



XXXII Panhellenic Conference on Solid State Physics and Materials Science

Ioannina, 18-21 September, 2016



Conference Program and Book of Abstracts

Organized by the University of Ioannina

Conference Center "Karolos Papoulias", University campus, Ioannina



Sponsored by



ΑΝΑΛΥΤΙΚΕΣ ΣΥΣΚΕΥΕΣ Α.Ε.
Δρ Κ.Ι. ΒΑΜΒΑΚΑΣ - ΕΠΙΣΤΗΜΟΝΙΚΟΣ ΕΞΟΠΛΙΣΜΟΣ



VECTOR
TECHNOLOGIES



Contact: xxxii@conf.uoi.gr <http://xxxii.materials.uoi.gr>

Under the auspices of



University of Ioannina



Materials Science & Engineering



Department of Physics



Research Committee

Sponsors



ΑΝΑΛΥΤΙΚΕΣ ΣΥΣΚΕΥΕΣ Α.Ε.
Δρ Κ.Ι. ΒΑΜΒΑΚΑΣ - ΕΠΙΣΤΗΜΟΝΙΚΟΣ ΕΞΟΠΛΙΣΜΟΣ



Committees

Local Organizing Committee

Eleferios Lidorikis (chair)
Christina Lekka (vice-chair)
Dimitrios Anagnostopoulos
Alexios Douvalis
Ioannis Panagiotopoulos
Dimitrios Papageorgiou
Dimitrios Vlachos

Chief Secretary

Kostas Prouskas

National advisory committee

Thomas Bakas (Ioannina)
Pantelis Kelires (Cyprus)
Stella Kennou (Patras)
Stergios Logothetidis (Thessaloniki)
Dimitrios Niarchos (Athens)
Costas Soukoulis (Crete)
Nikos Stefanou (Athens)

Preface

It is my distinct honor, and pleasure, to welcome you all to the "XXXII Panhellenic Conference on Solid State Physics & Materials Science" and to our beautiful city of Ioannina. This year the conference is held from 18 to 21 of September 2016 and is organized by the University of Ioannina at the Conference Center "Karolos Papoulias" within the University Campus. This is the National Conference of the Solid State Physics and Materials Science research communities. It is organized annually in a rotational basis within Greece and Cyprus, having started in 1982 at Thessaloniki. Typically more than 150 scientists from Greece and Europe, in fields of Physics, Engineering, Materials, Chemistry, and Biology, participate each year making this a thriving conference for over 3 decades! This great tradition has been an excellent forum for interactions between students, senior researchers and industry representatives. Many students have given here their first presentation, have discussed and exchanged ideas with experienced researchers and academics, while at the same time new research collaborations have been conceived and forged. It's been my privilege to be part of this for many years and a great honor to host this year's Conference in Ioannina.

About 180 researchers are attending and/or presenting their results this year. An exciting list of distinguished researchers from Greece and Europe have been invited to give lectures on the current experimental and theoretical issues in solid state physics & materials science: Andrea C. Ferrari (Cambridge), Wayne D. Kaplan (Technion-Israel Institute of Technology), Gregory Abadias (Univ. of Poitiers), Manfred Albrecht (Univ. of Augsburg), Kyriakos Porfyrakis (Oxford), Vassilios Kapaklis (Univ. of Uppsala), Maria Chatzinikolaidou (Univ. of Crete), George Dimitrakopoulos (Aristotle Univ), Ioannis Kallitsis (Univ. of Patras), Emmanuel Kymakis (TEI Crete), Argiris Laskarakis (Aristotle Univ.), Theodoros Leontiou (Frederic Univ., Cyprus), Athanasios Godelitsas (Univ. of Athens) και Ioannis Raptis (NCSR Demokritos). In addition, three special sessions have been organized: i) an industry forum, where representatives from instrument manufacturers present the newest scientific tools (Monday afternoon), ii) a presentation from representatives of the Greek General Secretariat for Research and Technology of the new calls on materials and round-table discussion (Wednesday afternoon), iii) the general assembly meeting of the "Hellenic Society for the Science and Technology of Condensed Matter (Wednesday afternoon).

I hope this conference, as it has happened year after year, will again live up to its main target, which is to become an inspiration for young scientists to continue and pursue their goals with passion and enthusiasm.

*With gratitude,
Elefterios Lidorikis*

Introduction

The 32nd Panhellenic Conference on Solid State Physics & Materials Science, held on 18-21 September 2016 in Ioannina, is a scientific meeting covering the modern trends and applications of Solid State Physics and Materials Science & Technology. This conference is held annually on a rotational basis. Recent past conferences were held in Thessaloniki 2015, Heraklion 2014, Athens 2013, Patras 2012, Limassol 2011 and Ioannina 2010. Researchers and scientists from Universities, Research Institutions, State Organizations and Industry get together to present and discuss the current state of the art in the area of physics, chemistry, materials science and materials engineering. At the same time, it provides a good opportunity for the young researchers (graduate and post graduate students) to present their first scientific results, investigate the possibility of scientific collaborations and explore employment opportunities. An exhibition of instruments and accessories also take part inside the conference centre.

Topics

The topics that will be discussed include: (1) electronics, photonics and optoelectronics, (2) structural-dynamical and mechanical properties of condensed matter, (3) strongly correlated systems, magnetism & superconductivity (4) surfaces, nanomaterials and low-dimensional materials & systems (5) polymers, organic materials and biomaterials, (6) ceramics, composites, minerals and metals.

The city of Ioannina

Ioannina is the capital and the largest city of Epirus. Founded by the Byzantine Emperor Justinian in the 6th century AD, Ioannina flourished following the Fourth Crusade, when many wealthy Byzantine families fled there in the early 13th century following the sack of Constantinople. It was part of the Despotate of Epirus from 1358 to 1416, before surrendering to the Ottomans in 1430. Between 1430 and 1868 the city was the administrative center of the Pashalik of Yanina. In the period between the 18th and 19th centuries, the city was a major center of the modern Greek Enlightenment. Ioannina joined Greece in 1913 following the Balkan Wars.



Venue

The conference is held at the Conference Center "Karolos Papoulias", located in the heart of the University of Ioannina Campus. You can get there, as following:

- From the Ioannina airport: By bus to the city center (runs every 30 min), then take bus 16 or 17 to the University (runs every 10 min)
- From the city centre: Take the bus 16 or 17 to the University (runs every 10 min) from the bus stop across the Justice Hall.
- By taxi: +30 26510 64777 (average cost: from airport 10-12 € from the city centre 6-7 €)



Presentations

Scientific program will include plenary, keynote, invited and contributed lectures as well as poster presentations which will provide an up-to-date state of the modern trends in Materials Science. Keynote and invited speakers should plan for a 35 and 25 minute talk respectively, followed by 5 minutes of questions. Oral presentations should be in done within 12 minutes in order to keep 3 minutes for discussion. Presentations should be in Microsoft Powerpoint or Adobe Acrobat Reader format and should be electronically handed by the speaker to the conference room at least one session before the lecture. Contributed papers describing original research work will be also presented as posters in order to promote scientific discussions and collaborations. The authors should hang their posters the morning of the presentation's day. The posters are recommended to be 80 cm (width) × 100 cm (height) while type size should be sufficiently large to allow people to read from 2-3 meters. All presentations should be in English.

Best presentation award

To encourage young students' participation a number of awards have been defined for high quality work based on their posters or oral presentations. These awards will be given to recognize excellence in research and presentation. The winners will be announced during the Closing ceremony on 21st September at 14:00.

Exhibition

Suppliers of analytical instrumentation and laboratory equipment will exhibit their latest offering during the Conference. The exhibition area is adjacent to the lecture area and within the poster, coffee break and lunch areas in the Conference Center "Karolos Papoulias".



International Technology Corporation was established 1977 by Mr Simaion Argyropoulos, who was active in the service of scientific instruments since 1973 for research and development film. Since 1977 I.T.C. provides in the territory of Greece and Cyprus later scientific equipment, supplies, software and also design, installation, training and service in vacuum systems,

surfaces analysis systems, vacuum measuring systems, leak detection systems, Mask aligners, Probers, Spin coaters and Hot plates. We also supply vacuum evaporation coaters, RTP-CVD systems, sputtering systems, mass spectrometers, wafers, spin on dopands, sputtering targets, pure metals and polymers, analytical and toploading balances. Over 35 years we represent in Greece and Cyprus companies like Varian (now Agilent Technologies) SUSS Microtech, AnnealSYS, Mantis Deposition Systems, V.G., Kemstream, Tristan technologies, Silvaco and more. Our customers are usually Universities, Research Institutes, public utilities, armed forces, industry, Hospitals etc. Recently the management of the company was transfer to Mr Leonidas Pennos who continues the good tradition of the company.



ThetaMetrisis designs & manufactures a wide range of turn-key instruments and holistic solutions for the non-destructive characterization of films and coatings (thickness, uniformity, refractive index, colour etc.) in the thickness range of 5nm – 500µm. ThetaMetrisis instruments are applied for both static and dynamic measurements in a wide spectrum of treatment conditions e.g. thermal processing, in liquids or gas environments etc. and for diverse applications, such as: Semiconductors, PV Industry, MEMS-MOEMS, Polymers, Optical Coatings, Hard Coatings Membranes, Liquid Crystal Display. ThetaMetrisis tools can be tailored to meet any particular customer's needs, are affordable in price, without any compromise in accuracy, quality & after sales support.



ΑΝΑΛΥΤΙΚΕΣ ΣΥΣΚΕΥΕΣ Α.Ε.
Δρ Κ.Ι. ΒΑΜΒΑΚΑΣ - ΕΠΙΣΤΗΜΟΝΙΚΟΣ ΕΞΟΠΛΙΣΜΟΣ

Analytical Instruments SA has been the exclusive representative in Greece for several decades of many renown scientific equipment manufacturers, such as

Bruker, Agilent, Leica-Microsystems, Horiba, Hitachi. This testifies its confidence and respect within the scientific community, as well as its commitment and dedication to its customers. It is accredited by TÜV

Germany according to ISO EN 9001:2008, EN 13485:2012, for quality assurance. Its calibration laboratory is in accordance with EN ISO 17025:2005 Its staff includes highly educated chemists, chemical engineers, physicists and electronic engineers, who are regularly trained and are thus continuously updated on the latest scientific and technological developments.



Klothakis Eleftherios & Co. E.E – Anelis E.E.: Our company supplies high quality scientific systems by well known manufacturers, in the field of research and industrial laboratories. Our skilled personnel and the long experienced collaborators, provide full scientific and technical support. We are supplying scientific systems in the fields of material science, research laboratories, for industrial and manufacturing applications, pharmaceutical testing, food and sample preparation techniques. Analyzers for process industry and environmental applications monitoring. Technical and Scientific support, spare parts and chemical consumables. Contact ANELIS (www.anelis.gr) for further information. **SPECS Surface Nano Analysis GmbH - A Story of Constant Innovation:** SPECS has more than 150 employees at its headquarters in Berlin and its subsidiaries in the USA and Switzerland. The company also has sales offices and international sales channels in more than sixteen countries. A team of scientists and engineers are involved in developing and producing scientific instruments for surface analysis, material science and nanotechnology. By constant innovation new techniques, components or system concepts are launched every year since more than 30 years, revolutionizing the field of surface analysis. Contact SPECS Surface Nano Analysis GmbH (www.specs.com) for further information.



Vector Technologies LTD was established 11 years ago as a value added distributor of Test and Measurement Instruments and Operational Support systems in the Telecommunications, Educational and Public Sector market specializing in sales, marketing, technical support and after-sales service of hi-tech products. It specializes also in the provision of troubleshooting, performance analysis and network consulting services of new technology networks. Our mission is to provide our customers with the right choice for their particular application combining the superior quality on a fair cost. Our strategic co-operations with leading international suppliers, together with the strong know-how of our people, provide a guarantee of the quality and the success of our solutions and services in every electronic application. It is our company's policy to continuously seek for new ways to improve our processes and our modes of operation in order to maintain our competitive edge and achieve our targets. Vector Technologies is offering a complete range of test & measurement products and systems and maintains partnership agreements with leading measurement systems manufacturers as follows: TEKTRONIX, KEITHLEY, AEROFLEX, AMETEK, Anite-NEMO, ACTIX, TTI, AARONIA, SPECTRACOM, AR, CAEN, AH Systems, etc. The company is located at Vrilissia area north of Athens - Greece The premises include warehouses, integration center, demo center, training facilities and offices.



LaborScience S.A. was established in 2003, with primary mission to provide customers with total reliable solutions on scientific / laboratory instruments and applications, to Universities, Institutes, Health and Biotechnology Institutions as well as to the Industrial Sector. In order to offer complete range of high quality products which fulfill the customer needs, currently represents in Greece carefully selected manufacturers in various fields, such as: NT MDT with Modular and Automated AFM / STM systems, Integration of AFM with cutting-edge optical methods for scientific research AFM - Raman - SNOM - TERS, NanoIndentation as well as AFM Probes. Carl Zeiss, Jenoptik, Linkam, Prior, Photonic, Dhs, Pyser and more with Research Optical Microscopes, Stereomicroscopes, Digital Cameras, Heating, Cooling, Motorized Stages, Micromanipulators, Graticules, Image Analysis Software, Cold Light, Metal Halide, LED Illumination Sources. Relion Industries, with cathodoluminescence instrumentation. Hesse Instruments with Heating Microscope and furnace with Automatic Image Analysis. Hirox with 3D Digital Video Microscopy from the Highest Optical Quality to the most Advanced 3D Measurement Systems. CRAIC Technologies with UV-visible-NIR microscopes and microspectrophotometers, Raman microspectrometers. Brookhaven Instruments Corp. with Particle size, Zeta Potential, and Molecular Weight Analyzers, Chromatography Detectors and Laser Light Scattering Instruments. RMC-Boeckeler, with Ultramicrotomes. Quorum Technologies, Agar Scientific and more with Carbon, Sputter Coaters and EM consumables. Fischione Instruments with Ion Beam Specimen preparation devices, Plasma Cleaner, specimen holders, and EM imaging detectors. General Laboratory Equipment, including Hermle range of centrifuges, Elma ultrasound baths, Consort pHmeters and conductometers, as well as ovens furnaces, distillation units, pumps, refractometers, tensiometers, polarimeters, balances, mills, sieves and sieve shakers and more.

Detailed program

Sunday 18 September 2016

16:00 Registration

Opening ceremony

18:50 E. Lidorikis (Conference Chair)

18:55 T. Bakas (Vice Rector of the University of Ioannina)

19:00 **Andrea C. Ferrari** (Cambridge University, plenary)

The Roadmap to Applications of Graphene, Layered Materials and Hybrid Systems

20:00 **Welcome Reception**

Monday 19 September 2016

Session 1: Surfaces, Interfaces and Nanomaterials I

chair: S. Agathopoulos (U. Ioannina)

9:00 **Wayne D. Kaplan** (Technion-Israel, keynote)

Adsorption Transitions and Microstructural Evolution

9:40 Thomas Kehagias (AUP)

Strain and composition variations in the (211)B GaAs/InAs quantum dot heterostructure

9:55 Maria Katsikini (AUP)

GaN nanocrystal formation in a SiO₂ matrix

10:10 **Theodoros Leontiou** (Frederic-Cyprus, invited)

Stress and Composition of SiGe Nanostructures on Curved Substrates

10:40 Theodore Pavloudis (AUP)

Hydrogen diffusion through the Pd/Mg interface of Pd nanoparticles deposited on Mg nanofilms

10:55 **Coffee break**

Session 2: Ceramics, composites, minerals and metals

chair: W. Kaplan (Technion-Israel)

11:30 **Athanasios Godelitsas** (U. Athens, invited)

Mineral Nanoparticles, Nanominerals and Natural Nanoporous Oxide Materials

12:00 George Litsardakis (AUP)

Low temperature synthesis of ferrites for LTCC applications

12:15 Petros Nikolaou (Cyprus U. Techn.)

Hydrogenated amorphous carbon with embedded plasmonic NPs of silver/gold: nanocomposite films for selective and broadband optical absorption

12:30 Maria Karampiperi (AUP)

Radiophotoluminescence for medical dosimetry

12:45 Simeon Agathopoulos (U. Ioannina)

The influence of wetting phenomena, thermodynamics and kinetics in the production of ceramic/metal composites

13:00 **Lunch break**

Session 3: 2D Materials

chair: A. Laskarakis (AUP)

- 14:30 **Emmanuel Kymakis** (TEI-Crete, invited)
Graphene and other 2D-based materials for organic and hybrid solar cells
- 15:00 George Kioseoglou (U. Crete)
Spin relaxation and intervalley scattering in 2D semiconductors
- 15:15 Georgios Kopidakis (U. Crete)
Electronic properties engineering of transition metal dichalcogenides: strained monolayers and nanoribbons
- 15:30 John Parthenios (ICEHT-FORTH)
Near field Raman scattering in Molybdenum disulfide
- 15:45 Maria Kandyla (NHRF)
Properties of graphene supported on gold-coated black silicon
- 16:00 George Kalosakas (U. Patras)
Controlled formation of carbon nanostructures through defect engineering in graphene
- 16:15 Coffee break**

Session 4: Photonics and Optoelectronics

chair: P. Patsalas (AUP)

- 16:45 **Ioannins Raptis** (NCSR-Demokritos, invited)
Monolithically integrated optoelectronic platform for Point-of-Need application in health & food safety
- 17:15 Georgios Kakarantzas (NHRF)
Silica nanowires with a highly nonlinear glass thin coating for flat extra-wide supercontinuum generation
- 17:30 Konstantinos Vyrsoinos (AUP)
Investigation of Silicon Photonics pn junctions for fast Electro-Optical Switching
- 17:45 D. Chatzitheocharis (AUP)
Investigation of Silicon Nanophotonic Single-Mode Polarization Insensitive Waveguides
- 18:00 Thomas Christopoulos (AUP)
Graphene-Based Nonlinear Resonators for Optical Bistability: A Coupled Mode Theory Approach

Special Session I: Sponsor Presentations

chair: K. Prouskas (U. Ioannina)

- 18:20 Vector Technologies LTD
- 18:28 Anelis E.E.- SPECS Surface Nano Analysis GmbH
- 18:36 LaborScience S.A.

Poster Session I: Topics 2, 4, 6

(18:45 – 20:30)

chair: Ch. Lekka (U. Ioannina), D. Anagnostopoulos (U. Ioannina)

Tuesday 20 September 2016

Session 5: Low dimensional materials and systems

chair: J. Kallitsis (U. Patras)

- 9:00 **Kyriakos Porfyrakis** (Oxford-UK, keynote)
Fullerenes: Production, Properties and Applications
- 9:40 **Argiris Laskarakis** (AUTH, invited)
In-line high precision optical metrology for mass production of Organic Electronics
- 10:10 Ioanna Zergioti (NTUA)
Laser fabrication of a hybrid platform combining electrical and optical interconnects
- 10:25 Dimitris Tsikritzis (U. Patras)
Energy level alignment regimes at P3HT and modified ITO interfaces: The influence of the substrate work function
- 10:40 Periklis Papadopoulos (U. Ioannina)
Wetting states on superoleophobic surfaces
- 10:55 Theodoros E. Karakasidis (U. Thessaly)
Molecular Dynamics to extract friction factor at the nanoscale
- 11:10 Coffee break**

Session 6: Structural and mechanical properties

chair: P. Kelires (Cyprus U. Techn.)

- 11:40 **Gregory Abadias** (U. Poitiers-France, invited)
Uncovering thin film growth dynamics from in situ and real-time diagnostics
- 12:10 **George Dimitrakopoulos** (AUTH, invited)
Plastic strain relaxation in heteroepitaxy: A critical comparison of mechanisms and processes in III-Nitride epilayers
- 12:40 Panagiotis Pappas (NTUA)
GIXRD Study of multiferroic EuTiO₃ with in-situ application of electric field
- 12:55 Marios Constantinou (Cyprus U. Techn.)
Nanomechanical characteristics of pulsed-laser deposited DLC films with metallic (Ag, Mo) nano-inclusions
- 13:10 Christina Kyrou (U. Athens)
Polarized micro-Raman Study of the impact of Nanoparticle Shape and Concentration on the Nematic Liquid Crystalline Orientational Order
- 13:25 Lunch break**

Session 7: Polymers and organic materials

chair: K. Porfyrakis (Oxford-UK)

- 15:00 **Joannis K. Kallitsis** (U. Patras, invited)
Polymeric Semiconductors and their Carbon Nanostructure Hybrids for Organic Photovoltaics
- 15:30 Athanasios Katsouras (U. Ioannina)
Chemical structure optimization in high performance electron donor conjugated polymers based on indacenodithiophene and indacenodithienothiophene for organic photovoltaic applications

- 15:45 Georgios Constantinides (Cyprus U. Techn.)
Buckling-Induced Patterning of PDMS Surfaces Through Argon Ion Bombardment
- 16:00 Alexandros Vanakaras (U. Patras)
Surface-induced alignment of liquid crystalline dendrimers
- 16:15 Efthymia Ramou (U. Patras)
Liquid Crystalline Behaviour of Dimeric Systems Exhibiting Two Nematic Phases
- 16:30 Apostolos Koutsioukis (U. Patras)
A simple route to increase electrical conductivity of Graphene/CNTs thin films by compression.
- 16:45 Coffee break**

Session 8: Surfaces, Interfaces and Nanomaterials II

chair: G. Dimitrakopoulos (AUTH)

- 17:15 Kalliopi Trohidou (NCSR-Demokritos)
Numerical Study of the effect of the Antiferromagnetic matrix on the Exchange Bias properties of diluted nanoparticle system
- 17:30 Dimitris Kehrakos (ASPETE)
Modeling domain wall velocity in bi-magnetic nanowires
- 17:45 Andreas Kaidatzis (NCSR-Demokritos)
Structural and magnetic properties of L10 FePt/{MgO, W, or Pt }/L10 FePt trilayers
- 18:00 Georgios Giannopoulos (NCSR-Demokritos)
Combinatorial sputtering method: Producing L10-FeNi films with coercivity in excess of 1 kOe
- 18:15 Loukas Kastanis (NTUA)
Electrical and structural characterization of memory devices with laser fabricated nanocrystals
- 18:30 Fotis Priftis (U. Patras)
On the role of entropy in the emergence of chirality in systems of achiral particles.
- 18:45 Alexandra Stamateri (AUTH)
A DFT study on the interface of prototype organic semiconductors and the silver surface

Poster Session II: Topics 1, 3, 5

(19:00 – 20:30)

chair: Ch. Lekka (U. Ioannina), D. Anagnostopoulos (U. Ioannina)

Conference Dinner at "Frontzu Politia" (21:00)

Wednesday 21 September 2016

Session 9: Strongly correlated systems and magnetism

chair: I. Panagiotopoulos (U. Ioannina)

- 9:30 **Manfred Albrecht** (U. Augsburg, Germany, keynote)
Future concepts and materials for magnetic data storage
- 10:10 **Vassilios Kapaklis** (U. Uppsala, Sweden, invited)
Thermal fluctuations in artificial spin ice
- 10:40 Margaritis Gjoka (NCSR-Demokritos)
Structure and magnet properties of $R1-xZrxFe10Si2$ alloys with $R = Nd, Sm$
- 10:55 Myrovali Eirini (AUTH)
Arranging at the nanoscale: Effect on magnetic particle hyperthermia
- 11:10 Antonios Makridis (AUTH)
Dancing with magnetism: An attempt to control cell fate
- 11:25 **Coffee break**

Session 10: Biomaterials

chair: G. Kalosakas (U. Patras)

- 12:00 **Maria Chatzinikolaidou** (U. Crete, invited)
Engineering biomaterials for tissue engineering with controlled immunomodulation
- 12:30 Marianna Vasilakaki (NCSR-Demokritos)
Monte Carlo Study of core/shell nanoparticles for enhanced hyperthermia performance
- 12:45 Maria Tassi (U. Athens)
Extra Carrier Transfer Oscillations in DNA Monomers, Dimers and Trimers
- 13:00 Stavros X. Drakopoulos (U. Patras)
Variation of Energy Density in Thermoplastic Starch-Cellulose Microcomposites with Humidity and Temperature. A new sensing capability?
- 13:15 **Coffee break and light snack**

Student Presentation Awards

(14:00 – 14:30)

chair: E. Lidorikis (U. Ioannina)

Special Session II: Presentation of the new calls on materials and round-table with GSRT

(14:30 – 15:00)

chair: D. Niarchos (NCSR-Demokritos)

Special Session III: Meeting of the "Hellenic Society for the Science and Technology of Condensed Matter"

(15:00 – 15:30)

chair: I. Zergioti (NTUA)

Closing Ceremony

chair: E. Lidorikis (U. Ioannina)

Monday 19 September 2016

Poster Session I: Topics 2, 4, 6 (18:45 – 20:30)

chair: Ch. Lekka (U. Ioannina), D. Anagnostopoulos (U. Ioannina)

Topic 2: Structural-dynamical and mechanical properties of condensed matter

P201	Theocharis Angeletos (U. Athens)	<i>Infrared Study of Defects in Nitrogen-Doped Electron Irradiated Silicon</i>
P202	K. Filintoglou (AUPh)	<i>High pressure Raman and photoluminescence studies of $\text{In}_x\text{Al}_{1-x}\text{N}$ ($x=0.72$)</i>
P203	S. Misopoulos (AUPh)	<i>Pressure response of the FC70 FluorinertTM studied by Raman spectroscopy</i>
P204	F. Sebro (AUPh)	<i>High pressure Raman study of Kevlar-29 aramide fibres</i>
P205	Calliope Bazioti (AUPh)	<i>Structural properties and strain relaxation in high alloy content InGaN films grown on $\text{AlN}/\text{Al}_2\text{O}_3$ templates by MBE</i>
P206	Marios Constantinou (Cyprus U. Techn.)	<i>PECVD/PVD hybrid deposition technology for developing Ag- and Ti-reinforced hydrogenated amorphous carbon nanocomposite coatings</i>
P207	Aikaterini Boutzi (AUPh)	<i>On the High Pressure Consolidation of Bi_2Te_3</i>

Topic 4: Surfaces, nanomaterials and low-dimensional materials & systems

P401	Anastasios Kotoulas (AUPh)	<i>Solvothermal synthesis of carbon encapsulated cobalt nanoparticles and their response in magnetic hyperthermia.</i>
P402	Mattheos Kamaratos (U. Ioannina)	<i>Yttrium and oxygen adsorption on silicon $\text{Si}(100)2 \times 1$ surface</i>
P403	Athanasios B. Bourlinos (U. Ioannina)	<i>Fluidized Carbon Nanotubes through Novel Modification Pathways</i>
P404	M. K. Niora (AUPh)	<i>Variation in the anomalous fading behavior of various luminescence signals from Durango apatite versus grain sizes; from micro to nano scale</i>
P405	Vassiliki Belessi (TEI-Athens)	<i>Gravure printing of highly conductive ink made by Graphene/MWNTs nanohybrids in polyacrylic resins</i>
P406	Athina Alevizaki (U. Le Havre, France)	<i>Hypersonic phononic crystals made of poroelastic spheres</i>
P407	Adam Stimoniari (TEI W. Macedonia)	<i>Thermodynamic characterization and behavior of epoxy / fly ash composites</i>
P408	Adam Stimoniari (TEI W. Macedonia)	<i>Structure – Properties Relationship of Thermoset and Thermoplastic Nanocomposites Filled with Fly Ash</i>
P409	Alexandra Ioannidou (NCSR-Demokritos)	<i>A novel one step synthesis and sintering of skutterudite CoSb_3</i>
P410	E.C Stefanaki (AUPh)	<i>The effect of synthesis technique on the microstructure of high performance PbSe thermoelectric materials</i>

P411	Georgios Skoulatakis (U. Patras)	<i>Chemical and electrical characterization of high-k ultra-thin films on Ge substrates.</i>
P412	Nikoletta Florini (AUTH)	<i>Finite Element Analysis of Quantum Nanostructures</i>
P413	Stavros Kozakos (AUTH)	<i>Study of structural characteristics of polycrystalline Si thin films, grown by Al metal induced crystallization of amorphous-Si, for solar cell applications by electron microscopy techniques</i>
P414	Martha A. Botzakaki (U. Patras)	<i>Al₂O₃/HfO₂/p-Si MOS structures: Electrical and structural characterization</i>
P415	Karanasios Anastasios-Nikolaos (AUTH)	<i>C-doped TiO₂ powder characterization via XRD-analysis and Photo-Electrochemical experiments</i>
P416	A. Konstantopoulou (U. Patras)	<i>Phononic band gaps in nanostructures</i>
P417	Marianna Vasilakaki (NCSR-Demokritos)	<i>Magnetic properties of FePt films in CD and Si patterned substrates</i>
P418	Philomela Komninou (AUTH)	<i>Strain distribution in ultra-thin In(Ga)N/GaN quantum wells</i>
P419	Carla Cutrano (U. Ioannina)	<i>Structural, magnetic and electronic properties of CuFe nanoclusters by density functional theory calculations</i>
P420	Nikolaos Pliatsikas (AUTH)	<i>Enhanced Photocatalytic Activity of Composite Semiconducting/Plasmonic Materials: Towards Withholding of Heavy Metal Ions from Aqueous Solutions</i>
P421	John Nikolaides (AUTH)	<i>A material scientist's guide to fractal analysis</i>
P422	Dimitris Bellas (U. Ioannina)	<i>Modification of Nanoparticle Arrays by Laser-Induced Self Assembly (MONA-LISA)</i>
P423	Charalambos Trapalis (U. Ioannina)	<i>Molecular Modelling of the OPV Active Material in the Vicinity of Ag Nanoparticles</i>

Topic 6: Ceramics, composites, minerals and metals

P601	Tomara Georgia (U. Patras)	<i>Dielectric characterisation of PA6/ Boehmite alumina nanocomposites. The effect of compounding method.</i>
P602	Antonios Theodorakakos (AUTH)	<i>Electrical Properties and Thermal Imaging of Commercial NiTi wires</i>
P603	Angeliki G. Lekatou (U. Ioannina)	<i>Surface degradation of aluminium matrix composites reinforced by WC nanoparticles and aluminide particles</i>
P604	Angeliki G. Lekatou (U. Ioannina)	<i>Corrosion and wear behaviour of HVOF WC-Co-Cr nanostructured and conventional coatings</i>
P605	Ioanna Maria Zougrou (AUTH)	<i>XAFS study of hydroxyapatite and fossil bone apatite</i>
P607	Theodoros Karakostas (AUTH)	<i>Vitrification and devitrification treatment for the stabilization of chromium containing tannery ash</i>
P608	Aristotelis Kazakopoulos (TEI-Thessaloniki)	<i>Ionic Conductivity comparative study of LiZnVO₄ and LiMgVO₄</i>
P609	Andreas Delimitis (CPERI-CERTH)	<i>Structural Analysis of Waste Material from Mafic Rock Quarries Used for CO₂ Sequestration</i>

Tuesday 20 September 2016

Poster Session II: Topics 1, 3, 5 (19:00 – 20:30)

chair: Ch. Lekka (U. Ioannina), D. Anagnostopoulos (U. Ioannina)

Topic 1: Electronics, photonics and optoelectronics

P101	Joseph Kioseoglou (AUTH)	<i>Ab-initio structure prediction and electronic properties of $[Si_xSn_{1-x}]_3N_4$ ternary nitrides</i>
P102	Dodoleri Loukia (AUTH)	<i>Comparison between beta and ultraviolet (UV) induced Thermoluminescence in Lithium Fluoride (LiF)</i>
P103	Tilema Georgakopoulos (U. Patras)	<i>Photoconductive properties of nanocrystalline TiO₂ powders prepared in acidic environment</i>
P104	Kesidou Panagiota (AUTH)	<i>Deconvolution on CaF:N glowcurves induced by ultraviolet (UV)</i>
P105	P. Konstantinidis (AUTH)	<i>Dose rate dependence of Anomalous Fading (AF) in natural apatites.</i>
P106	Vasilis Lionas (U. Patras)	<i>Electrical conductivity mechanisms of nanocrystalline TiO₂ powders prepared in acidic environment</i>
P107	Karagiannis Ioannis (AUTH)	<i>EIS studies in incandescent lamps' tungsten wires</i>
P108	C. Petridis (TEI-Crete)	<i>Solution-processed reduced graphene-based electrodes for organic photovoltaics</i>
P109	Spyros Doukas (U. Ioannina)	<i>Spectrometer free molecular sensing with graphene plasmons</i>
P110	Ioannis Vangelidis (U. Ioannina)	<i>Optimal designs of plasmonic organic photovoltaics</i>

Topic 3: Strongly correlated systems, magnetism & superconductivity

P301	Konstantinos Efthimiadis (AUTH)	<i>Finite Elements Micromagnetic Simulation of the domain wall resonance</i>
P302	Nikolaos Maniotis (AUTH)	<i>Numerical simulations of interactions between magnetic nanoparticles and living matter through magnetothermal and magnetomechanical experimental setups</i>
P303	Zoi Kalpaxidou (AUTH)	<i>Magnetic nanoparticle heating in an AC magnetic field; an ex vivo approach</i>
P304	Panagiotopoulos Ioannis (U. Ioannina)	<i>Study of Magnetization Reversal in Layered Heterostructures by Vector-Magnetometry</i>
P305	George Sempros (AUTH)	<i>Synthesis, processing and characterization of FeMnGa nanoparticles for permanent magnet applications</i>
P306	Charalampos Sarafidis (AUTH)	<i>Processing of MnBi particles by high energy surfactant assisted ball milling</i>
P307	Kostas Georgalas (U. Athens)	<i>Magnetic ordering and low field CMR in $La(Mn, Cr)O_{3+\delta}$ ($\delta \approx 0.09, 0.12$) compounds</i>
P308	Theodorou Andreas (U. Athens)	<i>Electrical properties of VO₂ layers on Y-ZrO₂ substrates</i>
P309	K. Trohidou (NCSR-Demokritos)	<i>Numerical Study of the Exchange Bias properties of MnFe₂O₄/γ-Fe₂O₃ core/disordered shell nanoparticles</i>

- P310 Sophia Karamanou (TEI-Crete) *A novel approach for Plastic Bonded Magnets of the type MQU-F melt spun NdFeGaB –type alloys*
- P311 Tzartzas Thanos (U. Ioannina) *"Motion of Magnetic Bubbles by Electric Currents in Perpendicular Anisotropy Films*
- P312 Ioannis Hanis (AUPh) *"Critical temperature investigation in high temperature superconductors by means of magnetic susceptibility measurements*
-

Topic 5: Polymers, organic materials and biomaterials

- P501 Sotirios Sakkopoulos (U. Patras) *Conductivity Degradation Study of Polypyrrole and Polypyrrole/5% w/w TiO₂ nanocomposite under Heat Treatment in He and Atmospheric Air*
- P502 Ioanna Zergioti (NTUA) *Laser Induced Forward Transfer technique for the immobilization of biomaterials*
- P503 Achilleas Pipertzis (U. Ioannina) *Ionic Conductivity in Discotic Liquid Crystals of hexa-peri-benzocoronenes (HBC) doped with lithium triflate (LiTf)*
- P504 Georgia K. Pouroutzidou (AUPh) *Synthesis of a glass-ceramic nano-material in the ternary system SiO-CaO-MgO-CuO: effect of ball milling on the particle size, morphology and bioactive behavior*
- P505 Aristoula Selevou (U. Ioannina) *Effect of Confinement on the Structure and Dynamics of two Rod-like Liquid Crystals*
- P506 Stelios Alexandris (U. Ioannina) *Glass Transitions of Amorphous Polymers Confined in Nanopores: Dependence on Interfacial Energy and Thickness*
- P507 Maria Katsikini (AUPh) *Spectroscopic study of the role of Br and Sr in colored parts of the Callinectes sapidus crab claw*
- P508 Thomas Nevolianis (U. Ioannina) *Liquid Crystals of Hexasubstituted Benzenes bearing ultra strong dipole moments*
- P509 George Kalosakas (U. Patras) *Modeling and quantifying drug release kinetics*
- P510 Christina Zacharaki (U. Athens) *Electronic structure of purines, pyrimidines and similar molecules with LCAO*
- P511 Evaggelia Efthymiou Zavvou (U. Patras) *Mesomorphic Behaviour and dielectric response of symmetric difluoroterphenyl methylene-linked dimers*
- P512 Eleni V. Christidi (U. Patras) *Modelling of drug particles behavior near the release boundary: a classical and fractional dynamics approach*
- P513 Violetta Georgiadou (AUPh) *CoFe₂O₄ Nanoassemblies as Dual agents: Carriers of Anti-inflammatory Drug and Imaging Probes*
-

The Roadmap to Applications of Graphene, Layered Materials and Hybrid Systems

Andrea C. Ferrari

Cambridge Graphene Centre, University of Cambridge, Cambridge CB3 0FA, UK

Disruptive technologies are usually characterised by universal, versatile applications, which change many aspects of our life simultaneously, penetrating every corner of our existence. In order to become disruptive, a new technology needs to offer not incremental, but dramatic, orders of magnitude improvements. Moreover, the more universal the technology, the better chances it has for broad base success. The Graphene Flagship has brought together universities, research centres and companies from most European Countries. At the end of the ramp-up phase significant progress has been made in taking graphene, related layered materials and hybrid systems from a state of raw potential to a point where they can revolutionize multiple industries. I will overview the progress done thus far and the future roadmap.

SESSION 1

Monday 19 September 2016, 9:00-10:55

+

*Surfaces, Interfaces and
Nanomaterials I*

Adsorption Transitions and Microstructural Evolution

W.D. Kaplan¹

¹*Department of Materials Science & Engineering, Technion – Israel Institute of Technology, Haifa, Israel*

Abstract: It is recognized that interfaces (including free surfaces, grain boundaries (GBs), and interfaces between dissimilar phases) can be described using diffuse interface theory, where the structure and chemistry of interfaces can go through 2-D transitions between thermodynamic states (termed complexions) in order to minimize the interface energy. As such, complexions for interfaces are analogous to phases in the bulk. To date, almost all experimental studies on potential complexion transitions have been conducted on GBs in single phase polycrystalline systems, which by definition are not at equilibrium. Similar questions have been raised regarding interfaces in thin film studies, where the deposition process may be very far from equilibrium.

This presentation will focus on an experimental approach to address the structure, chemistry, and energy of complexions at interfaces which are fully equilibrated, from which it can be demonstrated that a change in complexion minimizes interface energy. This will be compared with solid-liquid interfaces, where a region of ordered liquid exists adjacent to the interface at equilibrium, and the details of a solid-solid interface where the reconstructed interface structure accommodates lattice mismatch for a nominally incoherent interface. These three systems will be compared to known reconstructed solid surfaces, which can also be described as complexions, within a more generalized Gibbs adsorption isotherm.

From this basis, an example of the use of complexions to control grain growth dynamics in polycrystalline alumina will be presented, where experimentally measured dopant solubility limits at the sintering temperature are used to confirm if equilibrium grain boundary (GB) segregation or enrichment defines GB mobility. Analysis of GB mobility of alumina as a function of dopant concentration has shown that some segregating dopants, associated with complexion transitions, increase the GB mobility, i.e. the opposite of solute-drag.

Strain and composition variations in the (211)B GaAs/InAs quantum dot heterostructure

N. Florini¹, J. Kioseoglou¹, G. P. Dimitrakopoulos¹, S. Germanis^{2,3}, C. Katsidis²,
 Z. Hatzopoulos^{3,4}, N. T. Pelekanos^{2,3}, Th. Kehagias¹

¹Physics Department, Aristotle University of Thessaloniki, 54624 Thessaloniki, Greece

²Department of Materials Science and Technology, University of Crete, P.O. Box 2208,
 70013 Heraklion, Greece

³Microelectronics Research Group, IESL-FORTH, P.O. Box 1385, 71110 Heraklion, Greece

⁴Department of Physics, University of Crete, P.O. Box 2208, 70013 Heraklion, Greece

InAs QDs grown on high-index GaAs (*h*11) surfaces seem to exhibit superior optical properties compared to the usual QD growth on GaAs (001), due to their sizeable piezoelectric field, which can be efficient in nanophotonics and quantum computing. However, the morphology of the QDs and their strain state and chemical composition, influence the light emission and absorption, the lasing efficiency, and other optoelectronic properties of QD-based devices. To this end, we have explored the nanostructure, the strain properties, and the related chemical composition of buried InAs QDs grown on (211)B GaAs surface employing both quantitative HRTEM techniques and elastic strain field simulations by the Finite Elements Method (FEM). Local strain measurements by the geometric phase analysis (GPA) method showed that pyramidal buried QDs were pseudomorphically grown on GaAs. Assuming a plane stress state of the QDs, we found a systematic increase of the local GPA strain (decrease of the elastic strain) from the base area to their apex region (Fig. 1). Subsequently, we calculated the chemical composition of the QDs, which exhibited an indium composition gradient along the growth direction, implying gallium segregation inside the dots. While the gradual increase of indium concentration is a common trend for all QDs, various In-content maxima (0.50 to 0.92) were measured at the apex area of different QDs. This variation can be attributed to the corrugated form of the (211) surface, resulting in local compositional fluctuations of the wetting layer at the nucleation sites of the QDs. Therefore, gallium segregation is already involved at the onset of the Stranski-Krastanow QD growth. Photoluminescence (PL) and μ -PL experiments, as well as simulations of the QDs' transition energies, showed variations in their emission energy, which comply with the graded In-content along the growth direction revealed by the quantitative HRTEM analysis and FEM simulations.

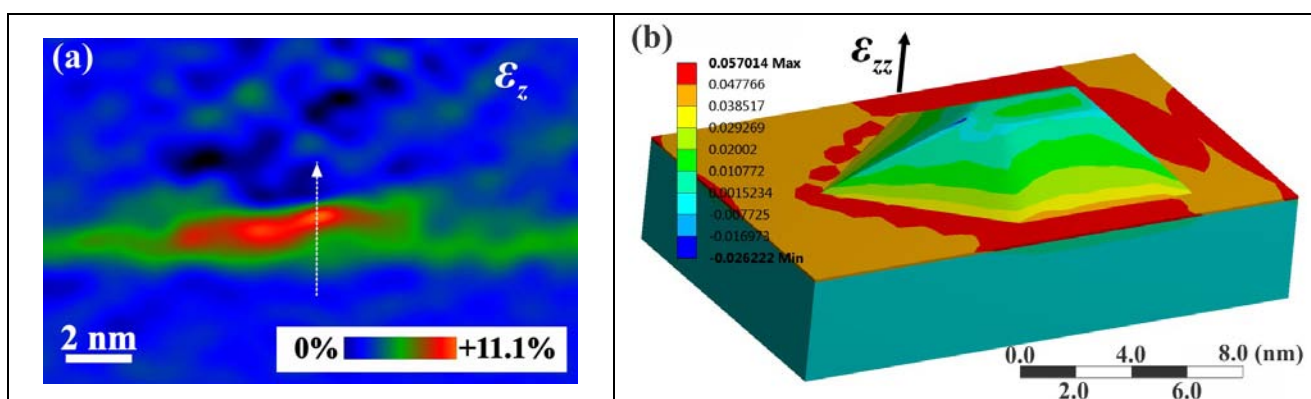


Fig. 1. (a) 2-D GPA strain map along the growth direction, illustrating the gradual increase of the ε_z strain inside an InAs QD with the GaAs lattice taken as the unstrained reference. (b) 3-D FEM simulated ε_{zz} elastic strain in an InAs QD model, showing gradual relaxation from the base toward the apex of the QD.

Acknowledgements

Work supported by the European Union (ESF) and Greek national funds - Research Funding Program: THALES, project "NANOPHOS", and Research Projects for Excellence IKY/Siemens.

GaN nanocrystal formation in a SiO₂ matrix

M. Katsikini¹, K. Filintoglou¹, F. Pinakidou¹, P. Kutza², Ph. Lorenz²,
 E. Wendler², K. Lorenz³, E. C. Paloura¹

¹School of Physics, Aristotle University of Thessaloniki, 54124 Thessaloniki, Greece

²Institut für Festkörperphysik, Friedrich Schiller Universität Jena, 07743 Jena, Germany

³Instituto Superior Técnico, P-2695-066 Bobadela LRS, Portugal

Abstract: The combination of ion implantation with annealing is an attractive process for the synthesis of semiconducting nanomaterials. Towards the integration of light emitting devices in Si substrates, GaN nanocrystals were fabricated *via* Ga and N implantation in a 1 μm-thick SiO₂ layer followed by rapid thermal annealing. The N and Ga atoms were sequentially implanted with energies 180 and 50 keV, respectively and fluences 6×10^{16} Ga ions /cm² and 7.5×10^{16} N ions/cm². The samples were annealed using a halogen flash lamp (rapid thermal annealing) for 30 sec in the temperature range 800 to 1300 °C. Rutherford backscattering spectroscopy, using 1.4 and 3.7 MeV He ions, revealed that Ga and N were implanted up to a depth of approximately 250 nm. Annealing at temperatures higher than 1000°C causes considerable loss of Ga, as identified in the X-ray fluorescence spectra (Fig. 1). The formation of GaN nanocrystals upon annealing at 1000°C is identified in the Ga-K-edge X-ray absorption fine structure spectra recorded at the KMC-II beamline of the synchrotron radiation facility BESSY-HZB (Fig. 2). Reduction in the coordination numbers is observed due to size effects. At annealing temperatures lower than 1000°C, only one nearest neighbouring shell, consisting of 3 oxygen atoms at the distance of 1.88 Å, is detected. This is also the case for the sample annealed at 1200°C, where middle-range order is lost. This result is attributed to loss of nitrogen which is characterized by much higher diffusion coefficient than Ga. The results suggest that ideal annealing temperature for GaN formation without considerable loss of Ga or N is 1000°C.

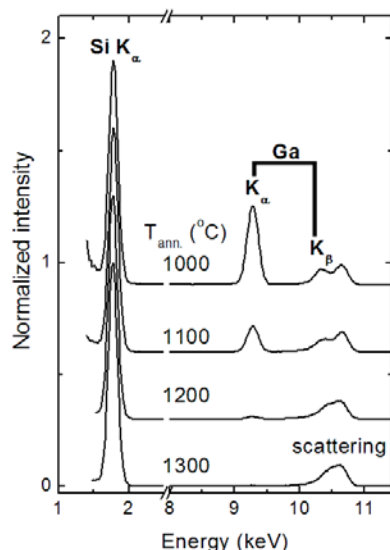


Fig. 1: X-ray fluorescence spectra of the samples annealed at 1000 to 1300 °C for 30 sec

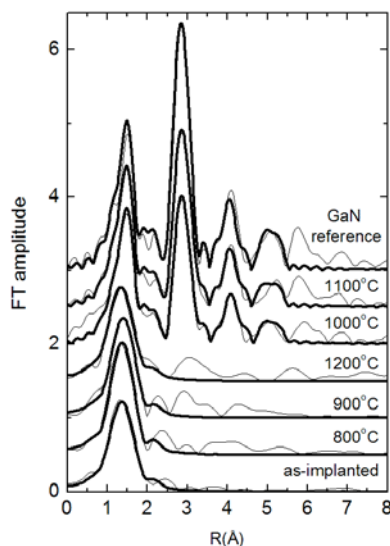


Fig. 2: Fourier transforms of the X-ray absorption fine structure spectra of a reference GaN as well as of the as-implanted and annealed samples for 30 sec at 800 to 1200 °C.

Acknowledgments: Financial support from the European Community's 7th Framework Programme (FP7/2007-2013-grant agreement Nr. 312284) and the IKYDA-2013 Greek-German bilateral program is greatly acknowledged.

Stress and Composition of SiGe Nanostructures on Curved Substrates

T. Leontiou¹, P. C. Kelires²

¹Department of Mechanical Engineering, Frederick University, Nicosia, 1036, Cyprus

²Department of Mechanical and Materials Science Engineering, Cyprus University of Technology, Limassol, 3603, Cyprus

Abstract: Experimental studies [1] of Ge nanoislands grown on Silicon-on-Insulator (SOI) substrates have shown that the strain distribution in such heterostructures is very different from that observed during Ge growth on thick Si substrates. This is accompanied by a defect-free strain relaxation mechanism through the bending of the substrate induced by the nanoisland. However, it is totally unknown how local bending affects the island composition and its distribution, something crucial to understand for device applications. Here, we present our recent work [2] aiming at clarifying this issue. Using atomistic Monte Carlo simulations and analytical modeling [3], we couple this bending relaxation mechanism with interdiffusion and alloying. We observe composition profiles that are completely different from those observed in flat nanoislands (Fig. 1, a). Moreover, for comparable SOI and island thicknesses, intermixing can be greatly reduced and Ge content in the islands is highly preserved (Fig. 1, b).

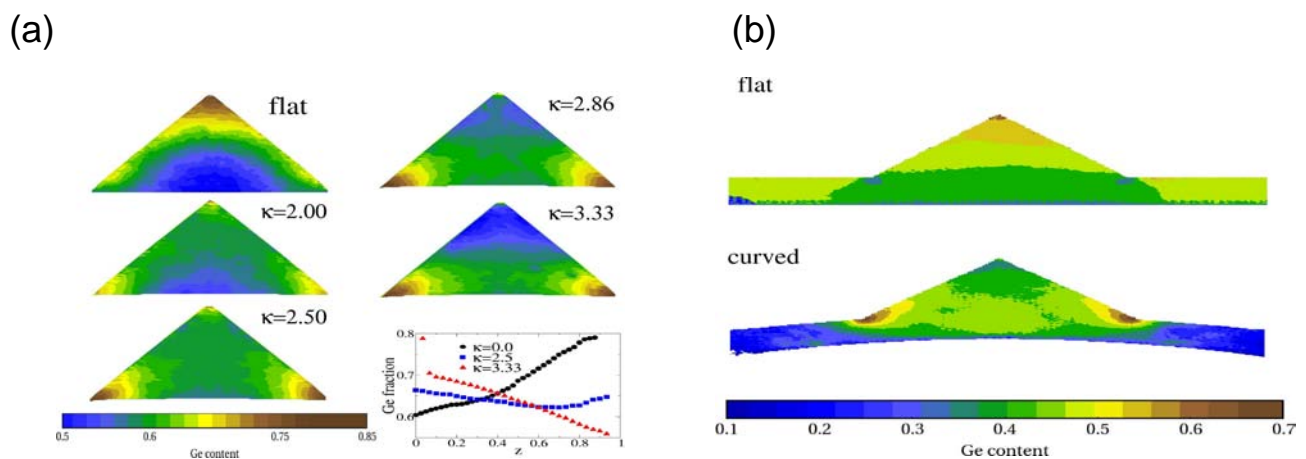


Figure 1: (a) The equilibrium composition profile at 900 K of a Ge-rich (65% Ge) {111} pyramid for both flat and curved geometries. The units of the curvature κ are 10^{-3} nm^{-1} . The graph shows the Ge fraction, averaged laterally, along the growth direction (in relative units). (b) The Ge composition profile of a SiGe pyramid on SOI for flat and curved ($\kappa = -5 \times 10^{-3} \text{ nm}^{-1}$) substrates.

References:

- [1] F. Liu *et al.*, Nature 416, 498 (2002); F. Cavallo and M. G. Lagally, Nanoscale Research Letters 7, 1 (2012).
- [2] T. Leontiou and P. C. Kelires, Phys. Rev. B 93, 125307 (2016)
- [3] T. Leontiou, J. Tersoff, and P. C. Kelires, Phys. Rev. Lett. 105, 236104 (2010).

Hydrogen diffusion through the Pd/Mg interface of Pd nanoparticles deposited on Mg nanofilms

Th. Pavloudis¹, S. Kumar², P. Grammatikopoulos², J. Kioseoglou¹, B. Clemens³, M. Sowwan²

¹Physics Department, Aristotle University of Thessaloniki, GR-54124 Thessaloniki, Greece

²Nanoparticles by Design Unit, Okinawa Institute of Science and Technology Graduate University, 1919-1 Tancha, Onna-Son, Okinawa, 904-0495, Japan

³Department of Materials Science and Engineering, Stanford University, Stanford, CA 94305-4045, USA

Abstract: Metal hydrides are a promising material for hydrogen storage, given their relatively low cost, abundance and high weight percent hydrogen absorption (e.g. 7.6 wt. % for magnesium hydride). However, to date, commercial application of metal hydrides has been limited by the relatively slow absorption and desorption kinetics, requiring high pressure and high temperature, respectively. A first approach for enhancing the properties of metal hydrides is nanostructuring, with the associated increase in surface area and reactivity that this inherently creates. Pd nanoparticles on Mg nanofilms may increase the efficiency of bulk Mg and offer an attractive alternative to bulk Pd for catalysis and hydrogen storage.

In this work, the diffusion of H in Mg nanofilms decorated with Pd nanoparticles is investigated by DFT using the VASP ab initio simulation package. Models of Pd and PdH on Mg and MgO are constructed and carefully relaxed and the specific reconstructions of the nanoparticle/nanofilm interface arising from the strain are examined. A single H atom is placed in a series of positions, starting from the nanoparticle region and ending deep in the nanofilm region and after the respective relaxations the diffusion path and energies are calculated and the diffusion barriers are extracted. The Pd nanoparticle is found to facilitate the diffusion of H in the first layers of Mg, significantly reducing the barrier compared to bulk Mg. This barrier is even smaller for PdH, suggesting that the diffusion is dependent on the H content of PdH_x. Finally, H diffusion is not preferable in MgO for both Pd and PdH, suggesting that the nanofilm surfaces should not be oxidized before the nanoparticle deposition.

SESSION 2

Monday 19 September 2016, 11:30-13:00

*Ceramics, composites, minerals
and metals*

Mineral Nanoparticles, Nanominerals and Natural Nanoporous Oxide Materials

A. Godelitsas¹

¹*National and Kapodistrian University of Athens, Zographou campus, 15784 Athens, Greece*

Abstract:

Of particular interest in Nanogeoscience is the study of nanometer-sized crystalline minerals or even poorly-, non-crystalline minerals, such as mineral nanoparticles, and nanominerals. Mineral nanoparticles are the nanoscale-versions of ordinary minerals (exhibiting different physicochemical properties compared to the micro- and macro-scale analogues), whereas nanominerals are distinctive phases occurring only in nanoscale without equivalents at larger scales. Besides, nanominerals are classified as naturally occurring crystalline substances (with a highly ordered, repeating atomic arrangement), having a specific chemical formula and exhibiting crystal dimensions -nanocrystals- that fall between 100 nm and 1 nm. Subsequently, it has been proposed that the classic definition of the term "mineral" has to be re-defined, down to the deep knowledge of atomic structure and arrangement. Moreover, naturally occurring nanoclusters, polyphasic nanominerals, nanoporous phases, amorphous nanomaterials, amorphous-nanocrystalline transitional phases, surface-disordered nanoparticles, and mesocrystals, all related to the natural progressive transition between amorphous and crystalline materials, have to be considered. The environmental importance of mineral nanoparticles and nanominerals, either crystalline or amorphous, is attributed to their vital role to mobility and (bio)geochemical cycles of hazardous elements and compounds in nature. Additionally, nanominerals and mineral nanoparticles are crucial in the study of raw materials & mineral resources, inasmuch they frequently occur in basic and noble metal deposits, as well as into related metallurgical products and wastes. On the other hand, natural nanoporous mineral oxides are important materials when studying the Earth and developing environmental technology and industrial applications. Tunnel-structured hydrated Mn-oxides with a 3×3 array of edge-shared MnO₆ octahedra, known as todorokites, exhibits a stable nanoporous molecular sieve structure similar to that of zeolite and have been proved to exhibit remarkable ion-exchange and catalytic properties. Finally, it has recently been revealed that common natural Fe-oxide minerals, such as hematite, may form nanocrystals containing a network of distinct nanopores.

Low temperature synthesis of ferrites for LTCC applications

G.Litsardakis and E.Halevas,
*Laboratory of Materials for Electrotechnics,
Department of Electrical & Computer Engineering,
Aristotle University of Thessaloniki, Greece*

Low temperature co-fired ceramics (LTCC) technology enables the integration of magnetic ceramics in the fabrication of high frequency and microwave devices, provided the magnetic materials achieve the desired properties at sintering temperatures as low as 800-900 °C. In order to obtain ferrites suitable for LTCC applications, soft chemistry methods are required. A modification of the citrate precursor synthesis route has been applied in spinel and hexaferrite compositions. The precursor gel is heated at 200 °C and, after the organic content is burned, it is fired at 600-800-1000 °C for 2 hours. XRD analysis shows that this method produces at a first stage single metal oxides and at higher temperature the mixed oxide. The microstructure and grain size has been examined by SEM and the crystallite size is compared to results from laser diffraction analyzer and to X-ray peak broadening through the Scherrer formula. Nano-sized, single-domain particles are formed (~40-60 nm), and grain growth is then dictated by the sintering temperature. VSM measurements have confirmed the development of the magnetic properties at 800 °C (eg. $M(@1T)=48,6$ emu/g, $H_c=435$ Oe for a Co spinel ferrite), and dielectric characterization of the samples has been performed at the 50Hz-5MHz range by means of an LCR bridge.

Hydrogenated amorphous carbon with embedded plasmonic NPs of silver/gold: nanocomposite films for selective and broadband optical absorption

P. Nikolaou¹, M. Constantinou¹, D. Bellas², P. Patsalas³, P. Kelires¹, E. Lidorikis², G. Constantinides^{1,*}

¹*Research Unit for Nanostructured Materials Systems, Department of Mechanical Engineering and Materials Science and Engineering, Cyprus University of Technology, Cyprus*

²*Department of Materials Science and Engineering, University of Ioannina, Ioannina, Greece*

³*Department of Physics, Aristotle University of Thessaloniki, Thessaloniki, Greece*

Abstract: The ability of plasmonic nanoparticles (PNPs) to absorb localized parts of the visible and infrared spectra depending on their size, shape and surrounding media are here explored for selective and broadband optical absorption applications, i.e. as potential solar harvesting materials collecting the sunlight energy that in turn heats a convective medium. Most of the materials currently in use exploit only a part of the solar radiation, leaving a great proportion unexplored. We here report on the making, measuring and modelling (previously designated as the 3M's principle) of hydrogenated amorphous carbon (a-C:H) matrices with PNPs (Ag and Au) to generate nanocomposite films with localized and tunable surface plasmon resonance (LSPR) characteristics and enhanced absorption capabilities. Free standing nanoparticles (NPs) of Ag and Au have been synthesized by thermally dewetting magnetron-sputtered films which have been subsequently capped with a layer of a-C:H. The NPs size was controlled through deposition time and annealing parameters. The a-C:H layer was deposited through an ion-beam source by cracking methane molecules using an RF plasma source. The morphological characteristics of the NPs have been investigated with SEM and AFM whereas optical measurements have been collected with a UV/VIS spectrophotometer. Roughness, density and thickness of the nanocomposite films have been probed using X-ray reflectivity. The factors that affect the LSPR peak position such as NP size, annealing conditions and host environment have been investigated, modelled and quantified. Finally, the solar photothermal performance of the produced films was evaluated in realistic conditions, using a thermocouple data logger system and monitored in real-time under sunlight. The experimental results are contrasted to photo-thermal theoretical predictions based on the effective medium theory.

Radiophotoluminescence for medical dosimetry

M.Karampiperi^{1,2}, J.P. Oliveira^{1,3}, F. Vanhavere¹, L.F.Nascimento¹

¹Radiation Protection Dosimetry and Calibration (RDC), Belgian Nuclear Research Centre (SCK-CEN), Belgium

²Physics department, Aristotle University of Thessaloniki (AUTH), Greece

³Physics department, University of Sao Paulo (USP), Brazil

Introduction : Aluminium oxide doped with carbon and magnesium ($\text{Al}_2\text{O}_3:\text{C},\text{Mg}$) can be used for radiophotoluminescence (RPL), a non-destructive method of luminescence[1] and for optically stimulated luminescence(OSL). The oxygen vacancies and the magnesium impurities cause the luminescent centers at 335 and 620nm, with emission at 750nm and lifetime $75 \pm 5\text{ns}$ [2].The aim of the project is to construct a reader for this material, with application in dosimetry (radiotherapy beams).

Materials and Methods : The samples from the $\text{Al}_2\text{O}_3:\text{C},\text{Mg}$ paper had 1mm thickness and 7mm diameter. The reader consists of UV LEDs and one red laser, filters and a multi-pixel photon counter (MPPC) detector. The samples were illuminated with the stimulation light and the luminescence is measured by the detector. The dose response is cumulative as the material cannot be bleached or annealed. Both β - and γ – sources were used for the irradiation.

Results and Discussion : Excitation with the red laser shows linear response from 160mGy to 20Gy while with the UV excitation the linearity is from 800mGy to 40Gy (Figure 1). The counts in the y-axis, represent the RPL counts, which is the total counts subtracted with the background coming from the zero dose.

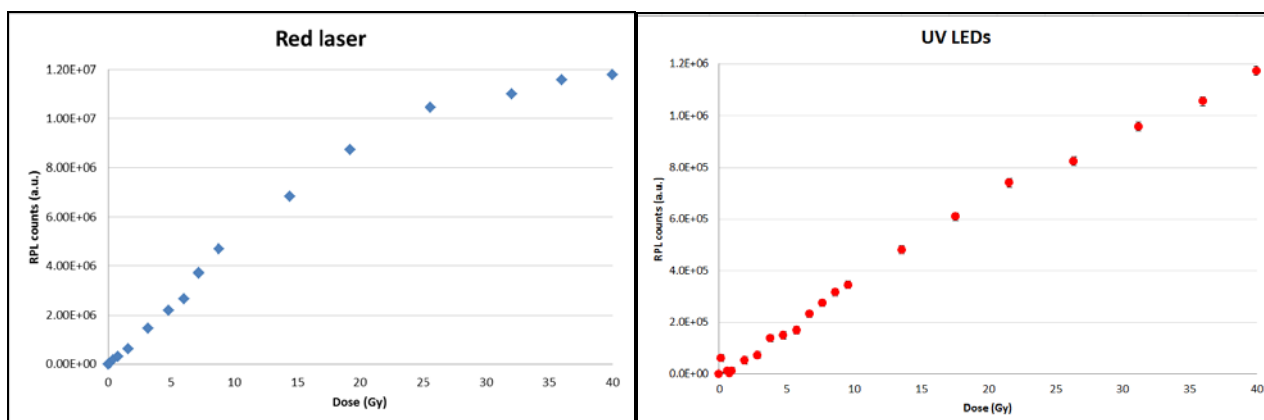


Figure 1 : Cumulative dose response for excitation source a) red laser and b) UV LEDs.

It is very important to be able to readout high doses, as the RPL technique is non-destructive, so the equivalent dose is added after each irradiation. However, the dose is given over different sessions, so the reader should separate low doses also. The UV exposure by the UV LEDs also add an OSL signal to the sample. The experiments showed that a pre-exposure by UV light is able to stabilize the OSL signal produced by ionizing radiation (which is not very reproducible alone), which gives opportunities to combine both the RPL and OSL signal after UV exposure.

References : [1] Ahmed, M. F., et al. "Comparison between different readout approaches for aluminum oxide radiophotoluminescent crystals." *Radiation Measurements*56 (2013): 361-364.

[2] Akselrod, Mark S., and Anna E. Akselrod. "New $\text{Al}_2\text{O}_3:\text{C}, \text{Mg}$ crystals for radiophotoluminescent dosimetry and optical imaging." *Radiation protection dosimetry* 119.1-4 (2006): 218-221.

The influence of wetting phenomena, thermodynamics and kinetics in the production of ceramic/metal composites

S. Agathopoulos^{*}, D. Gournis

Department of Materials Science and Engineering, University of Ioannina, Greece

^{*}: sagat@cc.uoi.gr, www.agathopoulos.org

The issue of thermodynamics (measured in equilibrium regime with surface and interfacial energies and wetting angles) and kinetics at ceramic-oxide/metal interfaces is important in joining techniques to obtain a mechanically strong interface. This presentation will focus in joining of alumina and zirconia either together or with metal devices, usually made of Ti or Ti6Al4V alloy. Whether direct bonding or brazing are considered, the system is seemingly simple, since it involves an oxide-ceramic (Al_2O_3 or ZrO_2), an active element (Ti), and noble metals (that ensure lack of oxidation, e.g. Pt, Au, Ag, or Cu), while high vacuum (10^{-6} mbar) is always applied during the experiments, due to high affinity of Ti for oxygen. Nevertheless, the microstructures of the interfaces developed at different temperatures, significantly differ one from the other, depending on each particular system. The general common features of the interfaces are the followings: (a) The reactive element (Ti) rapidly migrates towards the interface and reduces the ceramic oxide, yielding a Ti-oxide (not the same in every system) that is adjacent to the oxide, and (b) the sequence of reaction zones, whose thickness is determined by diffusion phenomena, is governed by the binary phase diagrams. However, (a) active elements, such as Al and V, can affect the microstructure of the interfacial reaction zone, (b) the features of other (more inert) elements crucially determine the microstructure and the strength of the interface, and (c) there is very different behaviour of Al_2O_3 (that is totally reduced) than ZrO_2 (that is blackened in the most of cases). Thermodynamic analysis of the experimental results suggests that the formation of the different oxides apparently depends on the kinetics of the reactions. The presentation will also briefly outline (a) phenomena which can be potentially observed at interfaces and influence interfacial strength, such as cracking (due to mismatch of thermal and mechanical properties of the contacting work-pieces), dissolution of ceramic, and penetration of reaction products along grain boundaries, including cases related to the production of glass-foams, and (b) the *in-situ* growth of superconductive nano-wires (with diameter of 15-35 nm) of Sn-mono-crystals, which exhibit a critical magnetic field (H_c) 30 times higher than bulk Sn, attributed to the nano-sized dimensions of Sn, encapsulated in C-nano-tubes, produced by catalytic chemical vapor deposition (CCVD) (Jankovic, et al. Nano Lett.2006;6:1131).

SESSION 3

Monday 19 September 2016, 14:30-16:15

2D Materials

Graphene and other 2D-based materials for organic and hybrid solar cells

Emmanuel Kymakis

*Center of Advanced Materials & Photonics and Department of Electrical Engineering, TEI of Crete,
 Estavromenos P.B 1939, Heraklion, GR 71 004, Crete, Greece*

<http://nano.teicrete.gr>

Abstract:

In this talk, I am going to present our recent progress on employing solution processable graphene like materials (GRMs) and other 2D crystals in high efficient organic (OSCs) and perovskite solar cells (PeSCs). The utilization of solution processable 2D crystals can simultaneously or individually optimize the photovoltaic parameters of an OSC by taking advantage of their high charge mobility to provide additional percolated pathways for efficient exciton dissociation and charge transport in the photoactive layer,¹⁻⁷ by adopting work-function (WF) tuned interfacial layers,⁸⁻¹¹ capable of providing a perfect energy match for either hole or electron transport, and by fabricating flexible transparent conductive electrodes (TCEs) with tailored optoelectronic properties.¹²⁻¹³

In particular, reduced graphene oxide (rGO) micromeshes were used as the TCE in flexible OSCs, achieving a power conversion efficiency (PCE) of 3.05%¹². A fast, non-destructive and r2r compatible photochemical method for the fabrication of chlorinated graphene oxide (GO-Cl) films with an increased WF of 5.23 eV⁸ and a facile process for lithium alkali metal functionalized graphene oxide with reduced WF, from 4.9 eV to 4.3 eV⁹, were presented. The utilization of these graphene-based HT and ET layers in PTB7:PC₇₁BM active layer devices, led to ~19% PCE compared to the reference graphene free devices, resulting in the highest reported PCE for graphene-based buffer layer OSCs of 9.14%.¹⁰

With respect to the photoactive layer, a photochemical route for the facile synthesis of tunable bandgap graphene-based derivatives, through controlled laser irradiation in liquid phase was demonstrated. Their incorporation as the electron acceptor material led to the highest reported PCE (2.41%) for graphene-based electron acceptors.³ In addition, functionalized LPE graphene nanoflakes (GNFs)¹ with controlled lateral size and graphene-inorganic nanocrystals hybrid materials (rGO-antimony sulphide, rGO-Sb₂S₃)² were demonstrated as electron cascade materials. Extending the research on other 2D materials, situ laser induced anchoring of noble metal nanoparticles onto the surface area of thin WS₂ nanosheets took place, leading to a PCE enhancement of ~13%.⁴ Finally, WSe₂ nanoflakes with different lateral sizes were utilized as the third components in high efficiency ternary OSCs, resulting in a PCE by 16%.

The utilization of 2D materials in PeSCs was also studied. In particular, GO-Li has been inserted between the perovskite sensitizer and m-TiO₂ layer, improving the electron injection by remarkably increasing the J_{SC} (+10.5%) and the stability.¹³ In another study, we presented a throughout analysis on the incorporation of reduced graphene oxide (rGO) in PeSCs, elucidating its main role in improving the electron transport when mixed with the m-TiO₂.¹⁴ By mixing rGO within the m-TiO₂ matrix, high efficient PeSC with PCE of 19.54% were recently realized.

References

- 1) Adv. Funct. Mater. 2015, 25, 3870-3880
- 2) ChemNanoMat 2015, 5, 346-352
- 3) Adv. Opt. Mater. 2015, 5, 658-666
- 4) 2D Materials 2016, 3, 015003
- 5) J. Mater. Chem. A 2016, 4, 1020-1027
- 6) Nanoscale 2015, 7, 17827-17835
- 7) J. Mater. Chem. A 2016, 4, 1020-1027
- 8) Nanoscale 2014, 6, 6925-6931
- 9) Chem. Mater. 2014, 26, 5988-599
- 10) J. Mater. Chem. A, 2016, 4, 1612-1623
- 11) Materials Today 2016, DOI: 10.1016/j.mattod.2016.03.01
- 12) Adv. Funct. Mater. 2015, 25, 2213-2221
- 13) Nanoscale Horiz. 2016, DOI: 10.1039/C5NH00089K
- 14) Adv. Funct. Mater. 2016, 26, 2686-2694

Spin relaxation and intervalley scattering in 2D semiconductors

G. Kioseoglou^{1,2}, I. Paradisanos^{2,3}, E. Stratakis^{1,2}, C. Fotakis^{2,3}, A.T. Hanbicki⁴, M. Currie⁴, A.L. Friedman⁴, B.T. Jonker⁴

¹Materials Science and Technology Department, University of Crete, Heraklion, 71003, Greece

²Institute of Electronic Structure and Laser (IESL), Foundation for Research and Technology-Hellas (FORTH), Heraklion, 71003, Greece

³Physics Department, University of Crete, Heraklion, 71003, Greece

⁴Naval Research Laboratory, Washington DC, 20375, USA

Monolayer transition metal dichalcogenides, MX_2 ($M = \text{Mo}, \text{W}$ and $X = \text{S}, \text{Se}$), are direct-gap semiconductors with some interesting properties. First, the low-dimensional hexagonal structure leads to two inequivalent K-points, K and K', in the Brillouin zone. Second, this valley index and spin are intrinsically coupled, and spin-dependent selection rules enable one to independently populate and interrogate a unique K valley with circularly polarized light^{1,2}.

Here we probe the degree of circular polarization of the emitted photoluminescence as function of the photo-excitation energy and temperature to elucidate spin-dependent inter- and intra-valley relaxation mechanisms. Monolayer flakes of MoS_2 and MoSe_2 show a strong depolarization as the excitation energy is increased³ (Figure). The difference in the excitation energy and photoluminescence emission energy, $dE = E_{\text{pump}} - E_{\text{PL}}$, governs the depopulation of carriers in each valley. Adding more energy above a distinct threshold characteristic of the longitudinal acoustic (LA) phonon for each material enables inter-valley scattering and produces a sharp decrease in the observed circular polarization. LA phonons in these two systems have different energies (30 meV for MoS_2 and 19 meV for MoSe_2), and we show that the threshold for the excess energy required to initiate the depolarization process clearly reflects the material specific phonon energy. In addition, our results show that independent of how many carriers are excited, i.e. whether you create neutral or charged excitons, the scattering process is the same. However, WS_2 maintains significant polarization⁴ for high excitation energies, even at room temperature when properly prepared and it will be discussed at the meeting.

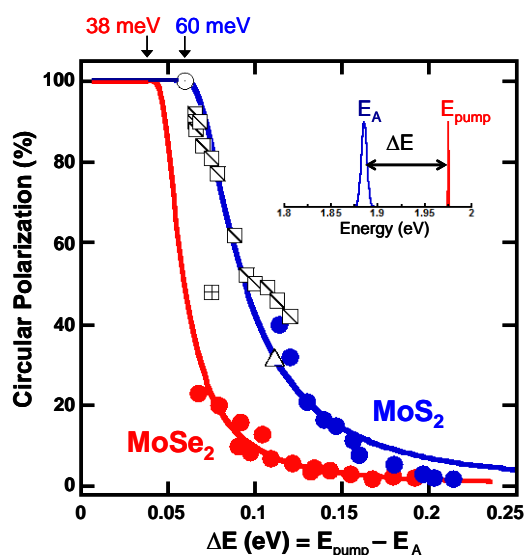
References

[1] K.F. Mak, K. He, J. Shan, and T.F. Heinz, *Nature Nanotechnology* 7, 494-498 (2012)

[2] G. Kioseoglou, A.T. Hanbicki, M. Currie, A.L. Friedman, D. Gunlycke, and B.T. Jonker, *Appl. Phys. Lett.* 101, 221907 (2012)

[3] G. Kioseoglou, A.T. Hanbicki, M. Currie, A.L. Friedman, and B.T. Jonker, *Scientific Reports* 6, 25041 (2016)

[4] A.T. Hanbicki, G. Kioseoglou, M. Currie, C.S. Hellberg, K.M. McCreary, A.L. Friedman, and B.T. Jonker, *Scientific Reports* 6, 18885 (2016)



Electronic properties engineering of transition metal dichalcogenides: strained monolayers and nanoribbons

G. Kopidakis, D. Davelou, A.E. Maniadaki, G.N. Kioseoglou, I.N. Remediakis
Dept of Materials Science and Technology, University of Crete, Heraklion, Greece.

Abstract: We present theoretical results for the electronic and dielectric properties of single-layer (2D) semiconducting transition metal dichalcogenides MX_2 ($M = \text{Mo}, \text{W}$; $X = \text{S}, \text{Se}, \text{Te}$) under isotropic, uniaxial (along the zigzag and armchair directions), and shear strain. Our Density Functional Theory (DFT) calculations show that electronic band gaps decrease while dielectric constants increase for heavier X. The direct gaps of equilibrium structures often become indirect under certain types of strain, depending on the material. The effects of strain and of broken symmetry on the band structure are discussed. Gaps reach maximum values at small compressive strains or in equilibrium, and decrease with larger strains. In-plane dielectric constants generally increase with strain, reaching a minimum value at small compressive strains. The out-of-plane constants exhibit a similar behavior under shear strain but under isotropic and uniaxial strain they increase with compression and decrease with tension. These DFT results are theoretically explained using only structural parameters and equilibrium dielectric constants [1]. We also discuss nanoribbon (quasi-1D) structures in comparison to the single-layer (2D) and bulk (3D) materials. Besides metallic edge states, our DFT results reveal several interesting electronic and dielectric properties which are interpreted with simple models and are consistent with available experimental data [2]. We also present results that show how strain can be used to tune atom adsorption on TMDs, such as hydrogen on MoS_2 nanostructures [3].

[1] A.E. Maniadaki et al, Solid State Commun. 227 (2016) 33.

[2] D. Davelou et al., Solid State Commun. 192 (2014) 42.

[3] A.E. Maniadaki and G. Kopidakis, Phys. Status Solidi RRL 10 (2016) 453.

Photographs / graphics may be used if necessary to substantiate results.

Near field Raman scattering in Molybdenum disulfide

John Parthenios¹, Kostantinos Papagelis^{1,2}, Rimma Dekhter⁴, Dimitris Anastopoulos¹, Spiros Grammatikopoulos¹, Costas Galiotis^{1,3}, and Aaron Lewis⁴

¹*Foundation of Research and Technology Hellas, Institute of Chemical Engineering and High Temperature Processes, P.O. Box 1414, GR-26504 Patras, Greece*

²*Department of Materials Science, University of Patras, GR-26504 Patras, Greece*

³*Department of Chemical Engineering, University of Patras, Greece*

⁴*Department of Applied Physics, Selim and Rachel Benin School of Engineering and Computer Science, The Hebrew University, Givat Ram, Jerusalem 9190401, Israel*

Abstract: Tip enhanced Raman scattering (TERS) employs the tip of a probe, under distance feedback with an ultraclose surface[1]. The resulting interactions amplify the intensity of vibrational Raman scattering of molecules on the surface. Although a general understanding of the TERS process is still to be elucidated, scanning tunneling feedback is often used in TERS with a noble metal tip and substrate. The possibility of tunneling induced plasmonic fields is investigated. The results of these investigations together with TERS of a 2D resonant, MoS₂ molecular system[2] are compared. Data on multiple excitation wavelengths of the resonant system in the near (TERS) and far-field are interpreted as arising from weak coupling interactions. This could explain the TERS enhancement within the framework of conventional resonance Raman scattering.

References:

[1] Schmid, T.; Opilik, L.; Blum, C.; Zenobi, R., *Angewandte Chemie* 2013, 52 (23), 5940-54.

[2] A. Michail, N. Delikoukos, J. Parthenios, C. Galiotis and K. Papagelis, *Appl. Phys. Lett.* 108, 173102 (2016)

Properties of graphene supported on gold-coated black silicon

M. Kandyla¹, N. Kelaidis², D. Palles¹, S.A. Giadini^{2,3}, M. Kanidi¹, J. Marquez^{2,4}, A. Dimoulas², E.I. Kamitsos¹

¹*Theoretical and Physical Chemistry Institute, National Hellenic Research Foundation, 48 Vasileos Constantinou Avenue, 11635 Athens, Greece*

²*Institute of Nanoscience and Nanotechnology, National Center for Scientific Research 'Demokritos', 15310 Athens, Greece*

³*Department of Physics, University of Athens, Zografou University Campus, 15784 Athens, Greece*

⁴*Department of Physics, National Technical University of Athens, 9 Iroon Polytechniou st., 15780 Athens, Greece*

Graphene-covered metallic nanostructures provide a unique platform for plasmonic-enhanced graphene devices. Recently, single-layer graphene was transferred and studied onto arrays of metallic nanoparticles, fabricated by lithographic methods.

Here, we integrate graphene with plasmonic Si substrates. We prepare arrays of nanopillars on the surface of Si (black Si) by laser irradiation in water. Laser nanostructuring of Si provides a simple, maskless, single-step, large-area, cost-effective method for the fabrication of plasmonic substrates. Coating the structured Si surface by a thin metallic layer results in the spontaneous formation of metallic nanoparticles, which cover the structured surface, instead of a smooth metallic film. The whole process is scalable and not inherently size-limited.

Single layers of graphene are prepared by chemical vapor deposition on transition metal catalytic substrates (Cu foil) and transferred on the plasmonic Si substrates by a PMMA scaffolding method. The properties of black Si-supported graphene are studied by scanning electron microscopy and optical reflectance spectroscopy. We probe the graphene layer for its plasmonic-enhanced Raman spectral signal via Raman spectroscopy.

Due to the coupling between localized surface plasmons and graphene, the Raman signal of graphene on black Si, coated with metallic nanoparticles, is enhanced by orders of magnitude, compared with the reference substrates employed, *i.e.*, graphene on flat Si with or without metallic coating. This result paves the way for future real-world applications of large-area hybrid nanomaterials.

CONTROLLED FORMATION OF CARBON NANOSTRUCTURES THROUGH DEFECT ENGINEERING IN GRAPHENE

G. Kalosakas^{1,2,3}, A.P. Sgouros⁴, M.M. Sigalas¹, K. Papagelis^{1,2}

¹ *University of Patras, Materials Science Department, GR-26504, Rio, Greece*

² *ICEHT/FORTH, P.O. Box 1414, GR-26504, Rio, Greece*

³ *Crete Center for Quantum Complexity and Nanotechnology (CCQCN), GR-71003, Heraklion, Greece*

⁴ *Chemical Engineering School, National Technical University of Athens, GR-15780, Athens, Greece*

Using numerical simulations we demonstrate the spontaneous formation of various 3D carbon nanostructures, like multi-tube carbon nanotubes, nanopyramids, nanocubes, artificially rippled graphene, and other exotic nanomaterials, starting from graphene nanoribbons and inducing controllably engineered defects consisting of carbon adatoms or inverse Stone-Wales defects. The evolution of the initial defected planar structures towards the final 3D nanoarchitectures is obtained through molecular dynamics simulations, using different force fields to ensure the reproducibility of the derived results [1].

It has been shown that periodic arrays of appropriate structural defects produce a stable and controllable inflection of a graphene sheet. This effect was used to obtain a variety of carbon nanotubes with different chiralities and sizes [2]. Lines of defects applied at the top or bottom side of graphene result in downward or upward, respectively, inflection of the sheet. Therefore, spatially designed defect distributions in graphene can spontaneously form a large variety of stable 3D nanostructures, of controllable size and shape, on demand.

The presented carbon nanostructures of different shapes, sizes, and morphologies, can be used in applications ranging from storage of hydrogen or other molecules, enhanced chemical reactions or catalysis in confined compartments, to drug delivery nanodevices and biosensors.

Acknowledgement: This work has been supported by the Thales project GRAPHENECOMP, co-financed by the European Union (ESF) and Greek national funds (ΕΣΠΑ) and by European Union's Seventh Framework Programme (FP7-REGPOT-2012-2013-1) under grant agreement n° 316165.

References:

- [1] "Exotic carbon nanostructures obtained through controllable defect engineering", A.P. Sgouros, G. Kalosakas, M.M. Sigalas, K. Papagelis, RSC Adv. **5**, 39930 (2015).
[2] "Transforming graphene nanoribbons into nanotubes by use of point defects", A. Sgouros, M.M. Sigalas, K. Papagelis, G. Kalosakas, J. Phys.: Condens. Matter **26**, 125301 (2014).

SESSION 4

Monday 19 September 2016, 16:45-18:15



Photonics and Optoelectronics

Monolithically integrated optoelectronic platform for Point-of-Need application in health & food safety

I. Raptis¹, P. Petrou², E. Makarona¹, S. Kakabakos², K. Misiakos¹

¹*Institute of Nanoscience & Nanotechnology, NCSR 'Demokritos' Athens, Greece*

²*Institute of Nuclear & Radiological Sciences & Technology, Energy & Safety, NCSR 'Demokritos' Athens, Greece*

Abstract: The biological and chemical optical sensors that are based on integrated waveguides require external active optical components resulting in operational complexity. To overcome these limitations, a radical photonic lab-on-a-chip platform, has been developed comprising planar waveguides self-aligned to VIS-NIR light-sources, and detectors, all monolithically integrated on the same silicon chip and fabricated with standard microelectronic/micromachining processes. The light sources (LEDs) are silicon avalanche diodes biased beyond their breakdown voltage and emitting in the VIS-NIR region of the spectrum. The LEDs are coupled to individually functionalized Broad-Band Mach-Zehnder Interferometric waveguides and the spectral shifts in the transmission spectrum due to the biomolecular adlayers are recorded through either an off-chip spectrometer or an on-chip one. The integrated nature of the basic biosensor scheme and the ability to functionalize each transducer independently with different recognition biomolecules allows for the development of miniaturized optical transducers tailored towards multi-analyte tests. An overview of the fabrication aspects and particular applications for fast and label-free optical immunochemical detection of markers related to human health and food safety will be presented.

Silica nanowires with a highly nonlinear glass thin coating for flat extra-wide supercontinuum generation

Grigoris Antonopoulos¹, Christos Riziotis¹, George Kakarantzas¹

¹*Theoretical and Physical Chemistry Institute, National Hellenic Research Foundation,
Vassileos Konstantinou Avenue, 11635, Athens, Greece*

Abstract: We report on the fabrication of hybrid photonic nanowires consisting of silica tapered fibers covered with a thin layer (< 100 nm) of a highly nonlinear sol-gel glass (HNG). These hybrid nanowires exhibit finely tunable waveguide properties: The positioning of a single layer of high index glass around the silica taper is found to be sufficient for obtaining zero-dispersion wavelengths at any point throughout the visible and near-infrared, and both positions and values of dispersion maxima can be adjusted according to design. It is, thus, possible to fine-tune the waveguide properties of the nanowires only by slightly adjusting, for example, the thickness of the HNG layer, while the silica taper diameter is kept constant.

The high-nonlinearity due to strong confinement and the tunability of the GVD make these hybrid nanowires extremely attractive and versatile candidates for different nonlinear applications, such as pulse compression and supercontinuum generation [1, 2]. Indeed, a 1- μm -diameter silica fiber coated with a 95-nm-thick HNG coating ($n = 1.81$) has been numerically shown to generate a flat, octave spanning, mid-infrared supercontinuum, far wider than what would have been possible with uncoated silica tapers [3].

The hybrid silica nanowires were fabricated in a specially designed platform that incorporates both the fiber tapering process and the controlled deposition of sol-gel thin layers [4]. The results and methodology presented in this work demonstrate the benchtop manufacturing and processing of this type of hybrid waveguides, even at room temperature.

References

- [1] Mark A. Foster, Amy C. Turner, Michal Lipson, and Alexander L. Gaeta, "Nonlinear optics in photonic nanowires," *Optics Express*, vol. 16, no. 2, p. 1300, 2008.
- [2] T. A. Birks, W. J. Wadsworth, and P. St. J. Russell, "Supercontinuum generation in tapered fibers," *Optics Letters*, vol. 25, no. 19, pp. 1415-1417, 2000.
- [3] Pantelis Velanas, George Kakarantzas, and Christos Riziotis, "Flat mid-infrared supercontinuum generation in tapered fiber with thin coating of highly nonlinear glass," in *SPIE LASE*, San Francisco, CA, 2015.
- [4] G. Kakarantzas, Leon-Saval S.G., T.A. Birks, and P.St.J. Russell, "Low-loss deposition of solgel-derived silica films on tapered fibers," *Optics letters*, vol. 29, no. 7, pp. 694-696, 2004.

Investigation of Silicon Photonics pn junctions for fast Electro-Optical Switching

M. Papadovasilakis, K. Vyrsoinos, S. Ves

School of Physics, Aristotle University of Thessaloniki, 54124 Thessaloniki, Greece

With the rapidly increasing aggregate bandwidth requirements in Data Centers (DCs) there is a demand to route the data at all hierarchy levels without optical-electrical-optical conversions. This task can be accomplished with high-radix, transparent and broadband optical switch fabrics based on the Silicon Photonics technology (SiP). Switching in SiP is achieved through the modulation from an external electrical control signal, of the electron plasma in a Si pn junction that forms a waveguide. The accumulated phase change induced from the carrier plasma in the propagating optical wave dictates if there will be constructive or destructive interference at the output port of an interferometric device and accordingly defines the switch's state. The junction is operated in a forward or reverse biasing with the injection or depletion of carriers. The injection scheme offers the advantage of lower losses at the expense of lower speed coming from the ns rate recombination rate of the carriers. Carrier Depletion switches on the other hand can operate with timing constants in the ps regime that is highly advantageous for fast reconfiguration of the DC network.

In this work we are presenting a model that verifies the experimental data recorded from a recently fabricated Mach Zehnder Interferometer (MZI) in the frames of the EU FP7 project PhoxTrot. The MZI employs pn junctions as phase shifters on both arms and is characterized in static conditions in depletion mode. The model fits very well the I-V curve, the propagation losses and the phase shift vs. applied voltage of the device. Further investigation reveals that optimization of the losses is possible with the right modification of the junction's p and n regions implantations.

Investigation of Silicon Nanophotonic Single-Mode Polarization Insensitive Waveguides

D. Chatzitheocharis, K. Vyrsoinos, S. Ves

*School of Physics, Aristotle University of Thessaloniki, 54124 Thessaloniki,
Greece*

Silicon nanophotonic platform has been considered so far as the straightforward solution for the implementation of Photonic Integrated Circuits (PICs). The ability to turn light in a few μm allows the implementation of very dense design layouts with small footprint, while also providing compatibility with CMOS process. These features enable unprecedented advantages in terms of cost, size and performance compared to circuits assembled from discrete devices or based on other material platforms e.g. III-Vs. However the nanophotonic waveguides exhibit one major drawback related to the high polarization sensitivity of the propagating light.

Usually due to this problem, the PICs operate only in one polarization (TE) or if they want to support both polarizations, they are duplicating the number of components; one for each polarization state that results doubling of its footprint. Towards the simplification of SiP PICs, in this work we are examining configurations of single mode waveguides that exhibit very low polarization sensitivity by exploiting the deposition of a SiN layer on top of the Si core. The investigation is extended to two sidewall angles; 3° and 8° in accordance with experimental data, while the SiN layer is covering either only the core or the whole waveguide. For each of the four generic configurations the parameters under variation are the height and width of the waveguide and the height of the slab. The simulation results for each waveguide profile reveal its single mode conditionality in both polarizations and their effective refractive index difference (Δn_{eff}). The investigation demonstrates that there are at least sixteen set of parameters where the Δn_{eff} is lower than 10^{-2} , while there are also three layout where Δn_{eff} is lower than 2×10^{-3} . These results pave the way for the realization of polarization insensitive SiP PICs. This work is conducted in the frames of H2020 ICT L3 matrix project.

Graphene-Based Nonlinear Resonators for Optical Bistability: A Coupled Mode Theory Approach

T. Christopoulos¹, O. Tsilipakos², N. Grivas¹, E. E. Kriezis¹

¹Department of Electrical & Computer Engineering, AUTH, 54124 Thessaloniki, Greece

²Institute of Electronic Structure and Laser, FORTH, 71110 Heraklion, Crete, Greece

Abstract: Graphene exhibits interesting properties in the THz frequency band and more specifically it has a surface conductivity consisting of both a linear and a third-order nonlinear contribution. The linear term has a significant negative imaginary part, allowing for the support of surface plasmon polaritons, while the third-order nonlinear term is, according to the literature, purely imaginary and of substantial magnitude, introducing a Kerr-type nonlinearity without extra nonlinear losses.

The combination of these unique properties of graphene with a simple travelling-wave resonator scheme providing feedback [Fig. 1(a),(b)], leads to optical bistability; a situation where the output power can potentially acquire two different states for a given input, depending on the history of the system [1].

To analyse this situation, we develop a framework combining first-order perturbation theory and temporal coupled mode theory (CMT). The framework is general, taking into account the inherent dispersion of graphene conductivity, expanding the available theory by additionally incorporating its nonlinearity. Importantly, we show that dispersive graphene can store energy due to the current density distribution on its surface. When dispersion is neglected, the stored energy on graphene becomes zero despite the fact that it still consumes reactive power produced by electric and magnetic fields.

To validate the framework developed, we compare the obtained results with full-wave nonlinear vectorial finite element method (NL-VFEM) simulations, while special care is taken to correctly model the current boundary conditions introducing graphene physically as a 2-D material [2]. Fig. 1(c) demonstrates excellent agreement between the two approaches.

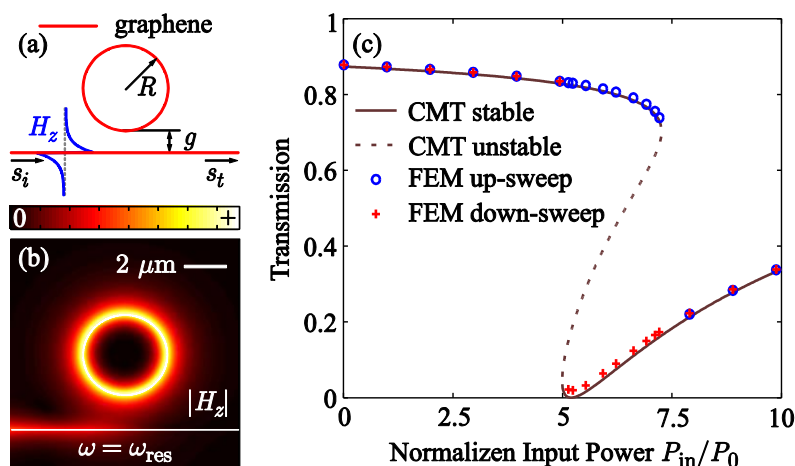


Figure 1. (a) Schematic of a graphene-based travelling-wave resonator, side-coupled with a graphene-based bus waveguide. (b) Magnetic field distribution on resonance (linear regime), revealing a travelling wave with zero transmission, since the resonator is critically coupled to the waveguide. (c) Bistability curve obtained both from CMT and NL-VFEM, indicating excellent agreement between the two.

[1] O. Tsilipakos, and E. E. Kriezis, *J. Opt. Soc. Am. B*, 31(7), 1698, 2014.

[2] D. Chatzidimitriou, A. Ptilakis, and E. E. Kriezis, *J. Appl. Phys.*, 118(2), 023105, 2015.

SESSION 5

Tuesday 20 September 2016, 9:00-11:10

*Low dimensional materials and
systems*

Fullerenes: Production, Properties and Applications

Kyriakos Porfyrakis

*Department of Materials and St. Anne's College,
University of Oxford, Parks Road, Oxford, OX1 3PH*
<http://www.materials.ox.ac.uk/>

Abstract:

Earlier this year, Sir Harry Kroto passed away. Harry Kroto was one of the discoverers of the fullerene molecule C₆₀. In this talk I want to pay tribute to Harry Kroto by revisiting the fascinating story of the discovery of one of the most famous molecules in Chemistry. The discovery of C₆₀ was somewhat accidental, but the brilliant insight of the scientists who discovered it, practically opened up the road for nanotechnology and led to numerous scientific breakthroughs. I shall also touch upon developments on how to increase the yields of production of endohedral fullerenes. Endohedral fullerenes are fullerenes with atom(s) or clusters trapped inside their interior. These molecules are arguably the most exciting family of the fullerene structures. I shall also describe progress in the chemical functionalization and the application prospects of endohedral fullerenes.

In-line high precision optical metrology for mass production of Organic Electronics

A. Laskarakis, S. Logothetidis

Lab for Thin Films - Nanobiomaterials - Nanosystems & Nanometrology (LTFN), Department of Physics, Aristotle University of Thessaloniki, 54124

Abstract

Optical metrology has the potential to revolutionize the manufacturing of high performance Organic Electronic devices on plastic substrates, as Organic Photovoltaics (OPVs), Organic Light Emitting Diodes (OLEDs), Organic Thin Film Transistors (OTFTs) etc, by large-scale Roll-to-Roll (R2R) manufacturing processes. Its unique advantages include non-destructive character, high measurement speed and sophisticated modelling methodologies that can provide significant information on the optical and structural properties, thickness and blend morphology of R2R printed nanomaterials in complex device architectures. This information is essential for the optimization of the morphology and thickness of the OE device nanolayers in order to manufacture OE devices with high performance and lifetime.

In this work, we present the innovative implementation of optical metrology tools (such as Spectroscopic Ellipsometry - SE in the visible to far ultraviolet spectral region, and Raman Spectroscopy -RS) on a unique R2R printing pilot line for the fabrication of polymer nanomaterials and OPV devices on flexible substrates that have the form of web rolls. The SE technique is combined with sophisticated modelling procedures and methodologies to obtain information on the optical properties, blend morphology, thickness homogeneity, surface roughness and quality of the different organic nanomaterials for OPVs in normal and inverted architectures. These include the transparent electrodes (e.g. PEDOT:PSS), and the bulk heterojunction (BHJ) photoactive layers that consist of electron donors (e.g. polythiophenes) and electron acceptors (e.g. PC₆₀BM, PC₇₀BM, IC₇₀BA, etc.). In addition, we present the advances on the Raman investigations of the bonding structure, quality and homogeneity of the printed OPV nanolayers on the plastic web roll of length of several meters.

Finally, the implementation of in-line optical metrology in the unique r2r printing pilot line will revolutionize the large scale production of printed OE devices (OPVs, OLEDs, OTFTs, etc.) with tailored properties, high performance and lifetime for commercialization to real-life consumer applications.

Laser fabrication of a hybrid platform combining electrical and optical interconnects

S. Papazoglou¹, M. Makrygianni¹, F. Zacharatos¹, M. K. Filippidou², S. Chatzandroulis²,
and I. Zergioti¹

1. *National Technical University of Athens, Physics Department, Heroon Polytehneiou 9, 15780, Zografou, Greece*

2. *Institute of Nanoscience and Nanotechnology, NCSR Demokritos, Agia Paraskevi, Greece, 153 10.*

Abstract:

With the evolution of flexible and stretchable devices during the last decade, the need for highly integrated components in multi-functional systems is now more urgent than ever. Furthermore, fabrication cost and process yield is of utter importance, while at the same time robustness and reliability are factors that need to be addressed in modern integrated circuits. In this work we report on a Polyimide (PI) based flexible platform, on which both electrical and optical interconnects are integrated by employing laser processing. Silver and copper nanoparticle inks and nanopastes were used to form highly conductive conformal interconnects for several types of multilevel devices residing on the PI substrate, by means of Laser Induced Forward Transfer technique (LIFT) and selective laser sintering. In particular, we have demonstrated the fabrication of electrical interconnects for the wire bonding of an all-laser printed resistive gas sensor device consisting of reduced graphene oxide as sensing element, with a printed circuit board (PCB). The aforementioned sensors were electrically characterized exhibiting good response upon the flow of humidity vapours (for humidity concentrations as low as 500ppm), with distinct resistance variations, avoiding cross-talk between adjacent sensors. On the same die, we have also applied selective laser curing for the direct writing of multi-mode optical waveguides operating at 1550 nm, and performed optical characterization in terms of performance, attenuation and reliability. These optical waveguides are of interest for short-distance optical interconnects which are key enablers for high-performance optoelectronic systems and can be particularly used as high speed optical interconnects for active optical components such as VCSELs and LEDs bonded on flexible substrates.

Energy level alignment regimes at P3HT and modified ITO interfaces: The influence of the substrate work function

D. Tsikritzis¹, C. Tselios¹, A. Douvas², S. Kennou¹

¹Department of Chemical Engineering, University of Patras, Caratheodory 1 GR 265 04 Patras, Greece

²Institute of Nanoscience and Nanotechnology, National Center for Scientific Research Demokritos, 15310, Aghia Paraskevi, Attiki, Greece

In organic based electronics the device performance and life time depend critically on the properties of both the active materials and their interfaces. In this work Photoelectron Spectroscopies have been utilized to characterize and determine the energy level alignment at interfaces of a hole-transporting organic semiconductor (P3HT) and ITO/polyoxometalate substrates. Polyoxometalates of Mo and W were deposited on ITO in order to tune the WF_{sub} from 4.4 eV up to 5.9 eV. Depending on the work function of the substrate, WF_{sub} , a transition between two different energy level alignment regimes has been observed: namely vacuum level alignment and Fermi level pinning (figure 1). The transition denotes the integer charge transfer state energy, E_{ICT+} , which represents the energy required to oxidize the organic polymer at the interface. Above this specific threshold value of 4.5 eV for P3HT, a spontaneous positive charge transfer across the interface to the organic semiconductor occurs. The charge transfer results in an interfacial dipole formation of a magnitude that scales with WF_{sub} . Within the Fermi level pinning regime, the barrier for hole injection remains constant and independent of the substrate work function, while within the vacuum level alignment regime, the barrier follows the Schottky- Mott limit behaviour, i.e., it scales linearly with the work function of the substrate. Thus, the charge-injection barriers can be reduced by modification of the electrode work function only within the limits established by the E_{ICT+} level.

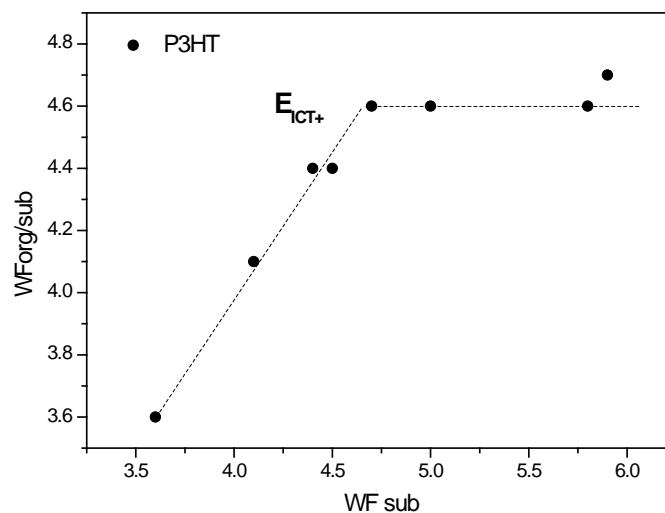


Figure 1. Evolution of work function of P3HT/sub ($WF_{org/sub}$) with respect to the work function of the substrate (WF_{sub}).

Wetting states on superoleophobic surfaces

Periklis Papadopoulos¹, Doris Vollmer² and Hans-Jürgen Butt²

¹*Department of Physics, University of Ioannina, GR-45110, Greece*

²*Max Planck Institute for Polymer Research, Mainz, D-55128, Germany*

Water repellency on superhydrophobic surfaces is achieved thanks to asperities that favor the entrainment of air cushions beneath the drop. This so-called Cassie state competes with the Wenzel state, in which the liquid fully wets the substrate. In case of liquids with low surface tension, the Wenzel state is always the thermodynamically stable one. A metastable Cassie state is obtained by using structures with overhangs. These structures are superoleophobic, repelling nearly all types of liquids. The Cassie-to-Wenzel transition can be triggered by vibrations, impact, rapid deceleration, or evaporation.

Here we image the Cassie-to-Wenzel transition of drops on superoleophobic surfaces, by laser scanning confocal [1] and reflection interference contrast microscopy [2]. Two scenarios are common: depinning and sagging. In depinning, the three phase contact line, or briefly contact line, unpins from the edge of the asperity. Then the contact line slides down the pillar wall, beginning the transition to a fully wetted state. The intermediate wetting states may be unstable, in case of pillars, or metastable, in case of overhangs. In the latter case these states may be long lived, effectively prohibiting the transition to the Wenzel state. On superoleophobic surfaces the energy barrier slows down the transition. Whereas most liquids with low surface tension are repelled efficiently at short times of a few seconds, at longer times – from minutes to hours – the liquid may penetrate slowly the structure.

References

- [1] Papadopoulos P., Mammen L., Deng X., Vollmer D., Butt H.-J., (2013) "How superhydrophobicity breaks down" *Proc. Natl. Acad. Sci. USA* 110(9), 3254–3258.
- [2] Papadopoulos P., Vollmer D., Butt H.-J., (2016) "Long-term repellency of liquids by superoleophobic surfaces" (submitted).

Molecular Dynamics to extract friction factor at the nanoscale

A. Liakopoulos¹, F. Sofos¹, T.E. Karakasidis¹

¹*Department of Civil Engineering, University of Thessaly, Volos, GR-38334, Greece*

Abstract: We perform Non-Equilibrium Molecular Dynamics simulations to describe the detailed atomistic behaviour of fluids moving in nanochannels. For some cases, flows at the nanoscale can still be investigated with Navier-Stokes equations, however, the modification scheme that has to be adjusted to the classical equation forms has a key-role and seems to depend on flow geometrical characteristics [1-2]. The question is how to incorporate phenomena existing at the nanoscale, such as shear stresses, slip lengths, non-constant viscosity and fluid density values, at the macroscale [3]. Molecular Dynamics (MD) is a common method for interpretation and investigation of nanoscale phenomena, describing particle interactions at the atomic scale. In this work we incorporate MD atomistic results in order to extract nanoscale properties to be used in the continuum N-S equations, such as the slip velocity at the wall and the shear viscosity profile. We find that classical continuum theory predictions of power dissipation do not apply in the case of nanochannels and have to be modified accordingly. However, the mathematical form of the friction factor expressions persists for quite small nanochannel widths and breaks down only when the channel walls are hydrophilic.

- [1] M. Gărăjeu, H. Gouin, G. Saccomandi, Scaling Navier-Stokes equation in nanotubes, *Physics of Fluids* 25, 082003 (2013).
- [2] A. Liakopoulos, F. Sofos, T.E. Karakasidis, Friction factor in nanochannel flows, *Microfluidics & Nanofluidics* 20, 1-7 (2016)
- [3] O.I. Vinogradova, A.V. Belyaev, Wetting, roughness and flow boundary conditions, *The Journal of Physics -Condensed Matter* 23, 184104 (2011)

SESSION 6

Tuesday 20 September 2016, 11:40-13:25

*Structural and mechanical
properties*

Uncovering thin film growth dynamics from *in situ* and real-time diagnostics

G. Abadias¹, J. J. Colin¹, C. Furgeaud¹, A. Michel¹, L. Simonot¹, B. Krause²

¹Institut Pprime, CNRS-Université de Poitiers-ENSMA, F 86962 Chasseneuil-Futuroscope, France

²Institut für Photonenforschung und Synchrotronstrahlung, KIT, Karlsruhe, Germany

Abstract:

The understanding of morphological and microstructural development during thin film growth is of particular relevance to control islands shape, nucleation and growth of nanoparticles, phase transformation, texture or surface roughness. Due to oversaturated vapour fluxes employed in physical vapor deposition (PVD) techniques, dynamics usually prevails over thermodynamics in dictating growth and microstructural evolution in PVD films. Depending on the material mobility, different growth modes occur, driven by kinetically limited surface diffusion processes and/or interfacial reactions. This has important implications in areas where nanoscale materials are involved, such as plasmonics, spintronics or next-generation of nano-devices.

In this presentation, we will provide some examples of *in situ* and real-time diagnostics based on optical techniques (wafer curvature, surface differential reflectance spectroscopy) and electrical resistance measurements to probe with high sensitivity the early growth stages of a variety of metal films on Si during sputter-deposition. In particular, we will show by coupling simultaneously two optical sensing techniques that the tensile stress generated upon island coalescence exhibit a maximum value at a film thickness that coincides with the onset of film continuity, for films growing in a Volmer-Weber mode (Ag, Au, Cu, Pd). The tensile stress magnitude is found to increase with decreasing material mobility, in relation with a lower percolation threshold, revealed from *in situ* resistivity measurement.

For films with lower adatom mobility (e.g., Mo, W), interfacial reaction with silicon favors a 2D growth mode and the initial formation of an amorphous film, followed by a phase transition to the equilibrium bcc phase above a critical thickness. In the case of Mo and Fe films, our *in situ* measurements reveal a structural transition at a film thickness of ~ 2-3 nm manifested by a concomitant tensile stress variation and decrease in electrical resistance. Insights on the kinetics of the amorphous-to-crystalline phase transformation were gained from *in situ* synchrotron studies, coupling simultaneously X-ray diffraction, X-ray reflectivity and wafer curvature during sputter-deposition of a series of Mo_{1-x}Si_x alloys. These unique measurements evidenced an interface-controlled crystallization process, taking place spontaneously above a composition-dependent critical thickness, with a constant growth front velocity (~13 nm/s).

**Plastic strain relaxation in heteroepitaxy:
A critical comparison of mechanisms and processes in III-Nitride epilayers**

G. P. Dimitrakopoulos

Department of Physics, Aristotle University of Thessaloniki, 54124 Thessaloniki, Greece

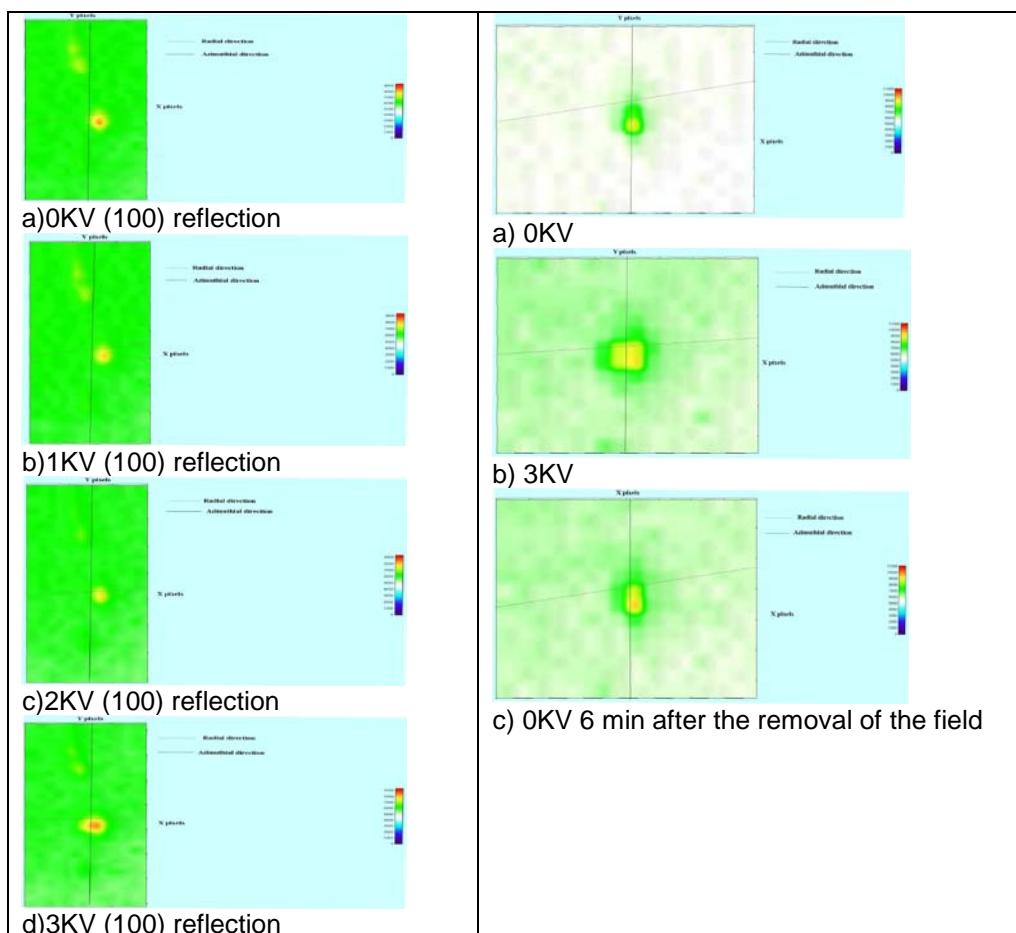
The concept of critical thickness has been dominant in defining the plastic behaviour of epitaxial layers. In this respect, the description of the phenomenon is based on the introduction of misfit dislocations at the heteroepitaxial interface in order to relieve the elastic strain due to the substrate. On the other hand, a crucial issue concerns the availability of glide mechanisms that will permit this to actually take place. If such an availability is limited, the system will seek other routes as an alternative to cracking.

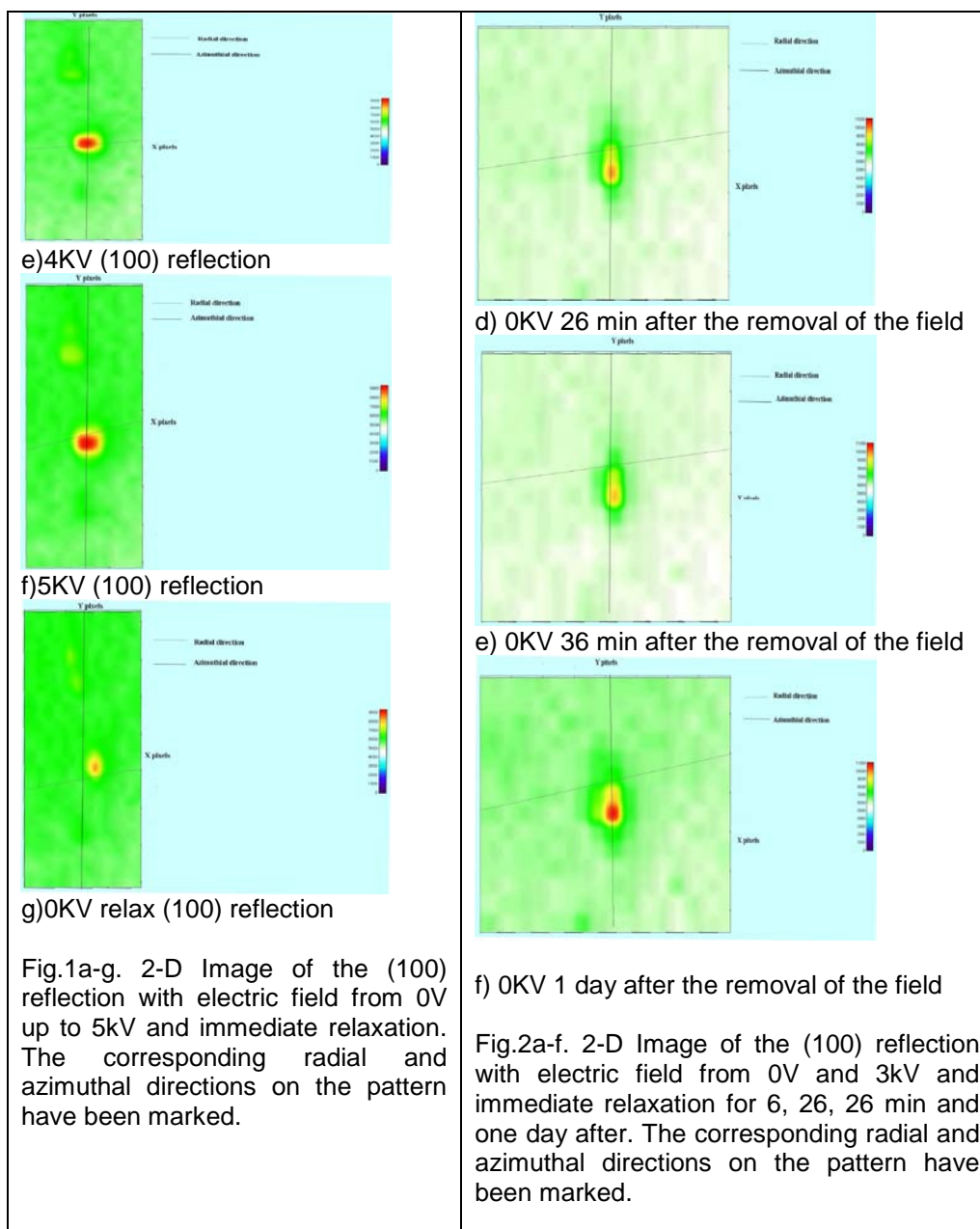
III-nitrides constitute a model system to demonstrate this, since, due to the hexagonal lattice, there is no resolved shear stress on the primary slip systems in the cases of polar and nonpolar growth. Only when the epitaxial orientation is semipolar, such a resolved shear stress can exist. Also, in addition to being grown in alternative orientations, III-nitrides are usually grown as alloys of the general form $\text{In}_x\text{Al}_y\text{Ga}_{1-x}\text{N}$, so that a compositional interplay is also possible under the influence of elastic strain.

We will compare the response of $\text{In}(\text{Ga})\text{N}/\text{GaN}$ and $\text{Al}(\text{Ga})\text{N}/\text{GaN}$ heterostructures to the misfit-induced plane stress. InGaN and AlGaN alloys differ significantly on the bond strength and adatom mobilities. Based on detailed structural observations by transmission electron microscopy (TEM) and high resolution TEM (HRTEM) methods, we will discuss the alternative routes to misfit dislocation introduction such as the inclination of the threading dislocations, stacking fault folding, opening of V-pits, chemical grading or zoning of the films, and interfacial grading versus interfacial roughening. Such mechanisms pertain to either films or very thin layers such as quantum wells, and it is important to consider the cumulative elastic strain energy stored in the system for the onset of plastic relaxation. Overall, a description of the strain relaxation of such heterostructures requires a separate definition of a critical thickness for each mechanism, as they may operate in succession in response to the residual elastic strain.

GIXRD Study of multiferroic EuTiO_3 with in-situ application of electric fieldP.Pappas¹, E. Liarokapis¹, A. Bussmann-Holder², J. Köhler²¹Department of Physics, National Technical University of Athens, GR15780, Athens, Greece²Max-Planck-Institut für Festkörperforschung, Heisenbergstr. 1, 70569 Stuttgart, Germany**Abstract:**

EuTiO_3 (ETO) has been discovered many decades ago [1]. Its antiferromagnetic properties below $T_N=5.5\text{K}$ [ii] excluded any technological applications, so for a long time it was discarded scientifically. The discovery of a strong magneto-dielectric effect as the temperature approaches T_N [iii] has revived the interest for this material. However, for the bulk material the soft mode frequency tends to zero at around -170K [iv, v], thus there is only a tendency towards a ferroelectric lattice instability. Nevertheless, a tuning of the dielectric constant by a magnetic field reveals that ETO is a strong coupling magneto-dielectric compound. Mainstream thin film technology enables to enhance the multi-functionality in many oxides and also provides valuable information about technological applications. Attempts have been made to realize with these techniques the desired properties for ETO. We have studied a high quality $1\ \mu\text{m}$ ETO thin film grown along the (100) axis on a SrTiO_3 (STO) substrate under the application of an external electric field along the (100) axis with the grazing incident angle xrd (GIXRD) technique at the Elettra Sinchrotrone Trieste facility. We have clear evidence that the electric field induces a significant reduction of the disorder of the crystal. The crystal structure itself changes, some crystallographic planes tilt and also there is a profound d-spacing change for planes parallel to the surface (Fig.1a-f), but a symmetry lowering was not observed. The effect shows a hysteresis, but the structural modifications are reversible (Fig.2a-e). Also there seems to be a permanent alteration of the disorder of the crystal as we can see from the profile of the spot (comparison of Fig.2a and Fig.2f). We have observed similar behavior in bulk samples with XRD and Raman spectroscopy. These observations open a new and interesting path for microelectronic applications for ETO thin films as it is obvious that there is a clear effect on the crystal structure with the electric field at room temperature.





[ⁱ] Brous J, Frankuchen I and Banks E 1953 *Acta Crystallogr.* **6** 67

[ⁱⁱ] McGuire T R, Shafer M W, Joenk R J, Halperin H A and Pickart S J 1966 *J. Appl. Phys.* **37** 981

[ⁱⁱⁱ] Katsufuji T and Takagi H 2001 *Phys. Rev. B* **64** 054415

[^{iv}] Kamba S, Nuzhnyy D, Vaněk P, Savinov M, Knižek K, Shen Z, Santav' a E, Maca K, Sadowski M and Petzelt J 2007 *Europhys. Lett.* **80** 27002

[^v] Goian V, Kamba S, Hlinka J, Vaněk P, Belik A A, Kolodiaznyi T and Petzelt J 2009 *Eur. Phys. J. B* **71** 429

Nanomechanical characteristics of pulsed-laser deposited DLC films with metallic (Ag, Mo) nano-inclusions

M. Constantinou¹, M. Pervolaraki², P. Nikolaou¹, C. Prouskas³, P.C. Kelires¹, P. Patsalas⁴, J. Giapintzakis², G. Constantinides¹

¹*Research Unit for Nanostructured Materials Systems and Department of Mechanical Engineering and Materials Science and Engineering, Cyprus University of Technology, Limassol, Cyprus*

²*Department of Mechanical and Manufacturing Engineering, University of Cyprus, Nicosia, Cyprus*

³*Department of Materials Science and Engineering, University of Ioannina, Ioannina, Greece*

⁴*Department of Physics, Aristotle University of Thessaloniki, Thessaloniki, Greece*

Abstract: We here report on the systematic synthesis and characterization of diamond like carbon (DLC) films with metallic (Me) nano-inclusions and explore their potential for mechanical (protective coatings or solid lubricants) or other functional (solar harvesting films) applications. The objective of this experimental study is to investigate and analyze DLC:Me nanocomposite films with silver (Ag) or molybdenum (Mo) as reinforcing material, such as to develop structure-property relations for material optimization purposes. DLC:Ag film is optically efficient, mechanically tough, has low residual stress and its design methodology differs from the one adopted for single phase amorphous carbon film, as it has to take into consideration the metallic inclusions' influence for tailoring purposes. Similar attention is placed on the mechanism at which molybdenum influences the chemical, physical and mechanical properties of DLC films. A single deposition method, Pulsed Excimer Laser Deposition (PELD) of sector targets, is used for the growth of DLC:Me amorphous carbon films with varying compositions of Ag or Mo. A range of characterization techniques is used for the in-depth study of materials in terms of their density, thickness, surface roughness, atomic bonding, crystallinity and phase compositions. Particular emphasis is placed on the nanomechanical and nanotribological characteristics of the nanocomposite films using an instrumented indentation platform and testing protocols based on the classical nanoindentation or nanoscratch modes. Scanning electron microscopy is used for visualizing residual plastic, fracture or delamination phenomena while atomic force microscopy is applied for morphological measurements. The increase of both metal amounts within the host amorphous carbon matrix is found to be beneficial as it increases the ductility of the material system and reduces film deterioration and film fracturing during scratching.

Polarized micro-Raman Study of the impact of Nanoparticle Shape and Concentration on the Nematic Liquid Crystalline Orientational Order

C. Kyrou¹, Y.S. Raptis², D.Tsiourvas³, G.Nounesis⁴, M. Panagopoulou² and I. Lelidis¹

¹ Department of Physics, University of Athens, Panepistimiopolis, Zografos, GR 157 84, Athens, Greece

² School of Applied Mathematical & Physical Sciences, National Technical University of Athens, GR 157 80 Athens, Greece

³ Institute of Nanoscience and Nanotechnology, National Centre for Scientific Research Demokritos, GR 15310 AghiaParaskevi, Greece

⁴ Biomolecular Physics Laboratory, National Centre for Scientific Research Demokritos, GR 15310 Aghia Paraskevi, Greece

Abstract:

Liquid Crystals (LCs) exhibit mesophases, which are intermediate between the solid and the liquid state of matter, characterized by unique physical properties such as long range orientational order coupled with anisotropic behaviour. Over the last fifteen years, scientists have shown great interest in liquid-crystalline nanotechnology and serious efforts have been devoted in order to investigate the interactions between liquid crystalline molecules and nanoparticles.

In order to explore the impact of nanoparticles of different shapes upon the nematic orientational order, we report measurements of the temperature dependence of Raman depolarization ratios in the nematic phase of the liquid crystal 5OP8OB (4-Pentyloxyphenyl-4'-Octyloxybenzoate) made of uniaxial rod-like molecules, doped with spherical hydrophobic semiconducting quantum dots CdSe-ZnS and also with hydrophobic Perfluorinated Silica Nanoplates. Both systems have been studied for various weight-concentrations. The measurement of the orientational order has been achieved by the determination of the first two expansion coefficients of the orientational distribution function, known as order parameters $\langle P_2 \rangle$ and $\langle P_4 \rangle$. The order parameters have been calculated by the Raman depolarization ratios in a direct way, since the polarized Raman spectra provided information on the macroscopic symmetry of the nanocomposite materials.

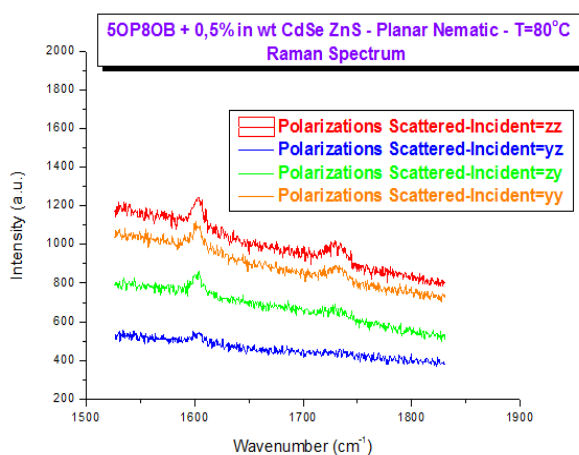


Fig.1: Polarized & Depolarized Raman Spectra of the Nanocomposite Nematic 5OP8OB with 0,5 % in wt CdSe-ZnS quantum dots at 80°C, (z -direction: parallel to the molecular axis of symmetry, y direction: perpendicular to the molecular axis of symmetry)

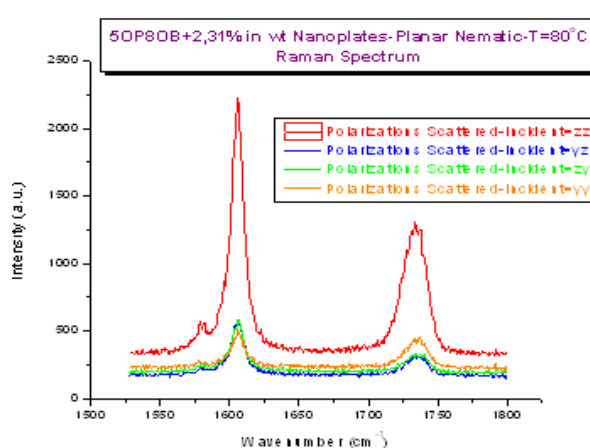


Fig.2: Polarized & Depolarized Raman Spectra of the Nanocomposite Nematic 5OP8OB with 2,3 % in wt Perfluorinated Silica Nanoplates at 80°C, (z -direction: parallel to the molecular axis of symmetry, y direction: perpendicular to the molecular axis of symmetry)

The analysis and the evaluation of our experimental measurements performed by a polarized micro-Raman technique, show that both, shape and nanoparticle concentration have a critical impact on the nematic liquid crystalline order.

SESSION 7

Tuesday 20 September 2016, 15:00-16:45

Polymers and organic materials

Polymeric Semiconductors and their Carbon Nanostructure Hybrids for Organic Photovoltaics

Joannis K. Kallitsis

*Department of Chemistry, Univeristy of Patras & Institute of Chemical Engineering Science,
Foundation of Research Technology Hellas FORTH/ICE-HT, Patras, Greece
E-mail: j.kallitsis@upatras.gr*

Organic Photovoltaics is an emerging topic due to their potential low cost high throughout device production using continuous manufacturing processes. One of the most successful device architecture is bulk heterojunction (BHJ) solar cells in which the donor and the acceptor are blended to form a bicontinuous interpenetrating network. Intensive research efforts resulted in a performance increased over 10% recently. For the efficiency optimization of these devices, design of either new electron donating semiconducting polymers with broaden absorption spectra and narrow bandgap or new fullerene derivatives as electron accepting materials, as well optimization of the architecture of the device have been made. However, device's performance and stability is strongly affected by the morphology of the active layer. The phase separation between the donor and the acceptor materials have to be controlled to provide an about 10nm phase separated mixture.

Working in the direction of electron donors, low bandgap polymers have been synthesized in our laboratory for the application of these materials in large areas OPVs. Besides that, we have developed a straightforward methodology to create tailor made hybrid materials, composed of the selected polymeric electron donor and any fullerene derivative chosen. These hybrid polymers could be used to control the morphology of the active layer as well as the stability performance of BHJ device. A large number of materials have been synthesized and after tedious purifications the final materials were characterized in terms of structural, electronic and morphological properties.

Acknowledgments:

This research has been co-financed by the project SMARTONICS – 310229 - FP7-NMP-2012.1.4-1 (2013-2017) "Development of Smart Machines, Tools and Processes for the Precision Synthesis of Nanomaterials with Tailored Properties for Organic Electronics".

Chemical structure optimization in high performance electron donor conjugated polymers based on indacenodithiophene and indacenodithienothiophene for organic photovoltaic applications

Athanasios Katsouras, Christos L. Chochos, Apostolos Avgeropoulos

Department of Materials Science Engineering, University of Ioannina Ioannina 45110, Greece

Abstract: Conjugated polymers represent one of the most important class of materials for the fabrication of many optoelectronic applications, such as light emitting diodes, field effect transistors, organic photovoltaics, sensors, etc. In the field of organic photovoltaics, the design of novel conjugated polymers with appropriate frontier orbital energy levels, optical band gap and suitable carrier transport properties are needed to improve the power conversion efficiency (PCE).^[1,2] Among various materials developed for bulk heterojunction devices, the multifused-ring conjugated polymers are particularly interesting due to their superior optical and electrical properties.^[3] The highly fused aromatic/heteroaromatic units enhance effective conjugation of the polymer backbone to facilitate electron delocalization and charge carrier mobilities.^[4] In this work, the design, synthesis and properties characterization of a new family of D-A copolymers based on Indacenodithiophene and Indacenodithienothiophene as the donor units with various electron deficient building blocks (benzothiadiazole, quinoxaline, thienopyrrolodione) will be presented (Figure 1).

In particular, model polymeric semiconductors were designed and successfully synthesized in order to explore, for the first time, the influence of the bond length alternation (BLA) through the polymer backbone enlargement on the optoelectronic properties, as well as the microscopic and macroscopic phenomena.^[5] A correlation between structures – properties relationship in this series of model D-A copolymers was achieved. Another important aspect is the role of the polymer's molecular weight. We will report our latest findings on the photovoltaic performance and optoelectronic properties of a donor-acceptor copolymer based on indacenodithieno[3,2-*b*]thiophene and 2,3-bis(3-(octyloxy)phenyl)quinoxaline moieties as a function of the number-average molecular weight (M_n).^[6,7] Current-voltage measurements and photo-induced charge carrier extraction by linear increasing voltage (Photo-CELIV) reveal improved charge generation and charge transport properties in these high band gap systems with increasing number average molecular weight, M_n , while polymers with low molecular weight suffer from diminished charge carrier extraction due to low mobility-lifetime ($\mu\tau$) product. By combining Fourier-transform photocurrent spectroscopy (FTPS) with electroluminescence spectroscopy, we demonstrate that increasing M_n reduces the non-radiative recombination losses.

We envision these insights will guide the synthetic chemists and materials scientists towards the optimization of a polymer chemical structure with predetermined optoelectronic properties, controllable supramolecular assemblies and morphologies for specific optoelectronic applications. Therefore, it is evident that the chemistry of functional conjugated polymers is facing major challenges and suitable materials have to adopt a broad range of specifications in order to be established as the best choice for high photovoltaic performance.

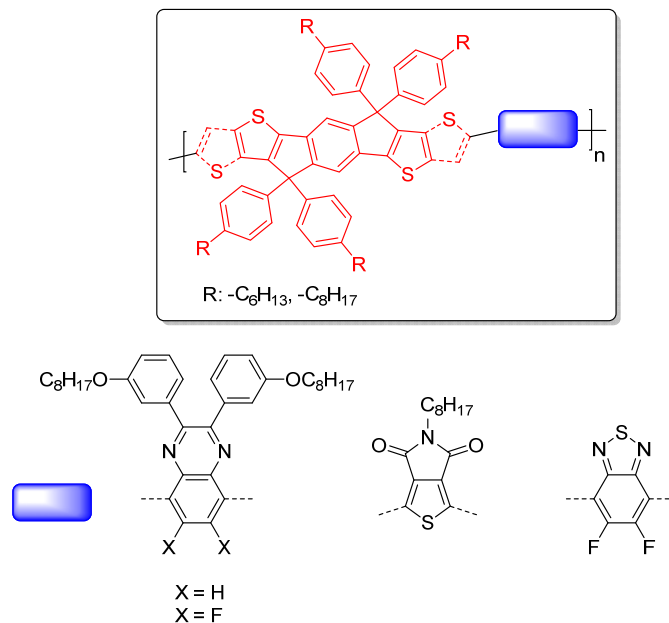


Figure 1: Chemical structures of the indacenodithiophene and indacenodithienothiophene copolymers developed in this work.

Acknowledgment

This project has received partial funding from the European Community's Seventh Framework Programme (FP7/2007-2013) under the Grant Agreement n° 331389 project ECOCHEM

References

- [1] G. Li, R. Zhu, Y. Yang *Nature Photon.* **2012**, *6*, 153.
- [2] C. L. Chochos, S. A. Choulis, *Prog. Polym. Sci.* **2011**, *36*, 1326.
- [3] J. You, L. Dou, Z. Hong, G. Li, Y. Yang, *Prog. Polym. Sci.* **2013**, *38*, 1909.
- [4] Y. Li, K. Yao, H.-L. Yip, F.-Z. Ding, Y.-X. Xu, X. Li, Y. Chen, A. K.-Y. Jen *Adv. Funct. Mater.* **2014**, *24*, 3631-3638.
- [5] Chochos, C. L.; Singh, R.; Kim, K.; Gasparini, N.; Katsouras, A.; Kulshreshtha, C.; Gregoriou, V. G.; Keivanidis, P. E.; Ameri, T.; Brabec, C. J.; Cho, K.; Avgeropoulos, A. *Adv. Funct. Mater.* **2016**, *26*, 1840-1848.
- [6] Katsouras, A.; Gasparini, N.; Koulogiannis, C.; Spanos, M.; Ameri, T.; Brabec, C. J.; Chochos, C. L.; Avgeropoulos A. *Macromol. Rapid Commun.* **2015**, *36*, 1778-1797.
- [7] Gasparini, N.; Katsouras, A.; Prodromidis, M. I.; Avgeropoulos, A.; Baran, D.; Salvador, M.; Fladischer, S.; Spiecker, E.; Chochos, C. L.; Ameri, T.; Brabec, C. J. *Adv. Funct. Mater.* **2015**, *25*, 4898-4907.

Buckling-Induced Patterning of PDMS Surfaces Through Argon Ion Bombardment

S. Pozov, G. Constantinides

¹*Research Unit for Nanostructured Materials Systems and Department of Mechanical Engineering and Materials Science and Engineering, Cyprus University of Technology, Limassol, Cyprus*

Abstract: Buckling, which relates to the onset of an elastic instability in which an in plane compressive force causes an out of plane deformation has been extensively studied within structural mechanics in an effort to avoid failure of columns or other compressively loaded elongated members. More recently, buckling has also been associated with the formation of patterns and morphological features that can either naturally occur (i.e., fingerprints) or engineered for specific applications. We here report on the formation of buckling induced wrinkling patterns on the surface of PDMS through argon ion bombardment. When argon ions are accelerated on the PDMS surface a hard thin film is generated through change in chemistry and the internal stresses generated during the thin film growth trigger the buckling instability of the surface that patterns the material with specific length characteristics. The effect of ion energy and fluence on the resulting patterns are studied using AFM, SEM and uv-vis spectrophotometry. The morphological details of the surfaces and subsequently its wetting and optical characteristics of the surface can be controlled indirectly through the ion characteristics, with potential applications of the produced surfaces in antibacterial coatings, energy harvesting materials, microfluidic devices, etc.

Surface-induced alignment of liquid crystalline dendrimers

Z. G. Workineh, A. G. Vanakaras

Department of Materials Science, University of Patras, 26504 Patras, Greece

Dendrimers are a class of monodisperse polymeric macromolecules with a well-defined and highly branched three-dimensional architecture. Liquid crystalline dendrimers (LCDrs) are usually derived through functionalization of common dendrimers with low molar mass liquid crystal molecules (mesogens) [1, 2]. The ability to control the macroscopic alignment of LCDrs is a key factor for many of their potential applications. For low molar mass liquid crystals (LC), robust and well-established techniques/materials are available for the precise alignment of the LC medium through surface-mediated interactions. Through controlling the surface-LC interactions, usually by means of chemical and/or mechanical treatment of the substrate, a variety of alignments (homeotropic, planar, tilted, etc.) of the LC medium with respect to the substrate are possible. The situation in LCDrs is quite different due to the rather strong positional/orientational constraints between the interconnected mesogenic units of the same dendrimer. Therefore the surface-mediated alignment in the case of LCDrs is determined by the fine interplay between the anchoring driven alignment of the mesogenic units and by the constraints the dendritic architecture imposes on them. We introduce a tractable coarse-grained force field for the inter-dendritic and the dendrimer-substrate interactions [3]. Based on this we present results from Monte Carlo simulations of LCDrs i) adsorbed on flat, impenetrable aligning substrates and ii) confined into nanopores of different geometries. Depending on the anchoring constraints to the mesogenic units of the LCDr and on temperature, a variety of stable ordered LCDr states, differing in their topology, are observed and analysed. The influence of the dendritic generation and core functionality on the surface-induced ordering of the LCDrs are examined.

References

- [1] Donnio, B.; Guillon, D. Liquid Crystalline Dendrimers and Polypedes. In *Supramolecular Polymers Polymeric Betains Oligomers*; 2006; pp 45–155.
- [2] Guerra, S.; Nguyen, T. L. A.; Furrer, J.; Nierengarten, J.-F.; Barberá, J.; Deschenaux, R., *Macromolecules*, **49**(9), 3222–3231 (2016).
- [2] Z. G. Workineh and A. G. Vanakaras, *Polymers*, **6**, 2082-2099 (2014); *Liquid Crystals*, **43**:7, 944-954 (2016); *J. Phys.: Condens. Matter*, **28** 115002 (2016).

Liquid Crystalline Behaviour of Dimeric Systems Exhibiting Two Nematic Phases

E. Ramou^{1,2}, J. Hussey¹, C. Welch¹, P.K. Karahaliou², G.H. Mehl¹

¹Department of Chemistry, University of Hull, HU6 7RX, UK

²Department of Physics, University of Patras, 26504 Patras, Greece

The uniaxial, apolar, achiral nematic phase (N), is the simplest and most widely studied liquid crystalline phase. Within this phase the molecules possess orientational order along a unique macroscopic axis, called the director and being an axis of full rotational symmetry, and no positional order. Recently, a fascinating new nematic phase was detected experimentally in certain types of symmetric liquid crystalline dimers with odd carbon-number alkyl spacers, upon cooling from the conventional nematic phase [1-4]. Under the microscope this low temperature phase displays features of a layered smectic-type structure, however X-ray investigations confirm its nematic character [1]. More interestingly, chiral domain formation associated with a very fast electro-optic response, has also been found in the new phase, although the constituent molecules are nonchiral [1,2]. Current investigations on the commonly termed Nx/tb phase are receiving close review in the field of liquid crystals, as the new mesophase is not yet fully characterized and its structure is a highly debated topic in the literature [5].

In the current contribution we investigate the mesomorphic behaviour of a new class of dimeric difluoroterphenyl systems that undergo the N-Nx/tb phase transition and exhibit a smectic phase at lower temperatures. Mixtures, of the difluoroterphenyl dimers with their corresponding monomer are also studied in order to gain insight on the stability of the phases upon adding a dopant that lacks the Nx/tb. The physical and structural characterization of the new materials are probed via complimentary characterization techniques, such as Polarizing Optical Microscopy (POM), Differential Scanning Calorimetry (DSC) and X-ray Diffraction (XRD). The results are discussed in connection to the rationalization of the structure-properties relationships that prevail the nature of the Nx/tb phase.

References

- [1] V. Borshch, et al., Nat. Commun., 4, 2635, (2013)
- [2] V. Panov, et al., Phys. Rev. Lett., 105, 167801, (2010)
- [3] E. Ramou, et al., Soft Matter, 12, 888, (2016)
- [4] Z. Ahmed, et al., RSC Adv., 5, 93513, (2015)
- [5] A.G. Vanakaras and D.J. Photinos, Soft Matter, 12, 2208, (2016)

E.R. acknowledges support by the EU through the ERASMUS+ Placements programme.

A simple route to increase electrical conductivity of Graphene/CNTs thin films by compression

Apostolos Koutsioukis, Vasilios Georgakilas
Department of Materials Science, University of Patras, 26505 Rio (Greece)

Abstract: Electrical conductivity is one of the most important and attractive properties of carbon nanoallotropes with graphenic structure. We demonstrate here a great improvement in the electrical conductivity of carbon nanostructured thin films by compression or polishing. It is shown that the sheet resistance of compressed thin films of carbon nanomaterials or hybrids is remarkably decreased in comparison with the as deposited films. The number and efficiency of the interconnections, the distance between the nanostructures as well as their orientation are highly altered by the compression favouring the electrical conductivity of the compressed samples.

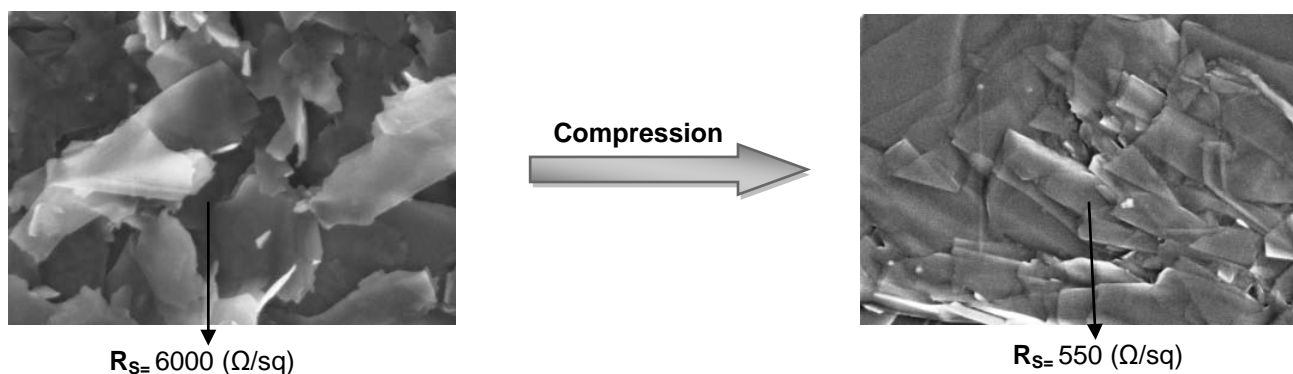


Figure: Characteristic SEM images of the pristine graphene thin films before (left) and after compression (right) and the impact of this on their sheet resistance.

SESSION 8

Tuesday 20 September 2016, 17:15-19:00

*Surfaces, Interfaces and
Nanomaterials II*

Numerical Study of the effect of the Antiferromagnetic matrix on the Exchange Bias properties of diluted nanoparticle system

G. Margaris¹, K. N. Trohidou¹, M. Vasilakaki¹, D. Peddis², D. Fiorani²

¹ *Institute of Nanoscience and Nanotechnology, NCSR Demokritos, Aghia Paraskevi, Greece*

² *Institute of Structure of Matter, Area della Ricerca, Viaalaria km 29,500, P.B. 10-00016, Monterotondo Scalo, Roma, Italy*

Abstract: Monte Carlo simulations of the static and dynamical magnetic properties of fine ferromagnetic (Co) particles dispersed (at 5 % volume filling fraction) in an antiferromagnetic film matrix (Mn) are reported and compared with the experimental results [1,2]. The model, assuming Co nanoparticles randomly placed on the nodes of a simple cubic lattice, accounts the significant degree of Co-Mn alloying, as shown by EXAFS measurements, responsible for a very small magnitude of the Co moment, as shown by XMCD measurements, and the Mn granularity, as shown by X-ray diffraction measurements, responsible for uncompensated magnetic moments in the antiferromagnetic matrix. Simulations replicate the zero-field-cooled and field-cooled low field susceptibility curves, providing an evidence of super spinglass freezing (SSG), the stop-and-wait effect in the ZFC curve (memory effect) and the observed Exchange Bias behaviour.

The results indicate that the observed super spinglass features in such a diluted nanoparticle system, unlike the dense ones as in usual SSGs, come from the interplay of dipolar interparticle interactions, transmitted through the uncompensated grain moments of the matrix which are also exchange coupled, and the non-uniform exchange interactions at the Co/Mn interface.

[1] M. Vasilakaki, KN Trohidou, D. Peddis, D. Fiorani, R. Mathieu, M. Hudl, P. Nordblad, C. Binns, S. Baker, *Phys. Rev. B (Rapid. Com.)*, 88 (2013) 140402 (pp 5)

[2] C. Binns, N. Domingo, A. M. Testa, D. Fiorani, K. N. Trohidou, M. Vasilakaki, J. A. Blackman, A. M. Asaduzzaman, S. Baker, M. Roy, and D. Peddis, *J. Phys.: Condens. Matter* 22, 436005 (2010).

Modeling domain wall velocity in bi-magnetic nanowires

A. Patsopoulos¹, D. Kechrakos², O. Chubykalo-Fesenko³,
 C. Simserides¹ and G. P. Triberis¹

¹Department of Physics, University of Athens, Zografos, 15784 Athens, Greece

²Department of Education, School of Pedagogical & Technological Education (ASPETE), N.
 Heraklion, 14121 Athens, Greece

³Instituto de Ciencia de Materiales de Madrid, CSIC, Cantoblanco, 28049 Madrid, Spain

We study the magnetic properties of exchange biased cylindrical nanowires (NW) composed of a ferromagnetic core and an antiferromagnetic shell, using atomistic modeling (Fig.1a) and the Metropolis Monte Carlo simulation algorithm. Emphasis is given to the interplay between magnetostatics and exchange biasing. The magnetic structure is described within a classical Heisenberg Hamiltonian on a simple cubic lattice with uniaxial anisotropy (K_{FM} , K_{AF}) and dipolar interactions (g). Our findings demonstrate that core-shell FM-AF nanowires exhibit an increase the coercivity (H_c) with length, reaching a saturation value (H_{c0}) that depends on the dipolar strength. The bias field (H_b) increases with wire length and reaches a saturation value (H_{b0}) whose behaviour depends on the competition between dipolar strength and anisotropy (K_{FM}). In particular, in nanowires with a hard FM core ($K_{FM}/g > 10$) the saturation value of H_{b0} increases with dipolar strength, while the opposite trend is observed when the FM core is soft ($K_{FM}/g \sim 1$). A systematic study of the time evolution of the magnetization profile demonstrated that magnetization reversal of FM-AF NWs proceeds by nucleation of a pair of domain walls (DW) at the opposite ends of the wire, propagation of the DWs towards the centre of the wire with constant and opposite velocities (Fig.1b) and eventually, their merge. The DW velocity is shown to decrease with increasing dipolar strength. Interestingly, the presence of the AF shell modifies the DW dynamics in two aspects: First, the DW nucleation process is delayed and the coherent rotation mechanism is restored for NWs with moderate dipolar strengths (anisotropic FM). Second, at a given reversing field, the DW velocity is higher in the FM-AF nanowire than their FM counterpart. The implications of our results to potential applications of magnetic nanowires are discussed.

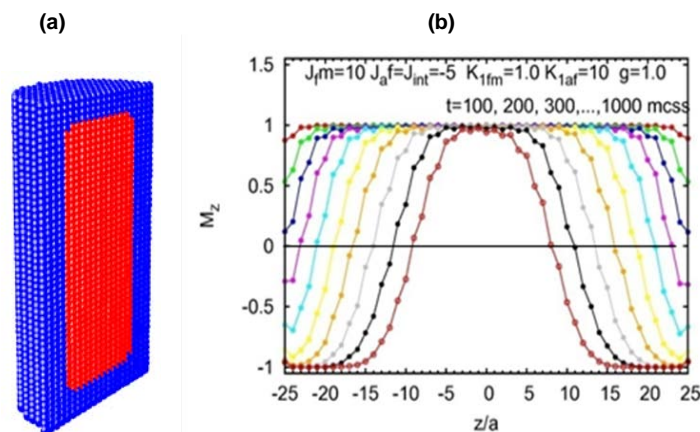


Figure 1 (a) Atomistic description of a cylindrical bi-magnetic nanowire with FM core – AF shell morphology. (b) Typical time evolution of the magnetization profile along the axis a bi-magnetic nanowire ($L_{FM}=50a$, $t_{AF}=3a$) shows nucleation and propagation of a pair of domain walls with constant velocity towards the center of the nanowire.

Acknowledgment. One of us (DK) acknowledges financial support by the Special Account for Research of ASPETE through project "Strengthening of research of faculty members of ASPETE"

Structural and magnetic properties of $L1_0$ FePt/{MgO, W, or Pt }/ $L1_0$ FePt trilayers

A. Kaidatzis¹, G. Giannopoulos¹, V. Psycharis¹, J. M. García-Martín², G. Varvaro³, A.M. Testa³, and D. Niarchos¹

¹ Institute of Nanoscience and Nanotechnology, NCSR Demokritos, Athens, Greece

² Instituto de Microelectrónica de Madrid, CNM-CSIC, Tres Cantos, Madrid, Spain

³ ISM-CNR, Area della Ricerca RM1, P.B. 10-00015, Monterotondo Scalo, Roma, Italy

Abstract: Nowadays there is an urgent need for enhancing data storage capacity of hard disk drives due to the rapid increase of digital data volume produced worldwide. New effective approaches are required to push the recording areal density beyond the limit of 1 Tbit/in² of state-of-art hard disk drives. A promising alternative is 3D-magnetic recording, where stacking magnetic layers with different magnetic properties are used [1].

In this work we report on the morpho-structural and magnetic properties of FePt/interlayer (MgO, Pt or W) /FePt magnetron sputtered trilayers, as a base structure towards 3D magnetic recording systems. The stack is grown on an MgO (100) substrate and consists of two magnetically hard FePt layers with a thickness of 20 and 10 nm separated by an interlayer of variable thickness (5 up to 50 nm). Fig 1a summarizes the coercivity for all MgO, W or Pt interlayer samples; the layers seem to be coupled even at 20 nm of MgO or W interlayer thickness. However, at 5 nm interlayer thickness, hysteresis loops for W or MgO interlayers are those of a film stack of partially coupled ferromagnetic layers (Figure 1b), whereas a fully decoupled magnetic trilayer is obtained for a Pt interlayer, in agreement to previous reports [2] and also supported by magnetic force microscopy imaging. Finally, electron diffraction patterns and dark field images analysis indicate that most of FePt grains grow in the $L1_0$ phase with the (001) planes parallel to the substrate and the MgO interlayer grows oriented as the substrate.

ACKNOWLEDGEMENTS

Funding from the E.C. is acknowledged (Grant No. 318144 and 280670) & MINECO (MAT2014-59772-C2-1-P)

REFERENCES

[1] N. Amos *et al.* PLoS ONE **7** e40134 (2012)

[2] A. P. Mihai *et al.* Appl. Phys. Lett. **94** 122509 (2009); O. P. Pavlova *et al.* Appl. Surf. Sci. **266** 100 (2013)

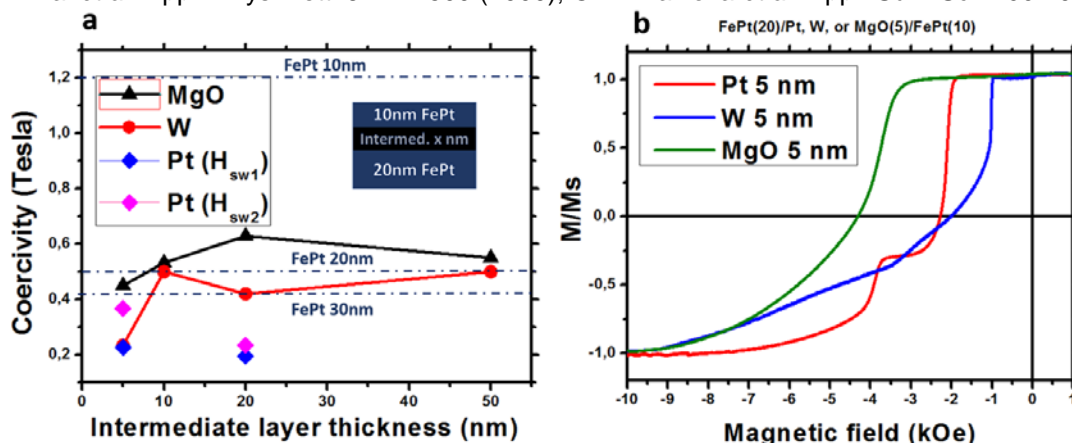


Figure 1a. Magnetic coercivity of the studied trilayers as a function of the interlayer thickness. **b.** Hysteresis loops of FePt (10 nm)/ W, MgO, Pt (5 nm)/FePt (20nm) samples. In the case of Pt interlayer, the magnetic layers are decoupled, whereas in trilayers with MgO and W a coupling behaviour was observed.

Combinatorial sputtering method: Producing L10-FeNi films with coercivity in excess of 1 kOe

G. Giannopoulos, A. Kaidatzis, V. Psycharis, and D. Niarchos

Institute of Nanoscience and Nanotechnology, NCSR Demokritos, Athens, Greece

Abstract: Combinatorial sputtering technique was used to deposit and characterize alloys with different stoichiometries [1]. This approach is a revolutionary step forward in the development of new materials. It involves the development and application of new tools for systematic and parallel synthesis and characterization of binary and ternary systems, thus being a very effective way to explore variable alloys stoichiometry.

L10-type magnetic compounds, including FeNi, possess promising technical magnetic properties of both high magnetization and large magnetocrystalline anisotropy energy and thus offer potential in replacing rare earth permanent magnets in some applications. FeNi estimated order-disorder transformation temperature is around 320°C, which is very low compared to the other L10-alloys. This results in very low diffusion of Fe and Ni atoms and makes the transformation extremely slow. This transformation can be enhanced either by the creation of vacancies, core-shell FeNi/L10-AuCu nanoparticles [2], or in the case of thin films by a strain mediated process [3].

In this work, we have employed a combinatorial sputtering process in order to study the conditions of fabricating the L10-FeNi phase and measure its magnetic properties. We have used Si(100) 100 mm wafer substrates and deposited multilayers of the following type: Si/Cr(10 nm)/Cu₃Au(70 nm)/combi-CuAuNi/NiFe(40 nm), where combi-CuAuNi is a compositional spread layer of various stoichiometries deposited using combinatorial sputtering, to match the lattice constants of the L10-FeNi. The final deposition of FeNi was performed at 200°C by co-sputtering Fe and Ni to a stoichiometry of 50/50 at%. We perform magnetic properties mapping of the multilayer by means of high-throughput polar Kerr effect magnetometry and we find that the coercivity increases from 0.3 kOe to 1 kOe as the Au content of the combinatorial interlayer decreases.

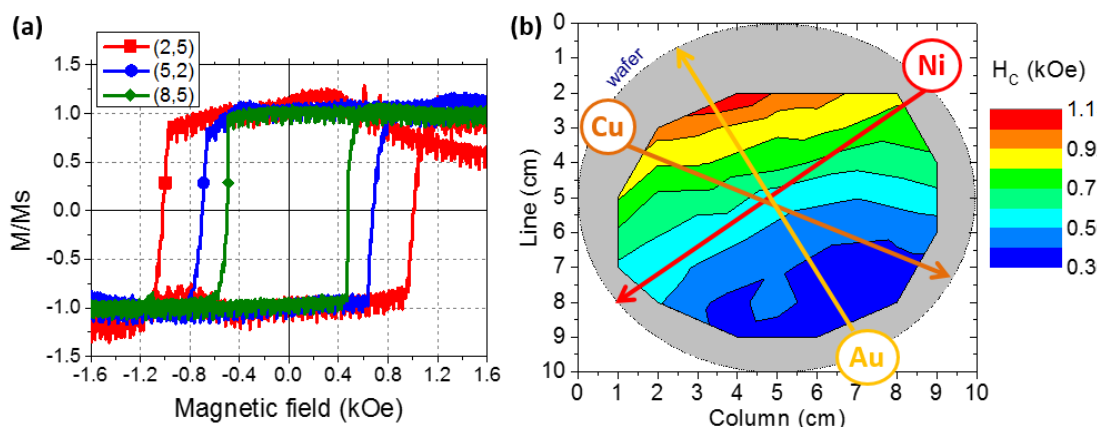


Figure 1 a. Representative hysteresis loops obtained by polar Kerr effect Magnetometry b. Map of magnetic coercivity across the wafer.

ACKNOWLEDGEMENTS

Funding from the E.C. is acknowledged (686056-NOVAMAG and 691235-INAPEM)

REFERENCES

- [1] X.-D. Xiang, X.-D. Sun et al, *Science* (1995) p. 1738
- [2] M. Gong et al., *Chem. Mater.*, **2015** (22) 7795
- [3] T. Kojima et al., *J. Phys.: Cond. Mat.* **26** (2014) 064207

Electrical and structural characterization of memory devices with laser fabricated nanocrystals

L. Kastanis¹, J.L. Spear², A. Angelou³, N. Kalfagiannis², Ch. Sargentis¹, D.C. Koutsogeorgis², E.K. Evangelou³, D. Tsamakis¹

¹*School of Electrical & Computer Eng., NTUA, 9 Iroon Polytechniou Str., Zografou Campus, 15780 Attiki, Greece.*

²*School of Science and Technology, Nottingham Trent University, Clifton Lane, Nottingham, NG11 8NS, UK*

³*Department of Physics, University of Ioannina, Panepistimioupolis, 451 10 Ioannina, Greece*

Abstract

Nonvolatile memory devices with metal nanocrystals (NCs) have the advantages of higher programming/erasing efficiency, lower operating voltage, wide work function and larger charge capacity. Metal NCs with high work-function such as Platinum (Pt) and gold (Au) are preferable materials [1] due to the deep voltage wells they create. A major challenge in manufacturing NCs is particles with small dimensions uniformity and high density. Fabrication of NCs via Laser Annealing (LA), is an alternative and promising technique because of its versatility and ease of application, offers a high degree of control of metal NC formation as well as advantages of defect minimization in the oxide or at the NC oxide interfaces [2,3]. In this work we present the results concerning electrical and structural characterization of memory devices consisting of n-Si/SiO₂/Y₂O₃/Al incorporating Au NCs and their characteristics. Laser annealing with a KrF laser was used to obtain uniformly spaced and small in dimensions (5-20 nm) Au NCs.

Capacitance vs Voltage (C-V), Conductance vs Voltage (G-V) and Current vs Voltage (I-V) measurements of n-Si/SiO₂/Au(NCs)/Y₂O₃/Al devices show a large memory window and a reduced leakage current.

Our results indicate that laser annealing leads to MOHOS-type flash memory devices with good electrical and structural characteristics due to the creation of high quality and high homogeneity metal NCs.

References

- [1] ChSargentis et al., SuperlatticeMicrost 44, 483-488 (2008)
- [2] J Y Yang et al., Current Applied Physics 7, 147-150 (2007)
- [3] A Siozios et al., Nano Lett. 12 (1), 259-263 (2012)

On the role of entropy in the emergence of chirality in systems of achiral particles.

F. Priftis, A. G. Vanakaras

Department of Materials Science, University of Patras, 26504 Patras, Greece

Spontaneous symmetry breaking is a fundamental concept that represents an underlying mechanism for a number of physical phenomena including the emergence of spontaneous self-organization in soft and condensed matter as well as in colloidal suspensions. When the constituent particles are chiral the self-organized ordered structures exhibits macroscopic chirality which, in soft matter liquid crystalline systems, expressed in the form of spontaneously twisted orientationally ordered states, known as cholesteric liquid crystals, or, in other cases in the form of helical nanofilaments. In this work we focus on the intriguing phenomenon of the emergence of macroscopic chirality in systems composed of achiral particles. We study, using molecular theory and computational experiments, the basic question: is it possible a spontaneous chiral symmetry breaking in systems of rigid, sterically interacting achiral particles?

Motivated by recent experimental studies on the self-organization of micron-sized equilateral triangular particles confined in two dimensions [1] we have performed large scale Monte Carlo simulations to study the order-disorder transitions of sterically interacting equilateral triangles [2]. This system, despite its simplicity exhibits a rich phase polymorphism. Besides the isotropic state the system upon compression exhibits a liquid crystalline phase that has quasi-long-range six-fold orientational order yet only short-range positional order. Upon further compression the liquid crystal phase continuously transform to a hexagonal close-packed crystal structure. Surprisingly, further compression leads, through a second order phase transition, to a novel crystalline phase where the triangles rotate collectively either in clockwise or anti-clockwise direction with respect to a fixed lattice vector. To analyze the structure of the various phases of the system we have introduced a number of appropriate multi-particle orientational/positional correlation functions that allow the study of the various phases both locally and on the macroscopic level. We discuss the entropic origins of the chiral symmetry breaking in this system and propose appropriate order parameters for the quantification of the degree of chiral ordering. Finally we discuss the role of the molecular shape in the ectopically driven self-sorting of the particles into chiral superstructures.

[1] K. Zhao, R. Bruinsma, and T. G. Mason, *Nature Communications*. 3, 801 (2012).

[2] F. Priftis, MSc Thesis (<http://hdl.handle.net/10889/9199>), Department of Materials Science, University of Patras, (2015).

A DFT study on the interface of prototype organic semiconductors and the silver surface

A. Stamateri¹, G. Volonakis², and S. Logothetidis¹

¹*Department of Physics, Laboratory for Thin Films Nanosystems and Nanometrology, LTFN, Aristotle University of Thessaloniki, GR-54124 Thessaloniki, Greece*

²*Department of Materials, University of Oxford, Parks Road, Oxford OX1 3PH, United Kingdom*

Abstract:

One of the most important factors that affect the performance and efficiency of organic electronic devices are the metal/organic interfaces. In this work, we employ first-principles Density Functional Theory (DFT) calculations in order to investigate the structural and probe the electronic properties of prototype organic materials (i.e. P3HT and PC₆₀BM) in the proximity of Ag. First, we examine the energetic stability of various conformations for the adsorption of PC₆₀BM on Ag(111) surface, depending on the position of PC₆₀BM's functional group. We also investigate the preference on the coverage rate of PC₆₀BM on the silver surface. Furthermore, we calculate the charge rearrangement at the interface and the respective interfacial dipole that is formed due to adsorption. We use the interfacial dipole, together with the intrinsic dipole of the adsorbed molecule to assess the total electrostatic potential step across the system. For the case of crystalline P3HT, the preferred adsorbed geometry is with the thiophene backbone parallel to the Ag surface. Results presented here, show that by controlling the adsorption details at the metal/organic interface, the charge rearrangement is modified and influences the energy level alignment of the different layers of the device.

SESSION 9

Wednesday 21 September 2016, 9:30-11:25

*Strongly correlated systems and
magnetism*

Future concepts and materials for magnetic data storage

Manfred Albrecht

Institute of Physics, University of Augsburg, D-86159 Augsburg, Germany

Due to the increasing demand in high-density recording media, magnetic thin films with high magnetic anisotropy are widely studied in order to overcome the superparamagnetic effect. To fulfill the requirements of thermal stability, hard magnetic alloys, i.e. FePt alloys in the $L1_0$ phase are promising candidates as storage layer. However, owing to the large magnetic anisotropy, the magnetic field required to reverse the magnetization of the media may become higher than the field provided by a conventional recording head. To solve this, so-called writeability issue, the concepts of exchange-coupled composite (ECC) media as well as bit patterned media based on $L1_0$ FePt were suggested, which will be discussed in this presentation.

Furthermore, ultrafast magnetization switching is at the heart of both modern information storage technology and fundamental science. In this regard, it was recently observed that ultra-fast magnetization reversal processes can be induced by circularly polarized laser pulses in amorphous ferrimagnetic GdFeCo alloy thin films [1]. This novel observation resulted in a broad range of exciting and challenging fundamental questions, and may enable new applications based on ultra-fast spintronics. An overview of our activities on all-optical switching in amorphous ferrimagnetic Tb-Fe alloy films [2-4] (see Fig. 1) will be presented.

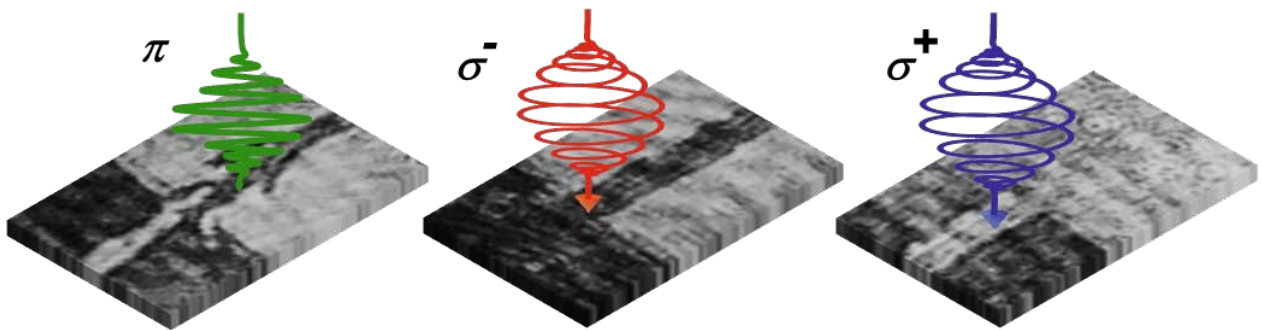


Fig. 1: *Demonstration of helicity dependent all-optical switching (AOS) in amorphous $Tb_{30}Fe_{70}$ thin films: The magnetization perpendicular to the sample surface is imaged by the Faraday effect. In the gray area the magnetization is pointing out of the sample plane ($M+$), while in the black area magnetization is pointing into the sample plane ($M-$). Linear polarization (π) results in formation of a disordered multidomain state. Left circularly polarized (σ^-) laser pulses cause a magnetization reversal, visible as a dark stripe ($M-$) written in the gray area ($M+$). Right circularly polarized (σ^+) laser pulses erase the written area and write a gray stripe ($M+$) into the dark region.*

- [1] C. D. Stanciu et al., Phys. Rev. Lett. 99, 047601 (2007).
- [2] B. Hebler et al., Frontiers in Materials 3, 8 (2016).
- [3] A. Hassdenteufel et al., Adv. Mater. 25, 3122 (2013).
- [4] A. Hassdenteufel et al., Phys. Rev. B 91, 104431 (2015).

Thermal fluctuations in artificial spin ice

Vassilios Kapaklis¹

¹*Department of Physics and Astronomy, Uppsala University, Box 516, SE-75120,
Uppsala, Sweden*

Abstract:

Magnetism has provided a fertile test bed for physical models, such as the Heisenberg and Ising models. Most of these investigations have focused on solid materials and relate to their atomic properties such as the atomic magnetic moments and their interactions. Recently, advances in nanotechnology have enabled the controlled patterning of nano-sized magnetic particles, which can be arranged in extended lattices. Tailoring the geometry and the magnetic material of these lattices, the magnetic interactions and magnetization reversal energy barriers can be tuned [1,2]. This enables interesting interaction schemes to be examined on adjustable length and energy scales. As a result such nano-magnetic systems represent an ideal playground for the study of physical model systems, being facilitated by direct magnetic imaging techniques [3]. One particularly interesting case is that of systems exhibiting frustration, where competing interactions cannot be simultaneously satisfied. This results in a degeneracy of the ground state and intricate thermodynamic properties [1-4]. An archetypical frustrated physical system is water ice. Similar physics can be mirrored in nano-magnetic arrays, by tuning the arrangement of neighboring magnetic islands, referred to as artificial spin ice. Thermal excitations in such systems resemble magnetic monopoles [4]. In this presentation key concepts related to nano-magnetism and artificial spin ice will be introduced and discussed, along with recent experimental and theoretical developments.

[1] V. Kapaklis et al., *New J. Phys.* 14, 035009 (2012).

[2] U. B. Arnalds et al., *Appl. Phys. Lett.* 105, 042409 (2014).

[3] A. Farhan et al., *Nature Physics* 9, 375 (2013).

[4] V. Kapaklis et al., *Nature Nanotech* 9, 514 (2014).

Structure and magnet properties of $R_{1-x}Zr_xFe_{10}Si_2$ alloys with $R = Nd, Sm$

M.Gjoka¹, V. Psycharis¹, Ch. Sarafidis², E. Devlin¹, D. Niarchos¹ and G. Hadjipanayis³

¹ Institute of Nanoscience and Nanomaterials, NCSR Demokritos, Athens, Greece

² Department of Physics, Aristotle University of Thessaloniki, 54124 Thessaloniki, Greece

³ Department of Physics and Astronomy, University of Delaware, Newark, De, USA

The tetragonal $R(Fe,T)_{12}$ alloys, where R is a rare earth and T is a stabilizing transition metal, are promising candidates for permanent magnet alloys due to their appropriate magnetic properties. Recently there is a resurgence of interest in the formation of the $R(Fe,T)_{12}$ structure, replacing now the rare-earth with Zr, which has produced very interesting results [1].

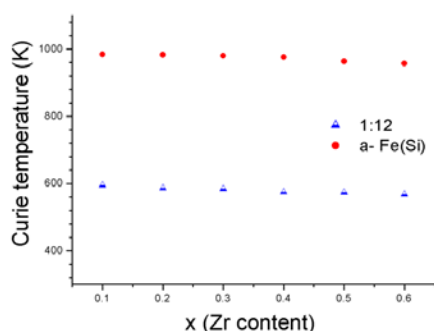


Fig.1 Dependence of Curie temperature from Zr for $Sm_{1-x}Zr_xFe_{10}Si_2$

Alloys with nominal composition $R_{1-x}Zr_xFe_{10}Si_2$, with $0.1 \leq x \leq 0.8$ ($R=Sm, Nd$), were prepared by arc-melting. Furthermore, rapidly solidified ribbons were prepared for the series $Sm_{1-x}Zr_xFe_{10}Si_2$ ($x=0.2-0.6$) using melt-spinning with wheel speeds of $15-55 \text{ ms}^{-1}$ and then annealed in the interval 773-1173K.

Structural and magnetic characterization of these alloys has been carried out using X-ray diffraction, Mössbauer spectroscopy and thermomagnetic analysis (Fig. 1). The alloys' microstructure has been investigated using a scanning electron microscope (SEM) with EDAX analysis.

After arc-melting and without further annealing, the formation of the tetragonal $ThMn_{12}$ -type structure with Zr substitution for Nd and $x \geq 0.3$ has been observed. For $x < 0.3$ the hexagonal $CaCu_5$ -type structure is formed. The Curie temperature of 1:12 phase decreases linearly with Zr substitution from 574K for $x=0.1$ to 558K for $x=0.8$. The saturation magnetization increases from

111 emu/g ($x=0.1$) to 145 emu/gr ($x=0.4$), and then decreases for $x > 0.4$, the anisotropy field following the same trend. This study contributes to the search for magnetic phases, lean or free of critical raw materials, suitable for the production of permanent magnets.

1. A. Gabay and G. C. Hadjipanayis, J. Alloys Compds. 657 (2016) 133-137

Arranging at the nanoscale: Effect on magnetic particle hyperthermia

E. Myrovali¹, N. Maniotis¹, A. Makridis¹, A. Terzopoulou¹, V. Ntomprougkidis¹, K. Simeonidis¹, D. Sakellari¹, O. Kalogirou¹, T. Samaras¹, R. Salikhov², U. Wiedwald², M. Spasova², M. Farle² and M. Angelakeris¹

¹Physics Department, Aristotle University of Thessaloniki, Thessaloniki, 54124, Greece

²Fakultät für Physik and Center for Nanointegration Duisburg-Essen (CeNIDE), Universität Duisburg-Essen, 47048, Germany

Magnetic particle hyperthermia is a synergistic cancer treatment technique that takes advantage of heat released by magnetic nanoparticles (MNPs) when they are exposed in an alternating magnetic field and may lead cancer cells either to a severe thermal shock or even induce their death. The heating efficiency of MNPs is quantified by the specific loss power (SLP). The aim of this work is to provide a deeper understanding on the evolution of Fe₃O₄ nanoparticles field driven orientation within an agarose gel network and its consequences on magnetic hyperthermia efficiency. We examined a 10 nm and a 40 nm magnetite nanoparticle system with the former being superparamagnetic and the latter ferromagnetic and fully successful in chain array formation. For this purpose, specimens were prepared by dispersing nanoparticles in an agarose solution followed by a natural gelation procedure under static magnetic field. The success of chain formation for varying particle concentration and agarose gel content was evaluated by electron microscopy observations while molecular dynamics simulations successfully represented experimental findings (as shown in Figure 1). Eventually, chain formation results to increased heating efficiency as quantified experimentally in calorimetric experiments and theoretically correlated with magnetic features via Stoner-Wohlfarth model extended to include the temperature and frequency dependence of the coercive field. The chain formation due to dipolar interactions results to uniaxial anisotropy evolution and directly influences collective magnetic features as verified by VSM and FMR measurements. Magnetic heating efficiency strongly correlated with collective magnetic features. By adequate selection of nanoparticles and colloidal parameters, the formation of oriented arrangements may be easily achieved, fine-tuned and result to enhanced magnetic particle hyperthermia efficiency.

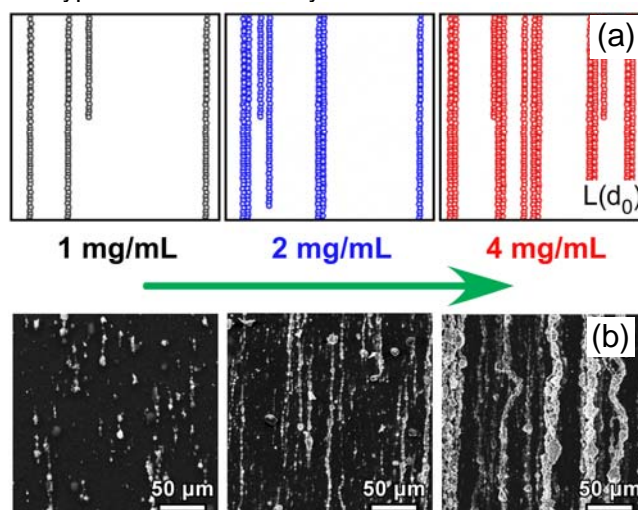


Figure 1: Results from Molecular Dynamics simulations of chains formation of 40 nm MNPs for various concentration values. (a) Chain formation of MNPs in an external field of 40 mT. The dimensions of our 2D computational space were $L(d_0) \times L(d_0) = (80d_0)^2$ where d_0 is the MNPs diameter of 40 nm. The number of MNPs was set to 380, 760, 1520 for the concentrations of 1, 2 and 4 mg/mL, respectively. (b) Corresponding experimental SEM images for three MNPs concentrations.

Dancing with magnetism: An attempt to control cell fate

A. Makridis¹, K. Spyridopoulou², N. Karypidou¹, N. Maniotis¹, E. Myrovali¹, T. Samaras¹, M. Angelakeris¹, K. Chlichlia², O. Kalogirou¹

¹Department of Physics, Aristotle University of Thessaloniki, 54124 Thessaloniki, Greece

²Department of Molecular Biology and Genetics, Democritus University of Thrace, Alexandroupolis, Greece

Mechanical or magneto-mechanical stress applied to the cell membrane, cytoskeleton, or organelles plays a very important role in crucial intracellular processes. In this work, we examine both experimentally and theoretically how a variable either in frequency (0-20 Hz) and/or in amplitude (up to 200 mT) magnetic field dictates magnetic nanoparticles' (MNPs) movements within a cellular environment and how these "dancing" modes affect cell fate. We present here a versatile device and its principle of operation affecting cell growth via mechanical forces exerted on cells during MNPs dancing movements as dictated by the external magnetic field gradients. A prototype 3D printout of a polymer rotating holder (Figure 1) was designed and manufactured. Its operation is based on a DC rotating motor at variable voltage resulting in tunable rotation frequency and in unique magnetic field patterns by different (in size, shape, magnetic force: Fig1c)ⁱ NdFeB block magnets placed in the slots of a rotating disk (Figs: 1d, 1e). To study, how cells respond to mechanical forces exerted on them during the MNPs "dancing" modes, we applied variable frequency, amplitude and field gradients to HT29 (human colorectal adenocarcinoma) cells incubated initially with commercially available MNPs ferrofluids (Chemicell GmbHⁱⁱ) consisting of an aqueous dispersion of magnetic iron oxides with average hydrodynamic diameters of 100 nm or 200 nm. Such magneto-mechanical effects mediated in HT29 cells generate coordinated cellular responses in both local biochemistry and higher-order biological processes leading to substantial variation on cell proliferation and viability which are strictly related to the applied forces induced by the generated magnetic field gradients as shown in Figure 2.

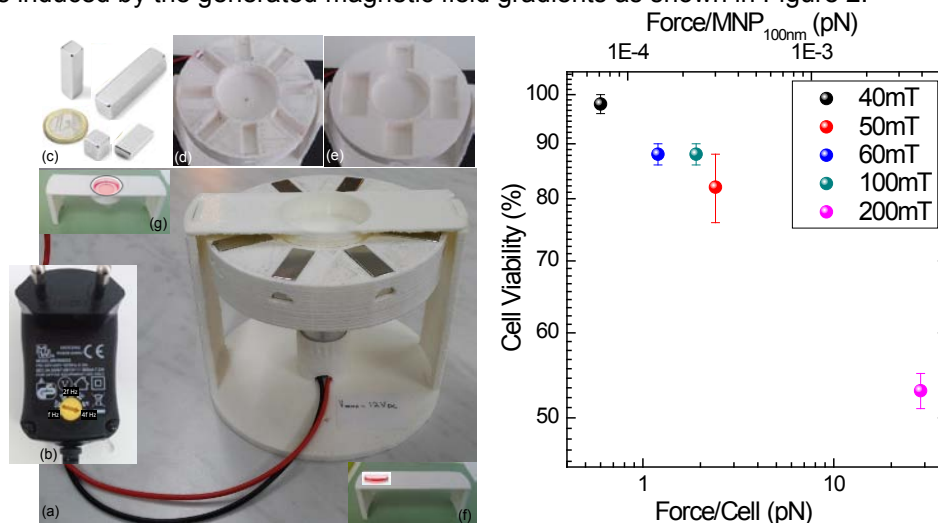


Figure 1

Figure 2

Figure 1: (a) 3D polymer printout rotating holder for static, alternating or rotating magnetic field penetration of cell samples (b) frequency adjustment of AC field (c) series of block magnets for variable magnetic field configurations (magnetic flux, axial components and gradient fields) (d), (e) Magnetic array setups to create variable magnetic flux modes in sample region. (f), (g) support tables for cell samples. **Figure 2:** Cell viability dependence on maximum forces extracted from a static external field on 100 nm magnetic nanoparticles (top) and from magnetic nanoparticles on cells (down) with magnetic flux density magnitudes in color scale per force.

ⁱ <http://www.supermagnete.de/eng/block-magnets-neodymium>

ⁱⁱ <http://www.chemicell.com/products/magneticfluorescent/index.html>

SESSION 10

Wednesday 21 September 2016, 12:00-13:15

Biomaterials

Engineering biomaterials for tissue engineering with controlled immunomodulation

M. Chatzinikolaidou^{1,2}, M. Kaliva^{1,2}, L. Papadimitriou^{1,2}, A. Georgopoulou^{1,2},
E. Mygdali², M. Vamvakaki^{1,2}

¹*IESL-FORTH, Heraklio, Greece*

²*Dept. of Materials Science and Technology, University of Crete, P.O. Box 2208,
71003 Heraklio, Greece*

Biodegradable biomaterial scaffolds are useful tools to conduct tissue development. At the same time biomaterials have an impact on the host immune response. The induced immune response is essential since it can facilitate the healing process. It is therefore important to predict and promote the proper immune response after implantation. The aim of the present study is to synthesize and characterize chitosan-*grafted*-poly(ϵ -caprolactone) copolymers (CS-*g*-PCL) with PCL contents of 20 wt% and 50 wt% and evaluate (i) their immunomodulatory potential by analyzing the differentiation of primary bone marrow derived macrophages (BMDMs) cultured on copolymeric films, (ii) the osteogenic differentiation potential of pre-osteoblastic cells on copolymeric films, and (iii) the angiogenic potential of the copolymeric materials.

We have successfully synthesized novel CS-*g*-PCL copolymers and prepared thin films on glass substrates. *In vitro* experiments of BMDMs onto CS-*g*-PCL films have shown a strong cell attachment and good cell proliferation after 7 days in cell culture. The CS-*g*-PCL copolymer with the higher PCL content exhibited anti-inflammatory action on macrophages, which was attributed to their higher CS content. We demonstrate an enhanced osteogenic response of pre-osteoblastic cells on CS-*g*-PCL copolymers and a pronounced angiogenic differentiation potential of human umbilical vein endothelial cells, supporting their potential use as scaffolds in vascularized bone tissue engineering.

Monte Carlo Study of core/shell nanoparticles for enhanced hyperthermia performance

M. Vasilakaki¹, K. N. Trohidou¹, G. Margaris¹, C. Binns²

¹ *Institute of Nanoscience and Nanotechnology, NCSR Demokritos, Aghia Paraskevi, Greece*

² *Department of Physics and Astronomy, University of Leicester, Leicester LE1 7RH, UK*

Abstract: Magnetic particle hyperthermia, namely the heating dissipation of magnetic nanoparticles (NPs) when exposed to an alternating magnetic field, is a promising cancer treatment technique with minima side effects. Active research is carried out to improve hyperthermia performance of NPs. The most studied and commercially produced colloids for magnetic hyperthermia contain iron oxide NPs. Recently, it has been demonstrated experimentally that complex nanoparticles Fe/Fe₃O₄ of core/shell morphology give higher SAR values than the single-phase oxides. [1]

We investigate theoretically the mechanism of magnetic hyperthermia due to susceptibility losses (SAR) in complex ferromagnetic (FM) core/ ferrimagnetic (FiM) shell nanoparticles. We use the Monte Carlo simulations technique with the Metropolis algorithm to simulate the magnetisation behaviour of complex FM/FiM nanoparticles of different core sizes and shapes. We calculate the magnetisation and we use our results in a modified linear Néel-Brown relaxation model [2] to calculate the SAR of Fe/ Fe₃O₄ nanoparticles. Our calculations show that for all the sizes and shapes the complex FM/FiM nanoparticles give higher SAR values than the pure ferrimagnetic ones due to their higher core saturation magnetisation. Our results have the same characteristics as the available experimental data from Fe/Fe₃O₄ nanoparticles, confirming that the complex nanoparticles with core/shell morphology can optimise the heating properties for hyperthermia. We also investigate the effect of interparticle interactions on the magnetic properties of assemblies of core/shell nanoparticles using a mesoscopic model of a few spins [3] that describes efficiently the complex structure of each nanoparticle. The dipole-dipole interparticle interaction effects on the heating performance are presented for various concentrations. Our simulations show that the hyperthermia performance reduces for higher concentrations in the case of random assemblies. For NP arrays we have increase of this performance with the concentration.

1. C Binns et al. J Nanopart Res (2012) 14:1136
2. M. Vasilakaki, C. Binns and K. N. Trohidou, Nanoscale, 7, 7753-7762 (2015)
3. G. Margaris, K. N. Trohidou, J. Nogués, Adv. Mat. 24 4331 (2012)

Extra Carrier Transfer Oscillations in DNA Monomers, Dimers and Trimers

M. Tassi¹, A. Morphis¹, K. Lambropoulos¹, K. Kaklamanis¹, R. Lopp², G. Georgiadis¹, M. Theodorakou¹, M. Chatzieftheriou³, and C. Simserides¹

¹ *National and Kapodistrian University of Athens, Faculty of Physics, Department of Solid State Physics, Panepistimiopolis, Zografos, GR-15784, Athens, Greece*

² *Current Affiliation: Georg-August-Universität Göttingen, Fakultät für Physik, Friedrich-Hund-Platz 1, D-37077 Göttingen, Germany*

³ *Current Affiliation: University of Copenhagen, Niels Bohr Institute, Blegdamsvej 17, 2100 Copenhagen, Denmark*

Abstract: The study of charge transfer (CT) in biologically important molecules is recently a great scientific challenge. Specifically, CT plays a central role in DNA damage and repair [1], it might be an indicator to discriminate between pathogenic and non-pathogenic mutations at an early stage [2] and it may be used as a building block in molecular electronics [3]. We study, theoretically, CT oscillations of an extra carrier (electron or hole) in DNA monomers (base pairs), dimers and trimers. To examine such oscillations we employ two variations of the Tight-Binding (TB) approach: (I) TB I, at the base-pair level, using on-site energies of base pairs and hopping parameters between successive base pairs [4,5,6], and (II) TB II, at the single-base level, using on-site energies of bases and hopping parameters between neighboring bases. For monomers, i.e., adenine-thymine and guanine-cytosine and for dimers we also employ Real-Time Time-Dependent Density Functional Theory (RT-TDDFT). With TB II, for monomers, we predict periodic carrier oscillations with frequency $f \approx 50$ -550 THz. For dimers, TB I gives oscillations with $f \approx 0.25$ -100 THz. For trimers made of identical monomers, with TB I the frequencies are $f \approx 0.5$ -33 THz. TB I and TB II show similar frequency content, giving complementary aspects of the oscillations. RT-TDDFT also predicts oscillations in a similar range.

[1] B. Giese, *Bioorganic & Medicinal Chemistry* **14** (2006) 6139

[2] C.-T. Shih, Y.-Y. Cheng, S.A. Wells, C.-L. Hsu, R.A. Römer, *Comp. Phys. Commun.* **182** (2011) 36

[3] C.H. Wohlgamuth, M.A. McWilliams, and J.D. Slinker, *Anal.Chem.* **85** (2013) 8634

[4] C. Simserides, *Chemical Physics* **440** (2014) 31

[5] K. Lambropoulos, K. Kaklamanis, G. Georgiadis, and C. Simserides, *Ann. Phys. (Berlin)* **526** (2014) 249

[6] K. Lambropoulos, M. Chatzieftheriou, A. Morphis, K. Kaklamanis, M. Theodorakou, and C. Simserides, *Phys. Rev. E* **92** (2015) 032725

Variation of Energy Density in Thermoplastic Starch-Cellulose Microcomposites with Humidity and Temperature. A new sensing capability?

S. X. Drakopoulos¹, G. C. Psarras¹, J. Karger-Kocsis^{2,3}, Á. Kmetty^{2,3}, L. Lendvai²

¹Department of Materials Science, University of Patras, Patras 26504, Greece

²Department of Polymer Engineering, Faculty of Mechanical Engineering, Budapest University of Technology and Economics,

Műgyetem rkp. 3., H-1111 Budapest, Hungary

³MTA–BME Research Group for Composite Science and Technology, Műgyetem rkp. 3., H-1111 Budapest, Hungary

Abstract:

Thermoplastic starch composites attracted the scientific interest due to their abundance in nature and their potential applications. In the present study, thermoplastic starch composites reinforced with microfibrillated cellulose were prepared and their electrical behaviour was investigated. The specimens were prepared via twin-screw extruder, internal mixer and compression molder, varying the filler concentration. Dielectric properties and related relaxation phenomena were studied via Broadband Dielectric Spectroscopy in the temperature range from 30 to 65°C and in the frequency range from 10⁻¹ to 10⁶ Hz. Each specimen was tested at least twice in the same frequency-temperature profile, in order to investigate the effect of the adsorbed water.

In the past few decades, considerable part of the scientific interest was focused to biodegradable plant-originated polymers, which exhibit renewable and ecologically friendly behaviour. Starch is one of the most examined agro-based polymers, which is abundant in nature, inexpensive and biodegradable.^[1,2] The dielectric properties and swelling characteristics of chemically modified starches have been studied before, but only for higher water-to-starch ratios.^[3] The past decade, the electrical response of agro-based biopolymers has attracted the research interest. The increasing energy requirements demand more efficient energy-conversion and storage systems with more affordable and environmentally friendly characteristics.^[4] The multifunctionality of some of these materials can be applied in more demanding applications requiring materials with smart behaviour. Here, we investigated the ability of thermoplastic corn starch to absorb and loose water depending on the current temperature and humidity, causing a variation in the energy density. In addition, microfibrillated cellulose was added as a reinforcement agent in order to improve this ability.

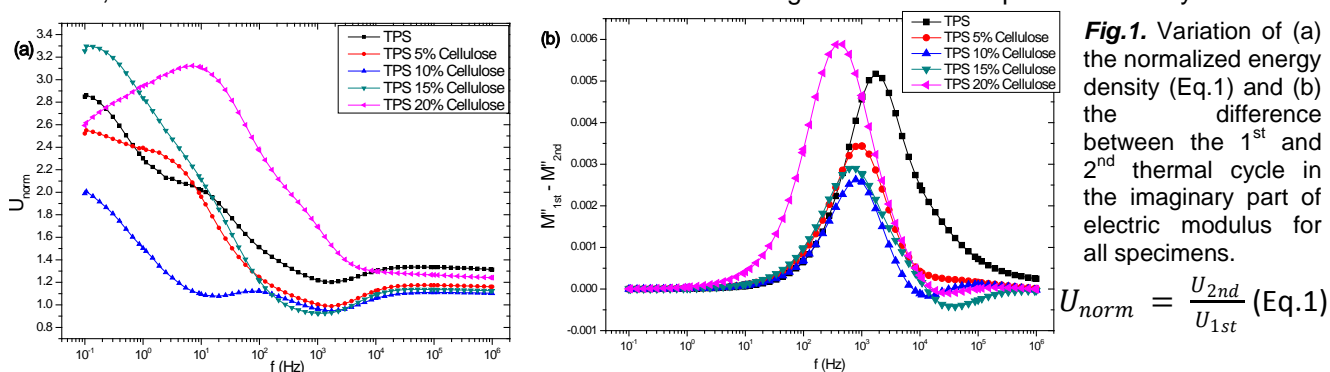


Fig.1. Variation of (a) the normalized energy density (Eq.1) and (b) the difference between the 1st and 2nd thermal cycle in the imaginary part of electric modulus for all specimens.

$$U_{norm} = \frac{U_{2nd}}{U_{1st}} \quad (\text{Eq.1})$$

References:

- [1] "Production and characterization of microfibrillated cellulose-reinforced thermoplastic starch composites", L. Lendvai, J. Karger-Kocsis, Á. Kmetty, S. X. Drakopoulos, Journal of Applied Polymer Science, 2016, 133 (2), 42397
- [2] "Preparation and properties of biodegradable starch-clay nanocomposites", Y.-L. Chung, S. Ansari, L. Estevez, S. Hayrapetyan, E. P. Giannelis, H.-M. Lai, Carbohydrate Polymers, 2010, 79, 391-396
- [3] "Dielectric and Thermal Transition Properties of Chemically Modified Starches During Heating", L. A. Miller, J. Gordon, E. A. Davis, Cereal Chemistry, 1991, 68 (5), 441-448
- [4] "Flexible Nanodielectric Materials with High Permittivity for Power Energy Storage", Z.-M. Dang, J.-K. Yuan, S.-H. Yao, and R.-J. Liao, Advanced Materials, 2013, 25, 6334-6365

POSTER SESSION I

Monday 19 September 2016, 18:45-20:30

*Structural-dynamical and mechanical
properties of condensed matter*

*Surfaces, nanomaterials and low-
dimensional materials & systems*

*Ceramics, composites, minerals and
metals*

Infrared Study of Defects in Nitrogen-Doped Electron Irradiated Silicon

T. Angeletos¹, N. Sgourou¹, A. Chroneos^{2,3}, C. A. Londos¹

¹*Solid State Section, Physics Department, University of Athens, Panepistimiopolis. Zografos, 157 84 Athens, Greece*

²*Department of Materials, Imperial College London, London SW7 2AZ, UK*

³*Faculty of Engineering and Computing, Coventry University, Priory Street, Coventry CV1 5FB, UK*

Abstract:

Silicon is the main semiconductor material for many electronic devices. Nitrogen is a key dopant in Cz-Si widely used to control properties of Si wafers in microelectronics. Most of these properties are affected by these defects and their processes. FTIR spectroscopy is an important experimental technique to investigate the properties and generally behaviour of defects in materials.

In this work we investigate the existence of N-related defects and their annealing characteristics as well as the impact of N-doping on the production and evolution of VO defect in irradiated Si, by means of FTIR spectroscopy. We used N-doped Cz-Si samples (with $[N] = 5 \cdot 10^{14} \text{ cm}^{-3}$) which were electron irradiated at a fluence of $2 \times 10^{18} \text{ cm}^{-2}$ and then subjected to 20 min isochronal anneals in 10°C steps up to 600°C . Fig.1 presents the Infrared spectra of the sample (a) before irradiation, (b) after irradiation.

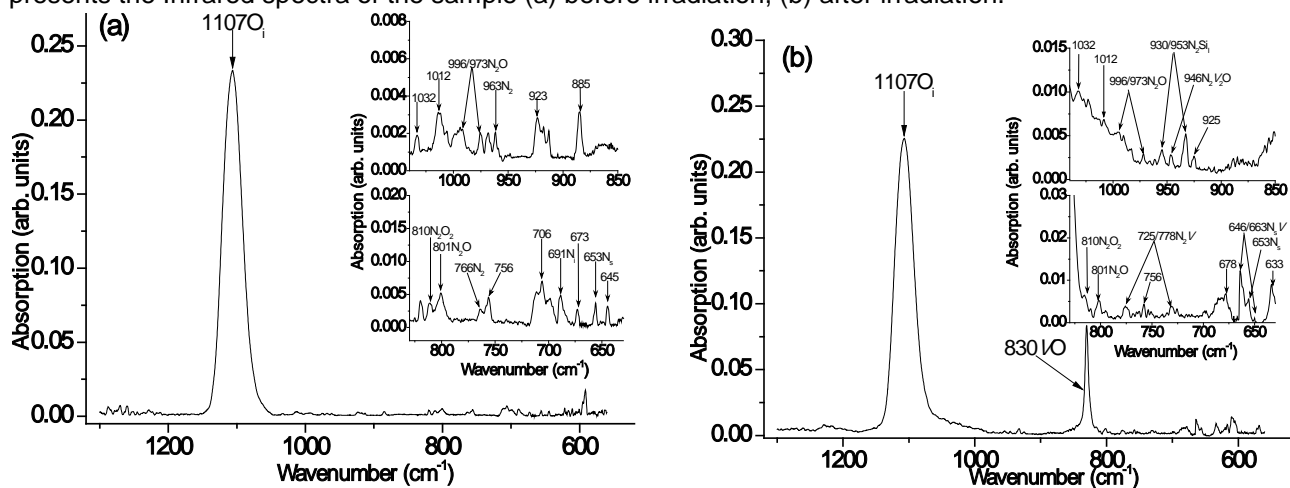


Fig.1 Infrared spectra of the sample (a) before irradiation, (b) after irradiation

Besides the well-known signals of substitutional (N_s) at 653 cm^{-1} , interstitial (N_i) at 691 cm^{-1} , N_2 at 766 cm^{-1} , N-O complexes at 801 , 996 and 1026 cm^{-1} and N_2O at 973 and 996 cm^{-1} , two bands at 646 and 663 cm^{-1} were attributed to a N_sV pair, two bands at 725 and 778 cm^{-1} were attributed to the N_2V complex and another pair of bands at 930 and 953 cm^{-1} were attributed to the N_2Si_i complex. Additionally we determined that N doping can reduce the formation of VO defects (Fig.2). The limitation of these defects will be beneficial as they can deleteriously impact materials properties and in turn the performance of devices. The evolution with temperature of the VO (830 cm^{-1}) and the VO_2 (888 cm^{-1}) defects of the N-doped and N-free samples.

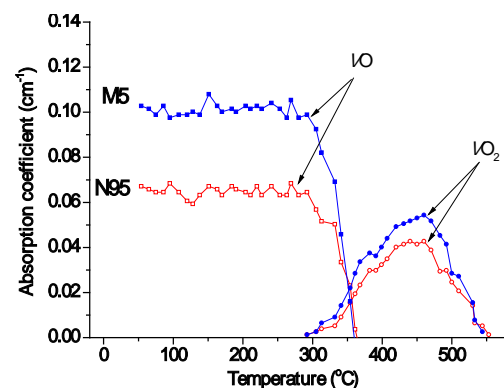


Fig.2 VO and VO_2 evolution with T in N-doped (N_{95}) and N-free (M_5) samples.

High pressure Raman and photoluminescence studies of $\text{In}_x\text{Al}_{1-x}\text{N}$ ($x=0.72$)

K. Filintoglou¹, J. Arvanitidis¹, D. Christofilos², S. Ves¹, G. A. Kourouklis², C. Bazioti¹,
 G. P. Dimitrakopoulos¹, A. Adikimenakis³ and A. Georgakilas³

¹Physics Department, Aristotle University of Thessaloniki, 54124 Thessaloniki, Greece

²Chemical Engineering Dept., Aristotle University of Thessaloniki, 54124 Thessaloniki, Greece

³Department of Physics, Microelectronics Research Group, University of Crete and IESL, FORTH, 71110 Heraklion, Greece

Abstract: $\text{In}_x\text{Al}_{1-x}\text{N}$ nanostructures are important for optoelectronic devices owing to their exceptional electronic properties. Their x -dependent bandgaps cover the spectral range from ultraviolet to near-infrared. Raman and photoluminescence (PL) spectroscopy are well-established, non-destructive techniques for the study of these systems. In this work, high pressure Raman and PL spectroscopies ($\lambda_{\text{exc}}=515$ nm) are used to probe the pressure response of the vibrational and electronic properties of a ternary $\text{In}_{0.72}\text{Al}_{0.28}\text{N}$ thin film grown by MBE on a $\text{GaN}/\text{Al}_2\text{O}_3$ substrate. Hydrostatic pressure up to 7 GPa was applied by means of a diamond anvil cell using the 4:1 methanol-ethanol mixture as pressure transmitting medium and the ruby fluorescence technique for pressure calibration.

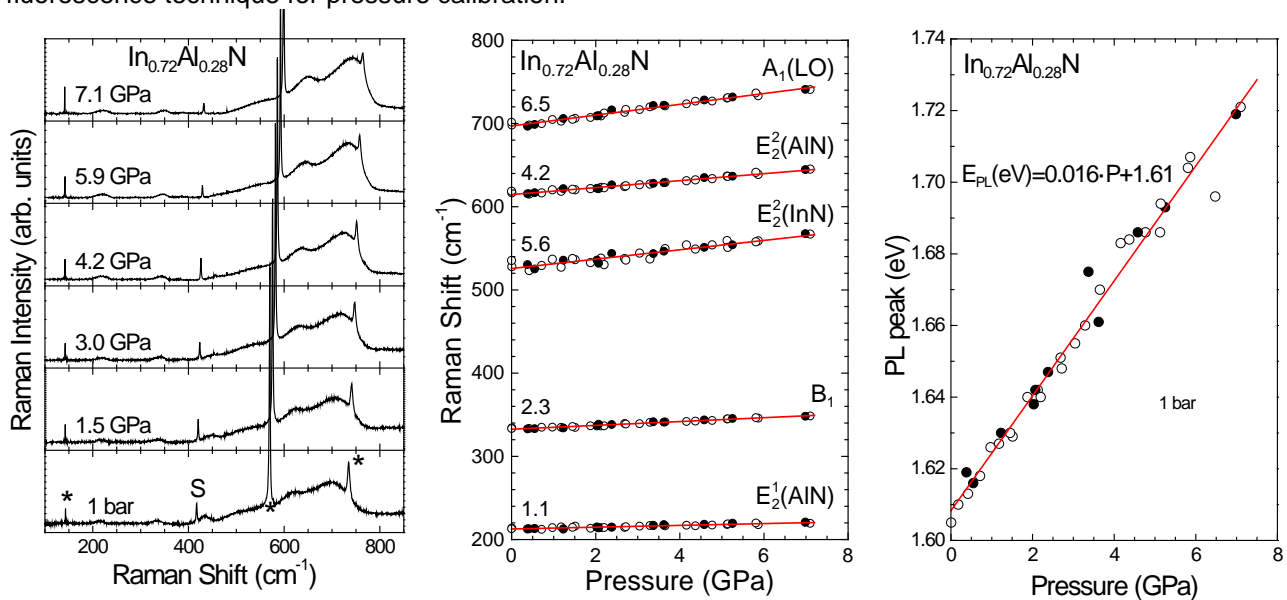


Figure 1. Pressure evolution of the Raman spectra of the studied $\text{In}_x\text{Al}_{1-x}\text{N}$ film and pressure dependence of its Raman peak frequencies and PL peak energy.

In the Raman spectrum of the $\text{In}_{0.72}\text{Al}_{0.28}\text{N}$ film (Figure 1), five broad Raman bands can be resolved at ambient conditions at 212 (E_2^1 , AlN-like), 334 (B_1), 528 (E_2^2 , InN-like), 611 (E_2^2 , AlN-like), and 699 cm^{-1} (LO, asymmetric peak). In addition to those of the film, the narrow Raman peaks of the GaN buffer layer at 143 (E_2^1), 570 (E_2^2) and 735 cm^{-1} ($A_1(\text{LO})$), marked by asterisks in Figure 1, as well as that of the sapphire substrate at 417 cm^{-1} (A_{1g}), marked by "S", are also present. Pressure application causes the reversible hardening of all the Raman bands of the film with slopes 1.1-6.5 $\text{cm}^{-1}\text{GPa}^{-1}$. While the pressure slopes for the two E_2^2 peaks {5.4 (InN-like) and 4.5 $\text{cm}^{-1}\text{GPa}^{-1}$ (AlN-like)} are similar to those for the corresponding end members of the $\text{In}_x\text{Al}_{1-x}\text{N}$ series, the pressure slope for the LO peak (6.5 $\text{cm}^{-1}\text{GPa}^{-1}$) is higher than those for the end members. This may be attributed to pressure induced changes of the electron-phonon coupling and the resonance conditions. On the other hand, the obtained pressure slopes of the Raman peak frequencies of the GaN/ Al_2O_3 substrate are in excellent agreement with the existing literature. The $\text{In}_{0.72}\text{Al}_{0.28}\text{N}$ PL peak appears at ~1.61 eV at ambient conditions, close to the absorption edge and in agreement with earlier studies. Its pressure slope is 16 $\text{meV}\cdot\text{GPa}^{-1}$, suggesting a possible clustered arrangement of the In atoms.

Pressure response of the FC70 Fluorinert™ studied by Raman spectroscopy

S. Misopoulos¹, A. Zerfiridou^{1,2}, K. Filintoglou¹, D. Christofilos³, S. Ves¹, G. A. Kourouklis³ and J. Arvanitidis¹

¹Physics Department, Aristotle University of Thessaloniki, 54124 Thessaloniki, Greece

²Food Technology Department, ATEI of Thessaloniki, 57400 Sindos, Greece

³Chemical Engineering Dept., Aristotle University of Thessaloniki, 54124 Thessaloniki, Greece

Abstract: FC70 Fluorinert™ (Perfluorotripropylamine) is an important liquid with a wide range of applications in electronics for vapor phase soldering and thermal management, as well as material science, because of its unique properties (thermal and chemical stability, compatibility with sensitive materials etc.). It has been also widely used in high pressure diffraction or spectroscopic studies as pressure-transmitting medium and, hence, knowledge of its Raman spectrum and pressure evolution is particularly useful. In this work, Raman spectroscopy ($\lambda_{\text{exc}} = 515 \text{ nm}$) has been used to study the pressure response of FC70. Hydrostatic pressure up to 5 GPa was applied by means of a diamond anvil cell, while pressure was calibrated by the ruby fluorescence technique.

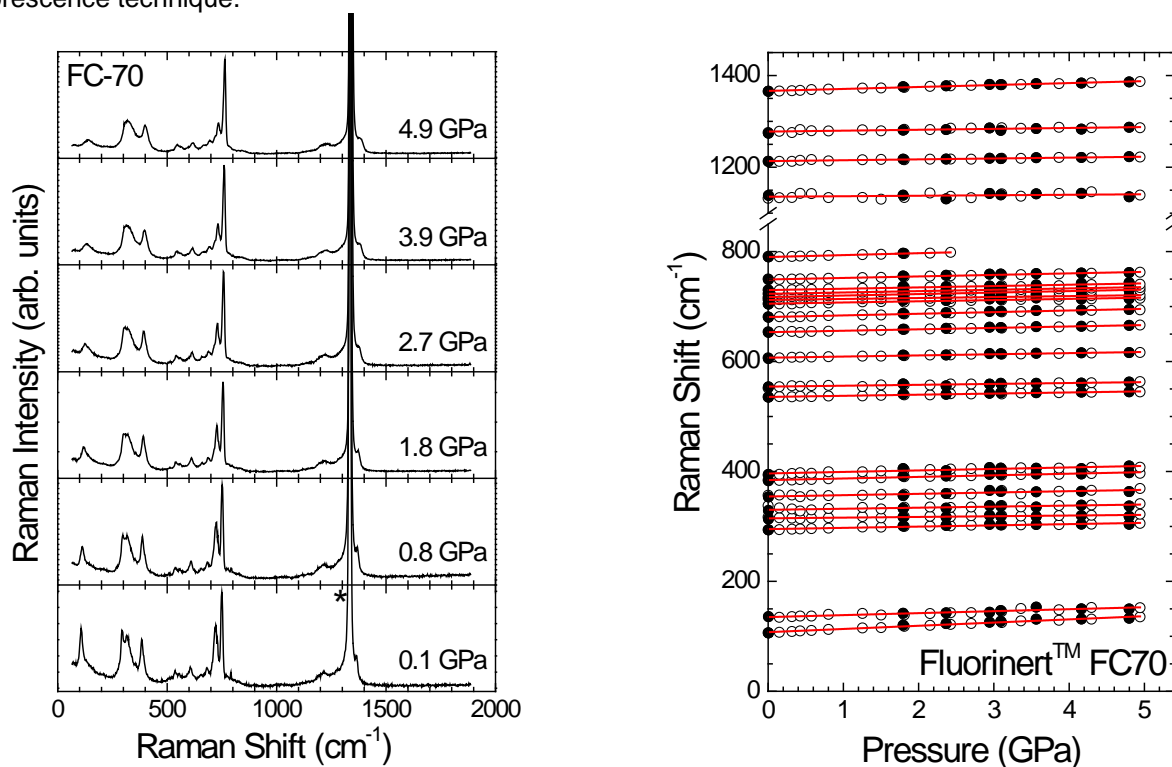


Figure 1. Pressure evolution of the FC70 Raman spectra and pressure dependence of its Raman peak frequencies.

With increasing pressure, all Raman peaks shift to higher frequencies, while no significant changes in the general spectrum profile occur up to 5 GPa with respect to the number of the Raman peaks, their linewidths and relative intensities (Figure 1). The only exception is the lowest frequency peak at 108 cm^{-1} that exhibits a continuous broadening and intensity attenuation with pressure. Previous studies have shown that FC70 becomes non-hydrostatic for $P > 0.6 \text{ GPa}$ due to its solidification. However, the pressure evolution of the frequencies of all the observed Raman peaks is quasilinear up to the maximum pressure attained in our experiments (5 GPa) with the corresponding pressure slopes ranging between 1.1 and $5.8 \text{ cm}^{-1}\text{GPa}^{-1}$. Moreover, the pressure-induced shifts of the frequencies of the Raman peaks are fully reversible upon pressure release. Consequently, despite its solidification, the pressure response of the frequencies of the Raman peaks and the overall spectrum profile remain unaffected for pressures at least up to 5 GPa, justifying its use as pressure transmitting medium.

High pressure Raman study of Kevlar-29 aramide fibres

F. Sebro¹, J. Arvanitidis¹, D. Christofilos², S. Ves¹, J. Parthenios³, G. Anagnostopoulos³,
 C. Galiotis^{3,4}, and K. Papagelis⁵

¹Physics Department, Aristotle University of Thessaloniki, 54124 Thessaloniki, Greece

²Chemical Engineering Dept., Aristotle University of Thessaloniki, 54124 Thessaloniki, Greece

³Institute of Chemical Engineering, FORTH/ICE-HT, 26500 Patras, Greece

⁴Chemical Engineering Department, University of Patras, 26504 Patras, Greece

⁵Department of Materials Science, University of Patras, 26504 Patras, Greece

Abstract: Kevlar-29 aramide fibres (poly-p-phenylene terephthalamide, PPTA) is a light weight, high strength material extensively used in ballistic applications, ropes and cables, protective apparel, helmets, vehicular armoring and plates, rubber reinforcement in tires etc. Kevlar fibres consist of polymeric chains where amide groups are attached directly between two aromatic rings. These long chains are highly oriented with many interchain hydrogen bonds and aromatic stacking interactions. In this work, Raman spectroscopy ($\lambda_{exc}=515\text{ nm}$) has been used to study the pressure response of Kevlar-29. Hydrostatic pressure up to 5.5 GPa was applied by means of a diamond anvil cell using glycerol as pressure transmitting medium and the ruby fluorescence technique for pressure calibration.

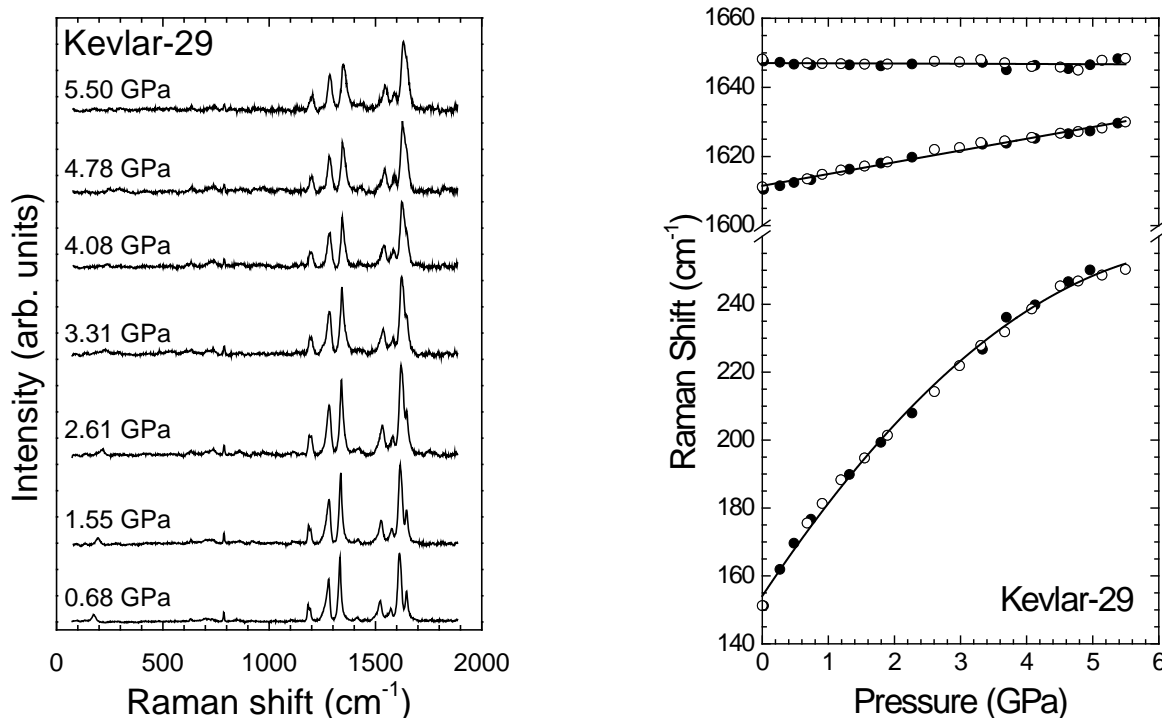


Figure 1. Pressure evolution of Kevlar-29 Raman spectra and pressure dependence of selected peak frequencies.

With increasing pressure, the majority of the observed Raman peaks shift to higher frequencies with slopes 1.2-6.2 $\text{cm}^{-1}\text{GPa}^{-1}$, without significant changes in their lineshapes and relative intensities (Figure 1). Interestingly, the Raman peak at 787 cm^{-1} , attributed mainly to ring puckering, exhibits a pressure slope of only $0.5\text{ cm}^{-1}\text{GPa}^{-1}$, suggesting that despite the volume reduction upon pressure application, the ring environment associated with this out-of-plane vibration is not significantly altered. Moreover, the peak at 1647 cm^{-1} , attributed mainly to the C=O stretching vibration (Amide I band), displays a nearly zero pressure slope ($-0.1\text{ cm}^{-1}\text{GPa}^{-1}$), indicating that the volume reduction is somehow absorbed by the much weaker hydrogen bonds. Finally, the lowest frequency Raman peak (154 cm^{-1}) exhibits a relatively strong intensity attenuation and a sublinear pressure response with initial slope as high as $29.4\text{ cm}^{-1}\text{GPa}^{-1}$, implying that it could be assigned to an external mode. All the observed changes are reversible upon pressure decrease.

Structural properties and strain relaxation in high alloy content InGaN films grown on AlN/Al₂O₃ templates by MBEC. Bazioti¹, E. Papadomanolaki², J. Smalc-Koziorowska³, E. Iliopoulos², and G. P. Dimitrakopoulos¹¹ *Physics Department, Aristotle University of Thessaloniki, GR 541 24, Thessaloniki, Greece*² *Microelectronics Research Group (MRG), IESL, FORTH, P.O. Box 1385, 71110 Heraklion Crete, Greece; and Physics department, University of Crete, 710003 Heraklion Crete, Greece*³ *Institute of High Pressure Physics, Polish Academy of Sciences, Sokolowska 29/37, 01-142 Warsaw, Poland*

InGaN alloy thin films of high indium content are a strong candidate for high efficiency photovoltaic and optoelectronic applications. In recent work [1] we made a systematic study on samples deposited by plasma-assisted molecular beam epitaxy (PAMBE) on GaN/Al₂O₃ templates by varying the growth temperature under almost stoichiometric conditions. In the current work, direct deposition on MOVPE (0001) AlN/Al₂O₃ templates was employed, as AlN exhibits high resistivity, a higher thermal conductivity compared to GaN leading to less self-heating, refractoriness, and transparency. Transmission electron microscopy (TEM) methods were used, including high resolution TEM (HRTEM), scanning TEM (STEM) and geometrical phase analysis (GPA), together with high resolution X-ray diffraction (HR-XRD), in order to study the complex microstructural behavior.

The defect content and crystalline quality of the films were characterized and a critical comparison of the microstructures of these films with films grown on GaN templates regarding the phenomena of compositional pulling, phase separation and sequestration was undertaken. The mechanism of TD introduction from BSFs was found to be operating also in this case. By lowering the growth temperature, the spontaneous formation of an InGaN sequestration layer was gradually suppressed. The InGaN/AlN heteroepitaxial interface was observed to have a prominent role in defining the defect content of the films. In particular, the large misfit promotes the creation of a defected interfacial region, characterized by regular misfit dislocation arrays, generating TD inverse half-loops due to the initial coalescence of InGaN nuclei. Furthermore, BSFs overlap during the initial stages of growth causing the introduction of interfacial areas with zinc-blende stacking. These phenomena are discussed in correlation to the growth conditions influencing indium adatom mobility.

[1] Bazioti et al., *Journal of Applied Physics* **118**, 155301 (2015).

Acknowledgement: Work co-financed by the EU (ESF) and Greek national funds - Research Funding Program: THALES, project NITPHOTO.

PECVD/PVD hybrid deposition technology for developing Ag- and Ti-reinforced hydrogenated amorphous carbon nanocomposite coatings

M. Constantinou¹, P. Nikolaou¹, P.C. Kelires¹, P. Patsalas², G. Constantinides¹

¹*Research Unit for Nanostructured Materials Systems and Department of Mechanical Engineering and Materials Science and Engineering, Cyprus University of Technology, Limassol, Cyprus*

²*Department of Physics, Aristotle University of Thessaloniki, Thessaloniki, Greece*

Abstract: This study aims to develop nanoparticle reinforced thin films with improved properties introduced through the inclusion of metals (Ag or Ti) than the ones exhibited by the hydrogenated amorphous carbon (a-C:H) matrix itself. The research motivation is to obtain films with tailored characteristics and optimum mechanical performances, that is, low friction coefficient and high toughness and abrasion resistance. For effective reinforcement, the particles should be small, with controlled geometrical characteristics, and evenly distributed throughout the matrix. These characteristics have been achieved through the use of a hybrid deposition technology, a combination of Plasma Enhanced Chemical Vapor Deposition (PECVD) and Physical Vapor Deposition (PVD). The amorphous carbon matrix is generated by the PECVD through carbon ions generated by an RF Plasma source by cracking methane, while the metallic nanoparticles are generated through a nanoparticle source based on PVD technology. The density and hydrogen content for the a-C:H matrix as well as the metal particle sizes and composition can be controlled during deposition. The physical, chemical, morphological and mechanical characterization of the films were accomplished through XRR, Raman Spectroscopy, SEM, AFM and nanoindentation, respectively. It is found that both Ag and Ti nanoparticles promote scratch resistance for the a-C:H:Me nanocomposite films. However, the different reactivity of each metal with the matrix leads to different percentage for critical load to fracture. The ability to form nanocomposite structures with optimum coating performance by controlling the carbon bonds (sp³, sp² or sp¹), the hydrogen content, and the type and content percent of metallic nanoparticles opens new avenues for a broad range of applications where mechanical, physical and/or optical properties are required.

On the High Pressure Consolidation of Bi_2Te_3

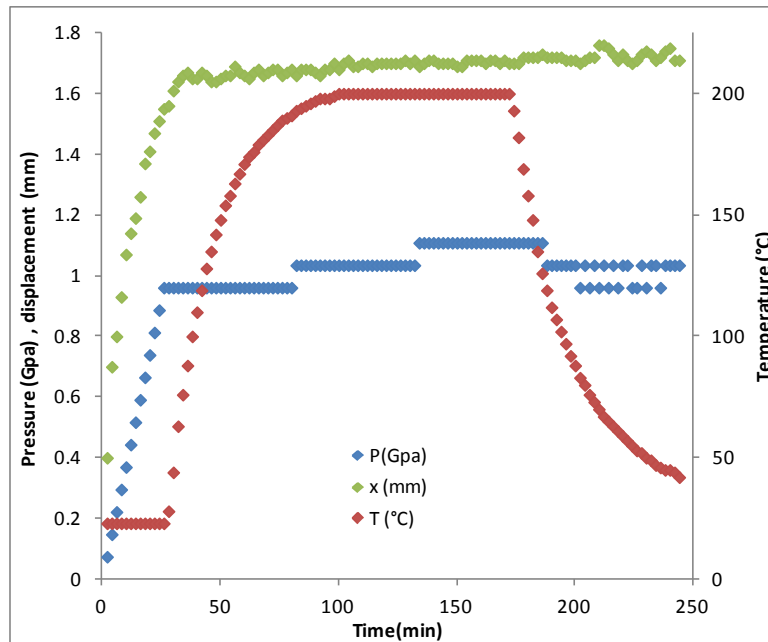
**K. Boutzi, S. Varitis, S. Kassavetis, E. Hatzikraniotis,
 S. Logothetidis, T. Karakostas, K.M. Paraskevopoulos**

Solid State Physics Section, Physics Department, Aristotle University of Thessaloniki, Greece

High-efficiency thermoelectric (TE) materials are very important for solid-state refrigeration as well as for power-generation devices. The conversion of wasted heat into electrical energy and vice-versa may play an important role in our challenge to develop alternative energy technologies. Bismuth telluride (Bi_2Te_3) and its alloys are widely used as materials both for commercial TE refrigeration (TEC) and as TE generators (TEG) when the temperature of the heat source is moderate. Optimized Bi_2Te_3 -based alloys have a figure of merit $ZT \sim 1$, $ZT = (S^2 \sigma / \kappa) \cdot T$, with S , σ , κ and T being the Seebeck coefficient, the electrical and thermal conductivity, and the temperature.

A TE device consists of p-type and n-type pairs of legs, connected electrically in series and thermally in parallel. The fabrication of a TE module starts from powders of polycrystalline material which are consolidated into pellets to improve the mechanical properties. One route for the consolidation is by cold pressing at high pressure (typically 0.8-1 GPa) and subsequent sintering of the cold pressed pellets at temperatures in the range of 200-500°C. Another route is by hot-pressing or SPS, at much lower pressures (typically 50-60MPa) at temperatures 400-550°C.

In this study, we report the consolidation of Bi_2Te_3 using a 13mm diameter hardened steel dry pressing die, capable of being heated up to 250°C and withstanding pressures up to 1.5GPa. Several heating/pressing profiles were applied, with holding times up to 2h. The maximum density of the obtained pellets reached 95% of the theoretical value. Knoop micro-hardness & nano-hardness and TE-properties on the pellets are presented.



A heating/pressing profile for high pressure consolidated Bi_2Te_3 pellet

Solvothermal synthesis of carbon encapsulated cobalt nanoparticles and their response in magnetic hyperthermia.

A. Kotoulas^{1*}, C. Dendrinou-Samara², J. Arvanitidis¹, G. Vourlias¹, M. Angelakeris¹, O. Kalogirou¹
¹Department of Physics, Aristotle University of Thessaloniki, 54124, Greece
²Department of Chemistry, Aristotle University of Thessaloniki, 54124, Greece

Abstract: Herein we report the synthetic procedure of carbon encapsulated cobalt (Co@C) nanoparticles. All samples were solvothermally prepared, via the wet chemical reduction of a cobalt complex or cobalt acetate tetrahydrated in the presence of different polyols, such as propylene glycol (PG), tetraethylene glycol (TEG) or triethylene glycol (TrEG) and NaOH. In all cases, the reaction temperature, the heating rate and the reaction time were maintained immutable (200 °C, 2.5 °C/min and 24h respectively).

The structural characterization of the samples was performed via X-ray diffraction (XRD) and scanning electron microscopy technique (SEM). X-ray diffraction revealed the fcc structure of cobalt and provided an approximate calculation of cell dimensions, while the presence of carbon was also indicated. The elemental analysis, illustrated by SEM, showed excessively presence of carbon, probably due to a core-shell structure effect. The presence of carbon was also evidenced by Raman spectroscopy, where peaks that correspond to G-band (1590 cm⁻¹) and D-band (1350 cm⁻¹) of carbon were revealed.

Co@C nanoparticles present saturation magnetization of 38.8 emu/g and coercivity of 274 Oe. Magnetic particle hyperthermia measurements at a frequency of 765 kHz were carried out and the observed values of specific loss power (SLP) at a concentration of 0.5 mg/mL were 241.1 and 154.2 W/g at a field amplitude of 0.03 T and 0.025 T, respectively.

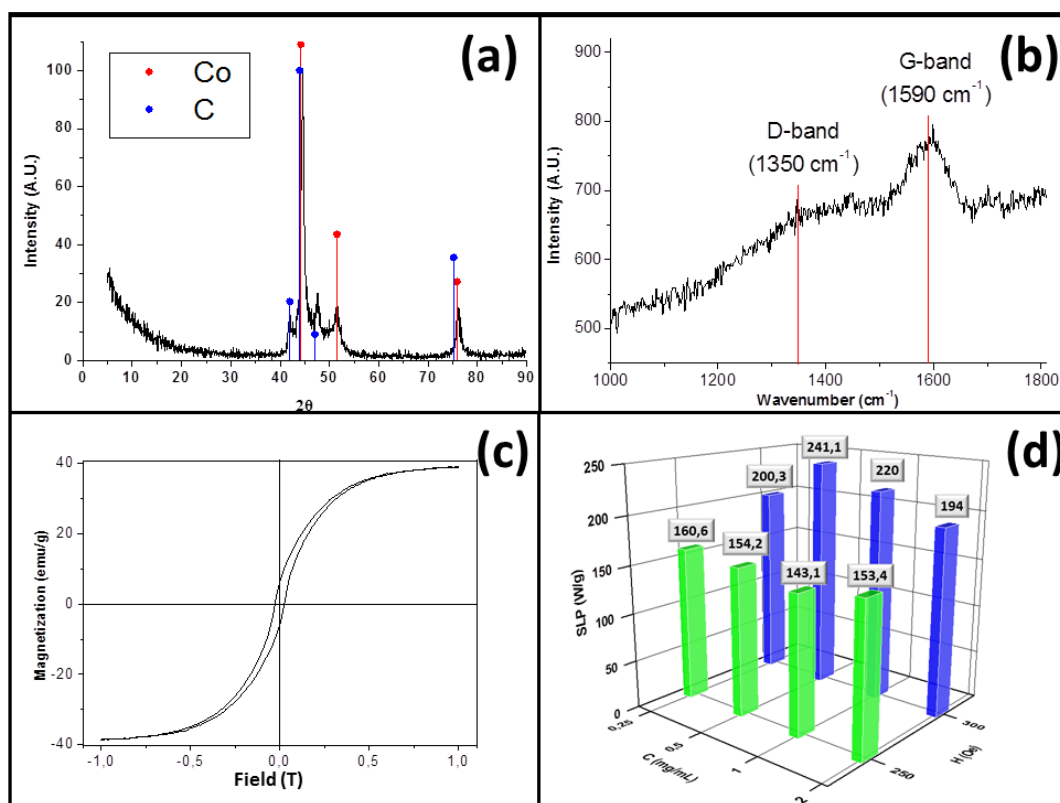


Fig. 1: (a) XRD pattern of Co@C nanoparticles, (b) Raman spectrum, (c) Magnetization loop, (d) SLP measurements for four different concentrations (0.25 to 2 mg/mL) at 0.025 T and 0.03 T.

XXXII Panhellenic Conference on Solid State Physics and Materials Science
Conference Center "Carolos Papoulias", 18-21 September 2016, Ioannina, Greece

Yttrium and oxygen adsorption on silicon Si(100)2x1 surface

M. Kamaratos, and D. Vlachos

Department of Physics, University of Ioannina, 451 10 Ioannina, Epirus, Greece

Abstract:

Oxygen adsorption on yttrium covered silicon Si(100)2x1 has been studied by Auger electron spectroscopy (AES), low energy electron diffraction (LEED), thermal desorption spectroscopy (TDS), electron energy loss spectroscopy (EELS) and work function measurements. The results show that oxygen penetrates underneath the yttrium overlayer and interacts with silicon substrate, by forming silicon oxide even at room temperature. In addition, a part of the adsorbed oxygen seems to interact with yttrium as well, forming yttrium oxide. Annealing of the oxidized surface results in the decomposition of both oxides, followed by yttrium partial desorption as yttrium silicide. A significant part of yttrium remains or/and diffuses into the silicon substrate, probably in the form of yttrium silicide compound.

XXXII Panhellenic Conference on Solid State Physics and Materials Science
Conference Center "Carolos Papoulias", 18-21 September 2016, Ioannina, Greece

Fluidized Carbon Nanotubes through Novel Modification Pathways

A. B. Bourlinos¹, V. Georgakilas², A. Bakandritsos², M. A. Karakassides³, D. Gournis³, A. Kouloumpis³, R. Zboril⁴, E. P. Giannelis⁵

¹ *Physics Department, University of Ioannina, Ioannina 45110, Greece*

² *Materials Science and Engineering, University of Patras, Rio 26504, Greece*

³ *Materials Science and Engineering, University of Ioannina, Ioannina 45110, Greece*

⁴ *Department of Physical Chemistry, Palacky University, Olomouc 77146, Czech Republic*

⁵ *Materials Science and Engineering, Cornell University, Ithaca NY 14853, USA*

Abstract: The dispersion of carbon nanotubes in liquids is critical in applications pertaining to polymer composites, thin films, nanoparticle hybrids and biomedicine. Generally, good dispersions can be obtained after surface modification of the nanotubes. This results in derivatives with long term colloidal stability, improved surface compatibility and exceeding solubility enabling for an easier manipulation of the dispersed solid through mixing, blending, impregnation, casting, spin-coating, evaporation and wet chemistry. Typical modifiers include organic reagents, polyaromatics, surfactants or polymers. Herein we present novel pathways towards the effective surface modification of multi-wall carbon nanotubes aiming to fluidized derivatives in the presence or absence of solvents. Solvent-dispersible adducts include perfluorinated carbon nanotubes and ionic cluster-carbon nanotube hybrids (ionic cluster: silica or fullerol polyanions). The first adduct is dispersible in perfluorinated solvents of low-boiling point, like hexafluoroisopropanol. Casting of the dispersion over a glass surface and evaporation of the solvent leads to high quality thin films with superhydrophobic properties. On the other hand, surface modification with silica or fullerol polyanions provides static repulsions that result in water-dispersible hybrids suitable for biomedical applications. Carbon nanotubes may exhibit fluid-like behavior in the absence of solvents after proper functionalization. In principle, the surface of the tubes is decorated with a soft organic corona that provides a liquid shell around the solid carbon core. Representative examples include adducts with a soft PEGylated amine or a liquid epoxy-silicone. In case of PEGylated amine, the derivative is isolated as a waxy solid that melts at 35 °C to afford a tar-like liquid. In case of silicone, the derivative is already a viscid fluid at room temperature. Such solvent-less nanofluids could be utilized in thermal dissipation and conductive inks.

Variation in the anomalous fading behavior of various luminescence signals from Durango apatite versus grain sizes; from micro to nano scale.

M. K Niora¹, G.S. Polymeris², I.K. Sfampa¹, E.C. Stefanaki³, E. Pavlidou³, V. Pagonis⁴, G. Kitis¹

¹ Nuclear and Elementary Particle Physics Laboratory, Physics Department, Aristotle University of Thessaloniki, GR-54214, Thessaloniki, Greece

² Institute of Nuclear Sciences, Ankara University, Beşevler 06100, Ankara, Turkey

³ Solid State Section, Physics Department, Aristotle University of Thessaloniki, GR-54214, Thessaloniki, Greece

⁴ McDaniel College, Westminster, MD 21157, USA

Introduction:

Durango apatite is a geological, naturally occurring luminescent material that yields very intense anomalous fading (AF)[1]. Thus, it is ideal for investigating theoretical models, which are based on the quantum mechanical tunneling origin of the AF effect. The localized tunneling transition model[2] is based on tunneling recombination within randomly distributed donor-acceptor pairs. Since the donor-acceptor distance is of crucial importance for the model, the present work is aiming at affecting this distance distribution by gradually reducing the grain sizes up to the nano-scale.

Materials and methods:

The grains of the sample (natural crystal of Durango apatite) were divided into different size fractions: coarse grains 80-200 μ m and nano-scale grains, achieved by applying ball milling to the sample, for various periods (between 2-48hours). The grain size distribution was yielded using Electron Microscopy techniques. All samples were firstly annealed up to 700 C for 1h, irradiated and then stored under dark room conditions for different storage times. All luminescence measurements (TL, OSL and thermally assisted OSL; TA-OSL) were carried out using a Risø TL/OSL reader.

Results and conclusions:

In the case of TL and OSL signals, AF effect is ubiquitous for all apatite grain size fractions subjected to the present study, but seems to be independent of the grain size (Fig.1- OSL fading rate); similar results were also yielded for TL. Furthermore, similarly to the case of coarse grains, very intense TA-OSL signal is yielded. The signal emerges from VDT, since each TA-OSL measurement follows a TL measurement up to 500°C[3]. Nevertheless, the intensity is somehow decreased as the ball milling time increases; the fading rate obtained is getting decreased as the grain size fraction is also decreased (clearly highlighted in Fig.1- for ball milling duration of 48h, TA-OSL seems to be un-affected by AF).

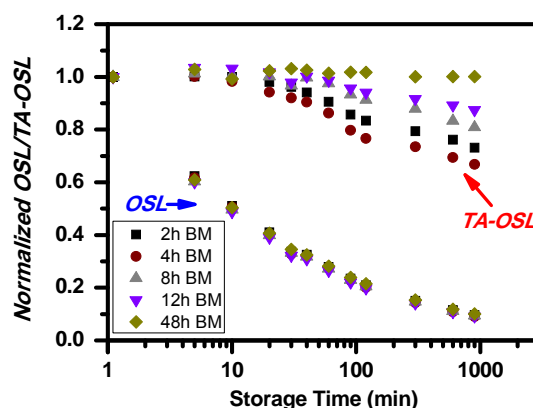


Fig. 1: Fading rates for OSL and TA-OSL for various ball milling durations.

References:

- [1] G.S. Polymeris, N.C. Tsirliganis, Z. Loukou, G. Kitis, Phys. Status Solidi A 203 (2006)578
- [2] M. Jain, B. Guralnik, M.T. Andersen, J. Phys. Condens. Matter 24 (2012)385
- [3] G. Kitis, G.S. Polymeris, V. Pagonis, N.C. Tsirliganis, Radiat. Meas. 49 (2013)73

**Gravure printing of highly conductive ink
made by Graphene/MWNTs nano hybrids in polyacrylic resins**

Vassiliki Belessi¹, Apostolos Koutsioukis², Vasilios Georgakilas²

¹*Department of Graphic Design, Section of Graphic Arts, Technological Educational Institution of
Athens, Ag. Spyridonos, 122 10 Egaleo, Athens, Greece*

²*Department of Materials Science, University of Patras, 26505 Rio, Greece*

Abstract: Gravure printing is a traditional printing method for high-volume applications such as magazines, catalogs or packaging with high printing speeds allowing for large numbers of prints in a short time. Gravure has the ability to print a variety of functional materials and fine lines with resolutions below 30 μm . It can therefore be used for printed electronics. In an effort to prepare conductive inks for gravure printing, a highly hydrophilic nano hybrid made of pristine graphene and hydroxy-functionalized multiwalled carbon nanotubes is homogeneously mixed with commercial polyacrylic resins that usually used in gravure printing. Thanks to the strong hydrophilic character of both components the non conductive resin can be highly loaded with the conductive carbon nano hybrid affording analogous conductive water based ink with acceptable characteristics for gravure printing technique.

Hypersonic phononic crystals made of poroelastic spheres

A. Alevizaki^{1,2}, R. Sainidou¹, P. Rembert¹, B. Morvan¹, N. Stefanou²

¹*Laboratoire Ondes et Milieux Complexes, UMR CNRS 6294, University of Le Havre, Normandie University, 75 rue Bellot, 76600 Le Havre, France*

²*Department of Solid State Physics, National and Kapodistrian University of Athens, University Campus, GR-157 84 Athens, Greece*

Abstract: Phononic crystals are composite materials consisting of a periodic array of objects (scatterers) with elastic properties (mass density, elastic wave velocities) different from those of the host medium in which they are embedded. This periodic modulation of the elastic parameters leads to the formation of regions of frequency, known as gaps, where elastic waves cannot propagate within the structured medium, whatever the direction of propagation; these composite materials behave as mirrors for the elastic waves, in analogy to crystalline solids where periodicity creates band gaps for the electronic states. Although frequency band gaps are their most known feature, phononic crystals can exhibit a plethora of interesting phenomena such as waveguiding, filtering, negative refraction, etc, which occur in a frequency range directly related to the scatterer size. In the last decade, self-assembly techniques allowed for the fabrication of colloidal crystals in nanoscale, thus leading to hypersonic phononic crystals operating at the GHz range, one of the most typical cases being silica spheres embedded in a water-like fluid. In this frequency range (up to 20 GHz) Brillouin Light Scattering experiments provide evidence that, at this scale, porosity in silica cannot be neglected [1,2]. For this reason, we shall be concerned with multiple scattering of acoustic waves in colloidal crystals of fluid-saturated porous silica spheres embedded in a fluid, involving study of the transition T-matrix for such a single sphere, after formulating the scattering in an appropriate vector spherical-wave basis. We discuss several physical models describing the effective viscosity present in the porous sphere [3] and provide a thorough analysis of the single-scattering based on density-of-state calculations [4]. Next, considering phononic crystals made of such spheres, we calculate the corresponding frequency band structure using layer-multiple-scattering techniques. For this purpose, the existing computer code MULTTEL [5] is extended by incorporating the above-mentioned T-matrix.

[1] H. S. Lim, M. H. Kuok, S. C. Ng, and Z. K. Wang, *Appl. Phys. Lett.* **84**, 4182-4184 (2004).

[2] T. Still, R. Sainidou, M. Retsch, U. Jonas, P. Spahn, G.P. Hellmann, and G. Fytas, *Nano Lett.* **8**, 3194-3199 (2008).

[3] S. Kargl and R. Lim, *J. Acoust. Soc. Am.* **94**, 1527-1550 (1993).

[4] R. Sainidou, N. Stefanou, A. Modinos, *Phys. Rev. B* **69**, 064301 (2004).

[5] R. Sainidou, N. Stefanou, I.E. Psarobas, and A. Modinos, *Comput. Phys. Commun.* **166**, 197-240 (2005).

Thermodynamic characterization and behavior of epoxy / fly ash composites

A. Stimoniaris^{1,4}, H. Zois², A. Kanapitsas³, C. Delides¹

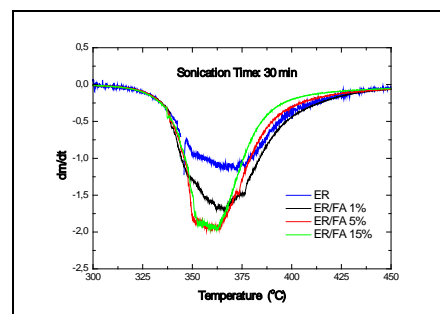
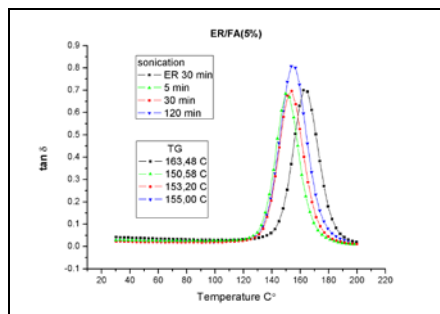
¹Department of Environmental Engineering and Pollution Control, Technological Educational Institute of West Macedonia, Kila, GR-50100, Kozani, Greece

²Merchant Marine Academy of Epirus, Vathi, GR-48100, Preveza, Greece

³Department of Electronic Engineering, Technological Educational Institute of Sterea Ellada, GR-35100, Lamia, Greece

⁴Department of Materials Science and Engineering, University of Ioannina, GR-45110, Ioannina, Greece

Abstract: The Fly ash (FA) is a waste by-product rich in oxides such as SiO₂, Al₂O₃ and Fe₂O₃, which has proved to have some favourable functions as filler in polymer composites [1, 2]. In this work, we have prepared epoxy resin (ER) composites filled with fly ash. The fly ash was produced at the power stations of Kozanis region in northern Greece and it is rich in CaO due to the origin of the burned lignite. An epoxy system (DGEBA) was used as matrix along with a triethilentetramine (TETA) curing agent. Optical and Scanning electron microscopy (SEM) was used to clarify the dispersion and the degree of aggregation/agglomeration of fly ash particulates in the matrix. In addition, DMA, DSC and TGA measurements are also employed to characterize dynamic mechanical properties, crystallinity and the heat-resistant performance of the composites. It was concluded that the mechanical stirring and ultrasonication was a useful combination to prepare highly dispersed fly ash composites. Interesting results concerning the effect of filler content and the sonication time on the dispersion and the deaggregation/deagglomeration of fly ash and on the thermomechanical properties of the composites were derived. Two DMA and TGA characteristic diagrams are shown below.



References

- [1] Ahmad, A. Mahanwam, J. Miner. Mater. Charact. Eng. 9, 183-198 (2010).
- [2] R.S. Raja, et al. Int. J. Min. Met. Mech. Eng. 1, 34 (2013).

Structure – Properties Relationship of Thermoset and Thermoplastic Nanocomposites Filled with Fly Ash

A. Stimoniaris¹, E. Skoura², A. Karanastasis², A. Avgeropoulos², M. Karakassides², D. Gournis²
and C. Delides¹

¹*Department of Environmental Engineering and Pollution Control, Technological Educational Institute of West Macedonia, 50100, Kozani, Greece*

²*Department of Materials Science & Engineering, University of Ioannina, 45110 Ioannina, Greece*

Abstract:

In this work the physicochemical properties of polymer/fly ash composites have been examined in relation to the nature of the matrix (thermosets and thermoplastics) and the surface modification of the filler as well. Pristine fly ash and that modified with organosilanes of the type $(RO)_3SiCH_2NH_2$ and $(RO)_3SiCH_2CH_3$ have been incorporated respectively into epoxy resin DGEBA (thermoset) and polystyrene-b-polybutadiene (PS-b-PB) (thermoplastic) matrices. Details for sample preparation are presented elsewhere [1, 2].

Scanning electron microscopy (SEM) was used to clarify the dispersion and the degree of aggregation/agglomeration of fly ash particulates in the matrix.

Pristine and modified materials as well as the final nanocomposites were characterized by a combination of analytical techniques including FT-IR, DMA, DSC and XRD. FT-IR spectra indicate the existence of surface modified fly ash in the final composite. DMA and DSC measurements show a clear dependence of the dynamic properties of the composites with the same filler loading on the matrix nature. The effect of surface modification is probably attributed to better compatibility of the modified filler with the matrices.

References

- [1] A. Stimoniaris, H. Zois, A. Kanapitsas, M. Karakassides, C. Delides, 6th International Conference on Structural Analysis of Advanced Materials, ICSAAM 2015, 08-11 September, Porto, Portugal.
- [2] E. Skoura, A. Karanastasis, A. Z. Stimoniaris, A. Avgeropoulos, M. Karakassides, D. Gournis, 7th Panhellenic Symposium on Porous Materials, June 2nd-4th 2016, Ioannina, Greece.

A novel one step synthesis and sintering of skutterudite CoSb₃

A. Ioannidou¹, T. Giannakis¹ and D. Niarchos¹
¹INN, NCSR Demokritos, Athens, Greece

Abstract:

Thermoelectric (TE) materials, which can be used to convert thermal energy to electric energy, have attracted a great deal of attention due to their promising applications in solid state cooling and power generation from waste heat. The production of these materials is based on a two-step procedure, first synthesis and then sintering.

Synthesis of CoSb₃ skutterudites with conventional method (furnace or ball milling) takes several days (~4 d) to obtain the final material for property measurements. Alternative routes have been proposed such as chemical routes and microwave assisted synthesis while sintering is usually been held by SPS (Spark Plasma).

In order to reduce the steps and the hours of preparation we introduce a novel way we termed RHS (Rapid Heating System). This system consists of an RF source and a mechanical press. RF has major potential and real advantages over conventional heating:

- Time and energy savings.
- Rapid heating rates (volumetric heating vs. conduction).
- Considerably reduced processing time and temperature.
- Fine microstructures and hence improved mechanical properties and better product performance.

In the proposed approach we are aiming to achieve single phase skutterudites in one step (synthesis and sintering at the same time) in less than 10 minutes, preserving the structure and the density of the materials.

X-ray diffraction analysis was used to examine the structure and the lattice parameters of the samples while SEM with EDX analysis was used to study the morphology of the compounds. We will also present data for thermoelectric properties and compare with materials synthesized with conventional approach.

The effect of synthesis technique on the microstructure of high performance PbSe thermoelectric materials

E.C. Stefanaki¹, Th. C. Chasapis², E. Hatzikraniotis¹, K. M. Paraskevopoulos¹, M. G. Kanatzidis²

¹ Physics Department, Aristotle University of Thessaloniki, Thessaloniki, Greece

² Department of Chemistry, Northwestern University, Evanston, IL, United States

Abstract: During the past decade, the scientific community has witnessed a tremendous increase of research activity in the field of high efficiency thermoelectric materials (TE). PbTe is the most widely studied lead chalcogenide with high efficiency in the intermediate temperature range (600-800K). The sister material PbSe has received comparatively little attention, due to a lower figure-of-merit in this range. However, PbSe has several advantages since Se is 50 times more abundant, much less expensive and it has lower thermal conductivity than Te. Furthermore PbSe melts at a relatively higher temperature than PbTe and thus can perform better on higher temperatures (900K).

Various synthesis methods are used to fabricate PbSe such as, vapour-liquid-solid (VLS), Bridgman, microwave irradiation for PbSe nanoparticles, sublimation and from the melt. In any of these cases, a microscopically homogeneous material has to be assumed in order to acquire a comprehensive understanding between the measured thermoelectric properties (Seebeck coefficient or free carrier concentration) and the microscopic intrinsic features of each material. However, the general assumption about electronically homogeneous materials was disproved and the limitations of conventional Hall and Seebeck effect measurements which provide only one bulk average value were illustrated in previous work.

In this work, we present the effect of the synthesis technique on the microstructure of high performance PbSe. Direct melt-cooling of Pb, Se, Na and Spark Plasma Sintering (SPS) were applied in order to prepare p-type $\text{Pb}_{1-x}\text{Na}_x\text{Se}$ ($0 \leq x \leq 0.04$). The chemical composition of all samples and the morphology was determined by SEM/EDS analyses using a Jeol 840A scanning microscope. Fourier transform infrared spectroscopy (FTIR) measurements were performed in the range of $700\text{-}4000\text{ cm}^{-1}$ using a microscope with $100\text{ }\mu\text{m}$ iris (PerkinElmer spectrometer with i-series microscope), which enables FTIR mapping of the samples (Figure 1). The Plasmon frequency derived by the $\mu\text{-FTIR}$ measurements and a Drude model analysis, was used as a probe for mapping local in-homogeneities in the microstructure induced by different dopant content diluted in the matrix.

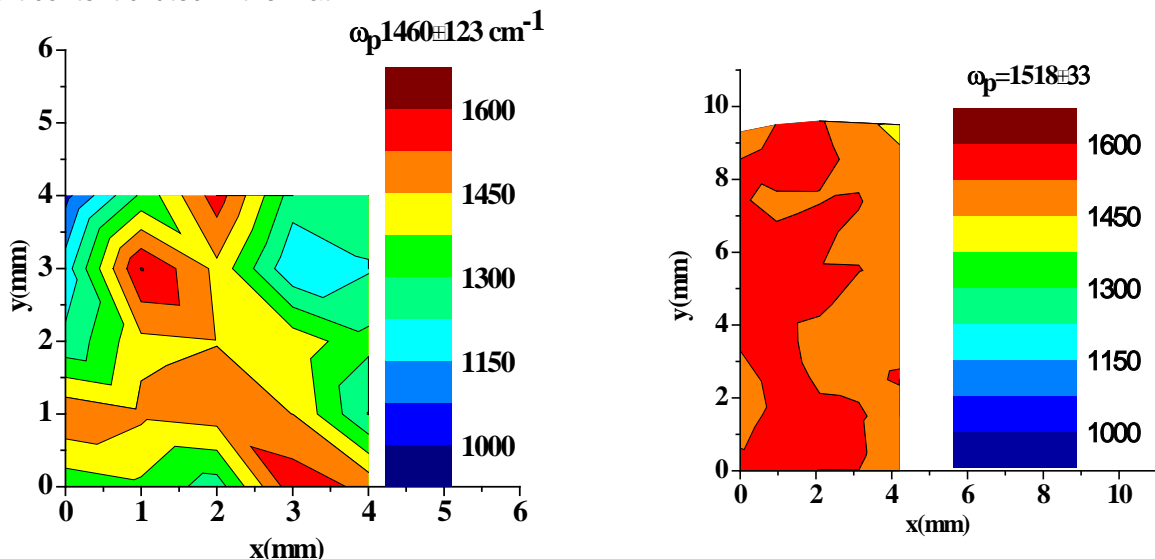


Fig.1 contour plots of plasmon frequency for two samples, by the melt (left figure) and SPS (right figure) with the same nominal Na content (1% Na). Sodium diluted in the matrix of SPS samples more homogeneously and in higher percentage, giving rise to higher plasmon frequency values.

Chemical and electrical characterization of high-k ultra-thin films on Ge substrates.G. Skoulatakis¹, M.A. Botzakaki², S.N. Georga², C.A. Krontiras², S. Kennou¹¹*Department of Chemical Engineering, University of Patras, Patras, Greece*²*Department of Physics, University of Patras, Patras, Greece*

Microelectronic engineering trends concern the replacement of SiO₂, as gate insulator in MOS devices, with high-k dielectrics and the possible substitution of Si with high-mobility substrates such as Ge [1,2]. For thermodynamic stability reasons, the choice of dielectrics is restricted to the oxides of Hf, La, Y, Zr and Al [3].

In this study, high-k ultra-thin films were grown by Atomic Layer Deposition (ALD) technique. ALD is one of the most known techniques in microelectronics field, which provides ultra-thin films with absolute control of thickness. Ultra-thin films of Al₂O₃ and HfO₂ were grown on Ge (100) substrates, at various deposition temperatures, from 80°C to 300°C, with nominal thickness of 5nm and 10nm. Furthermore, gate stacks of HfO₂/Al₂O₃/p-Ge were grown at different thicknesses.

The purpose of the present work is to investigate the influence of the ALD deposition temperature on the chemical composition and thickness of the deposited oxides. Furthermore, the possible formation of Ge oxide at the Al₂O₃/Ge and HfO₂/Ge interfaces, the oxide intermixing at ultra-thin layer HfO₂/Al₂O₃/Ge stacks as well as the electrical characteristics are also examined. All samples were studied by X-Ray Photoelectron Spectroscopy (XPS).

The experimental results revealed that the deposited films at higher temperatures (150 °C - 300 °C) are homogeneous and stoichiometric [4] while the ones deposited at 80°C are non-uniform. No chemical interaction, degradation or diffusion between the layers and the substrate were observed. The calculated equivalent film thickness of XPS was found in good agreement with the nominal one, estimated by the ALD recipes. The electrical measurements showed that the dielectric constant has a smaller value for the ultra-thin films compared to the bulk one and it is independent of the deposition temperature. The presence of ultra-thin Al₂O₃ layers, acting as passivation layer in the stacks, produced superior quality Ge-based MOS structures with negligible leakage currents and low density of interfacial traps (D_{it}) compared to the Al₂O₃/Ge and HfO₂/Ge structures.

[1] M.A. Botzakaki, N. Xanthopoulos, E. Makarona, C. Tsamis, S. Kennou, S. Ladas, S.N. Georga, C.A. Krontiras, *Microelectron. Eng.* **112**, 208-212 (2013).

[2] A. Delabie, R.L. Puurunen, B. Brijs, M. Caymax, T. Conard, B. Onsia, O. Richard, W. Vandervorst, C. Zhao, M.M. Heyns, M. Meuris, *J. Appl. Phys.* **97**, 064104 (2005).

[3] H. J. Hubbard and D. G. Schlom, *J. Mater. Res.* **11**, 2757 (1996).

[4] L. Sygellou, V. Gianneta, N. Xanthopoulos, D. Skarlatos, S.N. Georga, C.A. Krontiras, S. Ladas, and S. Kennou *Surf. Scien. Spec.* **18**, 58 (2011)

Finite Element Analysis of Quantum Nanostructures

N. Florini, Th. Stamou, G. P. Dimitrakopoulos, J. Kioseoglou, Th. Kehagias
Physics Department, Aristotle University of Thessaloniki, 54124 Thessaloniki, Greece

The elastic stress-strain fields build-up in III-V compound semiconductor nano-heterostructures, due to lattice mismatch, have a significant effect on their optoelectronic properties, for example the induced changes of levels in the conduction and valence bands and thus, affect the performance of III-V based microelectronic devices. Hence, we have used the Finite Element Method (FEM), in order to obtain an accurate description of the induced stress-strain fields. FEM is a versatile and efficient simulation technique, which can be applied in nanostructures of any geometrical shape, providing the right selection of the appropriate elastic constants. Here, FEM analysis is employed to simulate elastic strain fields, directional deformation and stresses in different quantum nanostructures, where the lattice misfit between the heterostructures is simulated in the framework of thermo-elasticity theory. In particular, we present FEM calculations for three different nanostructure geometries: (111)-oriented GaAs/Al_xGa_(1-x)As core-shell nanowires (NWs), (111)-oriented GaAs NWs comprising two consecutive In_xGa_(1-x)As quantum wells, and (211)-oriented InAs/GaAs surface and buried quantum dots (QDs). The effects of the chemical composition of the active regions and size of the heterostructures are studied. Specifically, for the GaAs/In_xGa_(1-x)As NWs the In concentration varied from 0.25 to 1, while for GaAs/Al_xGa_(1-x)As core-shell NWs the Al concentration varied from 0.2 to 0.65, respectively. In the latter case, shell-to-nanowire (S/NW) relative diameter ratios of 0.45 to 0.65 were studied and the results were compared with experimental and molecular dynamics results. FEM simulations showed that the strain distribution within the nanostructures is sensitive to both their chemical composition, as well as their size.

Acknowledgements

Work supported by the Research Projects for Excellence IKY/Siemens.

Study of structural characteristics of polycrystalline Si thin films, grown by Al metal induced crystallization of amorphous-Si, for solar cell applications by electron microscopy techniques

S. Kozakos¹, Ch. B. Lioutas¹, N. Vouroutzis¹, V. Gianneta² and A. G. Nassiopoulou²

¹ *Department of Physics, Aristotle University of Thessaloniki, GR-54124 Thessaloniki, Greece*

² *NCSR Demokritos/INN, Terma Patriarchou Grigoriou, Aghia Paraskevi, 15310 Athens, Greece*

The Al-induced crystallization and the simultaneous p-doping of amorphous Si thin films grown on n-type Si substrate have been investigated by transmission electron microscopy (TEM). This configuration is intended for use as the emitter in crystalline Si solar cells¹. The initial structure consists of an amorphous Si layer, deposited by sputtering on n-type Si, on top of which a layer of Al is deposited. During the annealing in N₂ ambient for several hours and different temperatures, the a-Si starts to crystallize from the Al/a-Si interface and proceeds downwards. The crystallized Si layer is highly doped with Al. A combination of different deposited nominal thickness a-Si thin films (10 and 20nm), annealing temperature (430 and 500°C) and annealing time (6 and 10 hours), were used in order to grow a set of samples.

Cross section and plane view conventional and high resolution transmission electron microscopy (CTEM, HRTEM) were used for the structural characterization of these films. The nanocrystalline layer was of high crystalline quality, with thickness around 10nm in all cases and the <111> crystallization direction to be mainly parallel to [100] of Si substrate. However, the samples with nominal thickness of 20nm, show also nanocrystals in the amorphous layer, between the nano-Si layer and the Si-substrate with no preferential orientation. A thickness around 2-9 nm and lateral size around 4-26 nm were measured, with the maximum lateral dimensions observed for 500°C and 10h annealing. Twins and other defects were observed in the Si nano-layer. Based on the TEM results, the crystallization mechanism will be discussed.

[1] S. Gardelis, A. G. Nassiopoulou, P. Manoussiadis, N. Vouroutzis, and N. Frangis, Appl. Phys. Lett. 103, 241114, 2013

Al₂O₃/HfO₂/p-Si MOS structures : Electrical and structural characterization

S. Korkos¹, M.A. Botzakaki¹, G. Skoulatakis², S. Kennou², S. Ladas², C. Tsamis³, S. N. Georga¹ and
 C. A. Krontiras¹

¹*Department of Physics, University of Patras, Rion 26 504, Greece*

²*Surface Science Laboratory, Department of Chemical Engineering, University of Patras, Rion 26
 504, Greece*

³*Institute of Nanoscience and Nanotechnology, NCSR "Demokritos", 153-10 Aghia Paraskevi,
 Greece*

The recent trends in Microelectronic technology concerns the replacement of SiO₂ with high-permittivity (high-k) dielectrics [1-3]. Taking advantage of the higher, compared to SiO₂, permittivity of high-k dielectrics, it is possible to create MOS devices exhibiting simultaneously low Equivalent Oxide Thicknesses (EOT) and low leakage currents. It is found that Al₂O₃ (k~8) is the most promising high-k gate material for future MOS devices, due to the high quality interface that create with the substrates. The main disadvantage of Al₂O₃ is the relative low dielectric permittivity, compared to HfO₂ (k~20) and ZrO₂ (k~20). HfO₂ was the first high-k gate dielectric material introduced, even from the technological node of 45nm, in the MOS technology [4]. In this study, we developed structures, using HfO₂ and Al₂O₃ as gate dielectrics. Specifically, 1.5nm HfO₂/p-Si and 2.5nm Al₂O₃/1.5nm HfO₂ /p-Si structures were grown via Atomic Layer Deposition Technique at 250°C. The precursors used for the growth of HfO₂ and Al₂O₃ were Tetrakis(Dimethylamido)Hafnium and Trimethylaluminum respectively. The co-reactant, in both cases, was H₂O. The stoichiometry and the thicknesses of both grown structures as well as the interfaces between Al₂O₃/pGe and HfO₂ /Al₂O₃ were evaluated and characterized through XPS analysis. For the electrical characterization of the developed structures, Al gate electrodes were grown through photolithography and lift of methods. C-V, C-f and J-V measurements were performed and analyzed in order to evaluate the density of interfacial traps (D_{it}), the EOT value as well as to determine the leakage currents through the structures [5].

[1] J. M. Rafi', M. Zabala, O. Beldarrain, and F. Campabadal "Deposition Temperature and Thermal Annealing Effects on the Electrical Characteristics of Atomic Layer Deposited Al₂O₃ Films on Silicon", Journal of The Electrochemical Society, 158 (5) G108-G114 (2011)

[2] M. J. Biercuk, D. J. Monsma, and C. M. Marcus, J. S. Becker and R. G. Gordon "Low-temperature atomic-layer-deposition lift-off method for microelectronic and nanoelectronic applications" Applied Physics Letters 83, 12 (2004)

[3] M.A. Botzakaki, N. Xanthopoulos, E. Makarona, C. Tsamis, S. Kennou, S. Ladas, S.N. Georga, C.A. Krontiras "ALD deposited ZrO₂ ultrathin layers on Si and Ge substrates: A multiple technique characterization" Microelectronic Engineering 112 (2013) 208–212.

[4] Interface-Engineered Ge Mosfets for Future High Performance CMOS Applications, Duygu Kuzum, Stanford University, December (2009).

[5] P. Svarnas, M.A. Botzakaki, G. Skoulatakis, S. Kennou, S. Ladas, C. Tsamis, S.N. Georga, C.A. Krontiras "Controllable growth of stable germanium dioxide ultra-thin layer by means of capacitively driven radio frequency discharge" Thin Solid Films 599 (2016) 49–53.

C-doped TiO₂ powder characterization via XRD-analysis and Photo-Electrochemical experiments

N. Karanasios^{1,2}, G. Litsardakis^{1,2} and S. Sotiropoulos^{1,3}

¹Post-graduate program "Processes and Technology of Advanced Materials",

²Department of Electrical & Computer Engineering,

³Department of Chemistry,

Aristotle University of Thessaloniki, Greece

Research towards the establishment of photo-electro-catalytic oxidation of organics as an advanced oxidation method for the degradation of organic pollutants, sometimes coupled with the production of hydrogen or electric energy, is timely. Special emphasis is given to its applicability under visible light illumination and to that direction photoanode materials that show visible light activity are highly demanded. These can be classified as single component semiconductors, bi-component semiconductors and modified TiO₂-materials. The latter include non-metal-doped (e.g. C-, N-, S-doped) as well as metal-decorated (e.g. Pt-, Au-, Ag-decorated) TiO₂ oxide powders or nanotubes. The aim of this study has been to produce C-doped TiO₂ nanopowders as visible-active photocatalytic materials. Catalyst preparation has been carried out by mixing TiO₂ (P25-Degussa) and carbon (Vulcan X) powders in ethanol, followed by drying and calcination at various temperatures in an inert or ambient atmosphere. Structure characterization was performed by powder XRD diffraction pattern analysis and photoelectrocatalytic testing towards water oxidation via cyclic voltammetry and chronoamperometry. XRD-analysis and 2θ-peak-indexing were accompanied by statistical analysis of the calculated crystal unit's dimensions. Photoelectrochemical experiments were carried out in a three-electrode cell by means of a potentiostat. Sample illumination by visible or UV light was achieved by appropriate lamps. Photocatalytic activity extended from the UV to visible range was recorded for certain samples. A direct correlation between variation of lattice parameters and photocatalytic activity, indicating that carbon enters the lattice of TiO₂ has not been observed. It is assumed that the beneficial effect of carbon is due to the creation of appropriate hetero-junctions at the catalyst surface rather than a change of its crystallographic structure.

Phononic band gaps in nanostructures

A. Konstantopoulou¹, M. M. Sigalas¹

¹*Department of Materials Science, University of Patras, Patra, Greece*

Abstract: Phononic band gaps (PBG), frequency areas where the propagation of phonons is not allowed, are created in nanostructures consisting of atoms of different atomic mass. For example, in graphene when C atoms are substituted with Si or Ge atoms wide PBGs may be created. Similarly, in WS₂ monolayers, PBGs can be created by replacing W atoms with Mo or S atoms with Se. Those systems were studied with Density Functional Theory for small sizes. For bigger sizes nanoparticles, molecular dynamics simulations with empirical potentials were used. PBGs in the nanoscale may be used to make phononic interconnects where the information can be transmitted with phonons. They can be also used to control the thermal conductivity.

Magnetic properties of FePt films in CD and Si patterned substrates

S. Karamanou¹, M. Vasilakaki¹, G. Giannopoulos¹, K. N. Trohidou¹, D. Niarchos¹

¹ *Institute of Nanoscience and Nanotechnology, NCSR Demokritos, Aghia Paraskevi, Greece*

Abstract: FePt magnetic thin films have attracted a lot of attention for many decades [1], because of their interesting physical properties. Magnetic anisotropy, magnetization switching processes, its high saturation magnetization and coercivity are examples of the most investigated properties of single thin films or multilayers for magnetic recording applications [2].

We have prepared FePt thin films deposited on CD-prepatterned and Si patterned substrates using the magnetron sputtering technique and we measured their magnetic properties. We found that their coercive field and magnetic anisotropy strongly depend on substrate and the deposition conditions [3].

Monte Carlo simulations with the Metropolis algorithm [4] replicate very well the observed magnetic behaviour. The developed model well explains the role of the interparticle interactions through exchange and dipole-dipole coupling between the moments of FePt grains and predicts the optimum conditions for the magnetic recording applications.

References

- [1] B. Ghebouli, A. Layadi, A. Guittoum, L. Kerkache, M. Benkerri, A. Klimov, V. Preobrazhensky, and P. Pernod, *Eur. Phys. J. Appl. Phys.* 48, 30503 (2009)
- [2] Z.H. Wang, K. Chen, Y. Zhou, H.Z. Zeng, *Ultramicroscopy*, 105, 343, (2005)
- [3] M. Mebarki, A. Layadi, A. Guittoum, A. Benabbas, B. Ghebouli, M. Saad, N. Menni, *Applied Surface Science*. 257, 7025, (2011)
- [4] C. Binns, K.N. Trohidou, J. Bansmann, et al. *J. Phys. D* 38, R357 (2005)

Strain distribution in ultra-thin In(Ga)N/GaN quantum wells

G. P. Dimitrakopoulos¹, C. Bazioti¹, Th. Pavloudis¹, J. Kioseoglou¹, S. Kret², J. Kozirowska³, T. Suski³, E. Dimakis⁴, T. Moustakas⁵, Th. Karakostas¹ and Ph. Komninou¹

¹Physics Department, Aristotle University of Thessaloniki, 54124 Thessaloniki, Greece

²Institute of Physics, Polish Academy of Sciences, Al. Lotników 32/46 02-668 Warsaw, Poland

³Institute of High Pressures Physics, UNIPRESS, 01-142 Warsaw, Poland

⁴Helmholtz-Zentrum Dresden-Rossendorf, 01328 Dresden, Germany

⁵Boston University, Boston, MA 02215, U.S.A.

Abstract: In the field of III-Nitride compound semiconductors, a lot of emphasis is being placed on the effort for growth of ultra-thin pure InN or high In-content InGaN quantum wells (QWs). It has been shown that, through tailoring of the internal polarization, it is possible that such layers exhibit topological insulator properties, making them suitable for applications in spintronics and quantum computing [1]. Two-dimensional electron gas properties and a temperature-independent behavior in the diagonal resistance, indicating the topological nature of the 2DES, were demonstrated in monolayer-thick, nominally InN QWs [2]. At the same time, the internal quantum efficiency of optoelectronic devices can be benefited by the band gap engineering that is feasible by short period In(Ga)N/GaN superlattices (SPSs). However, the stress-strain state of such heterostructures has not been clarified so far, as it may deviate from the conventional biaxial one, i.e. the plane stress state also referred to as 'tetragonal distortion'. In the present contribution we have considered the interfacial accommodation at SPS samples comprising nominally 1, 2, and 4 monolayer (ML) thick QWs that were grown by molecular beam epitaxy (MBE) on (0001) GaN templates. We have employed high resolution transmission electron microscopy (HRTEM), and high resolution Z-contrast scanning TEM (HRSTEM) in order to correlate the chemical composition with the strain, focusing on the influence of pseudomorphic accommodation on the out-of-plane strain component. Phenomena of interfacial sharpness and indium clustering have also been considered. Experimental observations were analyzed using geometrical phase analysis, peak finding, and Z-contrast quantification. Experimental results were compared to theoretical simulations, in particular, energetic calculations using *ab initio* density functional theory and molecular dynamics with a modified Tersoff interatomic potential. In both cases, deviation from the biaxial stress state of InN was identified for these QWs in agreement with the experimental observations.

Acknowledgement: Work partially supported by the Sonata 8 (2014/15/D/ST3/03808) project of the Polish National Science Centre

[1] M.S. Miao, Q. Yan, C.G. Van de Walle, W.K. Lou, L.L. Li, K. Chang, *Phys. Rev. Lett.* **109**, (2012) 186803

[2] W. Pan, E. Dimakis, G.T. Wang, T.D. Moustakas, D.C. Tsui. *Appl. Phys. Lett.* **105**, (2014) 213503

Structural, magnetic and electronic properties of CuFe nanoclusters by density functional theory calculations

C. S. Cutrano, Ch. E. Lekka

*Department of Materials Science and Engineering University of Ioannina
Ioannina 45110, Greece*

Abstract

Environmental sustainable magnetic nanoclusters and coatings have been proposed to meet specific technological demands (like superior magnetic properties) and being therefore promising for technological applications e.g. for the production of innovative nano-robotic platforms.

CuFe nanoclusters are very promising since they are free from hazardous and scarce raw elements. In this work we present density functional theory calculations on several CuFe_x ($x < 10\text{at}\%$) nanoclusters aiming to reveal the relationship between the energetically favoured configuration and the magnetic moment. We have used the 13, 55, 147 and 309 icosahedral nanoclusters while the thin CuFe_x coating on Cu(111) has been also studied for comparison reasons. We found that Fe atoms likes to aggregate inside the CuFe nanocluster revealing the pure Cu surface shell as the energetically favoured. The electronic density of states (EDOS) reveals the broad Cu bulk band from -5eV up to -0.5eV, mainly due to the Cu d electrons. In addition, the Fe atoms are mainly responsible for the spin majority and minority EDOS difference close to the fermi level introducing the magnetic character of the nanoclusters. Finally, the nanoclusters' magnetic moment is mainly due to the Fe d electron spin up – down mulliken charge population differences while it is found to be higher in the cases where the Fe atoms are segregated in the Cu surface cell. These results could be used for the design of environmental sustainable smart alloys with superior magnetic properties.

Acknowledgments: This work was supported by the SELECTA (No. 642642) H2020-MSCA-ITN-2014 project

XXXII Panhellenic Conference on Solid State Physics and Materials Science
Conference Center "Carolos Papoulias", 18-21 September 2016, Ioannina, Greece

Enhanced Photocatalytic Activity of Composite Semiconducting/Plasmonic Materials: Towards Withholding of Heavy Metal Ions from Aqueous Solutions

N. Pliatsikas², K. Symeonidis³, G. Vourlias², M. Mitrakas³, D. Koutsogeorgis¹, P. A. Patsalas²,
K. Sarakinos⁴, N. Kalfagiannis¹

¹*School of Science and Technology, Nottingham Trent Univ, Nottingham, United Kingdom*

²*Physics, Aristotle University of Thessaloniki, Thessaloniki, Greece*

³*Chemical Engineering, Aristotle University of Thessaloniki, Thessaloniki, Greece*

⁴*Physics, Chemistry & Biology, Linkoping University, Linkoping, Sweden*

Abstract: TiO₂ is a well-known photocatalytic material. Its combination with plasmonic nanoparticles (NPs) has been demonstrated in the literature in various ways. A vast majority of the publications have focused on reactions involving photocatalytic decomposition of organic compounds and water splitting. However, there is little evidence on the efficiency of such composite materials in the intermediate photo-oxidation step required to achieve the removal of heavy metals during water purification (e.g. Mn). In the present study we investigate the enhanced photocatalytic activity of TiO₂ (E_g = 3.2 eV) and TiO_xN_y (N content set to provide samples with E_g either 2.8 eV, or 2.4 eV) with optically active Ag and Au NPs towards oxidation of Mn aqueous species (10 mg/L). The photocatalytic templates were immersed on aqueous solutions of Mn(II) oxy-anions. For the illumination of the samples we used a simple white LED lamp. XPS has been used to identify the retention of the metal ions and their oxidation state during photocatalysis. We demonstrate that the performance of the photocatalysts is a strong function of the E_g of the semiconductor, the properties of the NPs and the structure of devices. Two different structures examined where the metallic NPs were either on the top or beneath of the TiO_xN_y layer; in both cases enhanced photocatalytic was observed compared to pure (no NPs) TiO_xN_y and TiO₂. We show that by tailoring the E_g and the size of the NPs it is possible to maximize the photochemical activity of a semiconductor and create more efficient devices for heavy metal purification of water.

A material scientist's guide to fractal analysis

J. Nikolaides¹, D. Anestakes², N. Nikolaides³

¹*Department of Electrical engineering, AUTH, Egnatia, Greece*

²*School of Medicine, AUTH, Egnatia, Greece*

³*Automation Department, ATEITH, Sindos, Greece*

Abstract: Abstract: In this poster, we introduce the reader to fractal analysis, underlining its strong connection to the shapes of different materials. We demonstrate what led to the development of fractal analysis, introduce some ways that relevant quantities can be measured, and expand on the measurement methods that we have developed. We then illustrate the particular characteristics of our algorithms that make them especially attractive for classifying wildly diverse imaging methods, such as MRI images, AFM images, and optical microscope images. We end by mentioning some highly promising preliminary results we have extracted with regards to Alzheimer's disease, cancer and material classification.

Modification of Nanoparticle Arrays by Laser-Induced Self Assembly (MONA-LISA)D. V. Bellas¹, N. Kalfagiannis², D. C. Koutsogeorgis², P. Patsalas³, E. Lidorikis¹¹ *Department of Materials Science and Engineering, University of Ioannina, GR-45110 Ioannina, Greece*² *School of Science and Technology, Nottingham Trent University, NG11 8NS, Nottingham, United Kingdom*³ *Department of Physics, Aristotle University of Thessaloniki, GR-54124 Thessaloniki, Greece*

Abstract: Large scale nano-structuring of metals is one of the challenges for the future of plasmonic and photonic devices. Such a technology calls for the development of ultra-fast, high-throughput and low cost fabrication techniques. Laser processing, accounts for the aforementioned properties, representing an unrivalled tool towards the anticipated arrival of modules based in metallic nano-structures, with an extra advantage: the ease of scalability. Specifically, laser nano-structuring of ultra-thin metal film or an alternative ceramic/metal film on a substrate results respectively on surface [1] (MNPs on the surface of the substrate) or subsurface [2] (MNPs embedded in a dielectric matrix) plasmonic patterns with many applications. In this work we investigate theoretically the photo-thermal processes involved in surface and sub-surface plasmonic nano-structuring and compare to experiments. To this end, we present a design process and develop functional plasmonic nano-structures with pre-determined morphology by tuning the annealing parameters like the laser's fluence and wavelength and/or the structure parameters like the thickness of the metallic film and the volume ratio of the ceramic metal composite. For the surface plasmonic nano-structuring we utilize the ability to tune the laser's wavelength to either match the absorption spectral profile of the metal or to be resonant with the plasma oscillation frequency (LSPR), i.e. we utilize different optical absorption mechanisms that are size-selective. Thus, we overcome a great challenge of Laser Induced Self Assembly by combining simultaneously large-scale character with nanometer scale precision. For subsurface plasmonic nano-structuring, on the other hand, we utilize the temperature gradients that are developed spatially across the metal/dielectric nano-composite structure during the laser treatment. We find that the developed temperature gradients are strongly depended on the nanocrystalline character of the dielectric host which determines its thermal conductivity, the composition of the ceramic/metal and the total thickness of the nano-composite film. The aforementioned material parameters combined with the laser annealing parameters can be used to pre-design the final morphology of the sub-surface plasmonic structure. The proposed processes can serve as a platform that will stimulate further progress towards the engineering of plasmonic devices.

[1] N. Kalfagiannis, et al., *Nanoscale* 8, 8236 (2016).[2] A. Siozios et al., *Nanotechnology* 26, 155301 (2015).

Molecular Modelling of the OPV Active Material at the Vicinity of Ag Nanoparticles

C. Trapalis¹, E. Lidorikis¹, D.G. Papageorgiou¹

¹*Department of Materials Science and Engineering, University of Ioannina, Ioannina 45110, Greece*

Abstract: Silver nanoparticles are used in the active layer of OPVs in order to increase performance. However little is known about their effect on the structure of the active materials. Using classical force fields and molecular dynamics simulations we studied the structural and energetic properties for PCBM and 3-hexyl-thiophene oligomers in the vicinity of fcc (111) silver nanoparticles surfaces. During this study we have developed a new set of parameters for Ag-organic interface interactions and we have adjusted appropriately the torsion parameters for the 3-hexyl-thiophenes. Through the simulations performed we have observed a preferred position for PCBM with the tail away from the Ag surface. Furthermore examining the adsorption energy, of the preferred PCBM positioning, at different temperatures and comparing to 3HT oligomers layers, lying flat on the Ag surface, we have discovered that while at temperatures below 100K the 3HT oligomers are the preferred phase to be adsorbed, while at higher temperatures the trend changes with the 3HT phase being less preferred to be adsorbed onto the surface.

Dielectric characterisation of PA6/ Boehmite alumina nanocomposites. The effect of compounding method.

G.N. Tomara¹, P. K. Karahaliou¹, G.C. Psarras², S. N. Georga¹, C.A. Krontiras¹

¹*Department of Physics, University of Patras, 26504, Patras, Greece*

²*Department of Materials Science, University of Patras, 26504, Patras, Greece*
 and

L. Lendvai³, J. Karger-Kocsis^{3,4},

³*Department of Polymer Engineering, Faculty of Mechanical Engineering, Budapest University of Technology and Economics, Műegyetem rkp. 3., Budapest H-1111, Hungary*

⁴*MTA-BME Research Group for Composite Science and Technology, Műegyetem rkp. 3., Budapest H-1111, Hungary*

Abstract: Water-assisted (WA) melt compounding gains an ever growing ground on the field of nanocomposites preparation due to its significant advantages compared to traditional methods. The most important of them are: the reduced health risk during melt mixing of nanoparticles in aqueous slurry compared to dry, volatile powders and the improvement of the dispersion even without surface modification of the filler [1, 2].

In the present study, nanocomposites of PA6 with 3 wt% boehmite alumina (BA) were prepared in two different ways: (i) dry and (ii) water dispersed BA powder was introduced into polyamide 6 (PA6) matrices via direct melt compounding. BA is easily dispersed in water due to the presence of hydroxyl groups on its surface. This, in combination with the hydrophilic character of polyamide chains, is expected to lead in a better dispersion of the nanofiller within the matrix.

Within the current study we investigate the dispersion and the dielectric response of the produced nanocomposites. Broadband dielectric spectroscopy was employed for the electrical characterisation of the samples, over a wide frequency (10^{-1} Hz to 10^6 Hz) and temperature (-100 °C to 150 °C) range. At least four relaxation mechanisms were recorded in the dielectric spectra of PA6 and PA6 based nanocomposites, which are associated with: (i) local motions of CH₂ segments involving dipolar amide groups (γ -mode of PA6), (ii) to local motion of the polar chain segments involving water molecules hydrogen bonded to free NH groups (β -mode of PA6), and (iii) the glass-rubber transition (α -mode of PA6) that can be deconvoluted into "wet" and "dry" relaxation modes, and (iv) interfacial polarisation (IP) due to the presence of the filler [3, 4]. The way these relaxation mechanisms are influenced by the presence of BA and the quality of the dispersion, as well as by the preparation technique is presented and analysed.

References:

1. Karger-Kocsis, J., Kmetty, Á., Lendvai, L., Drakopoulos, S. X., Bárány, T.: Water-Assisted Production of Thermoplastic Nanocomposites: A Review. *Materials*, 8(1) 72-95 (2014).
2. Siengchin, S. Dynamic mechanic and creep behaviors of polyoxymethylene/boehmite alumina nanocomposites produced by water-mediated compounding Effect of particle size. *Journal of Thermoplastic Composite Materials*, 26(7) 863-877 (2013).
3. Füllbrandt, M., Wellert, S., Von Klitzing, R., Schönhals, A. Thermal and corrosion (in) stability of polyamide 6 studied by broadband dielectric spectroscopy. *Polymer*, 75, 34-43 (2015).
4. Nikaj, E., Stevenson-Royaud, I., Seytre, G., David, L., Espuche, E.: Dielectric properties of polyamide 6-montmorillonite nanocomposites. *Journal of Non-Crystalline Solids*, 356(11) 589-596 (2010).

Electrical Properties and Thermal Imaging of Commercial NiTi wires

A. Theodorakakos¹, K. Zorbas¹, S.G.Stavrinides², E. Hatzikraniotis¹, K.M. Paraskevopoulos¹

¹Department of Physics, Aristotle University of Thessaloniki, 54124 Thessaloniki, Greece

²Computer Science Department, University of Thessaly, 35131, Lamia, Greece

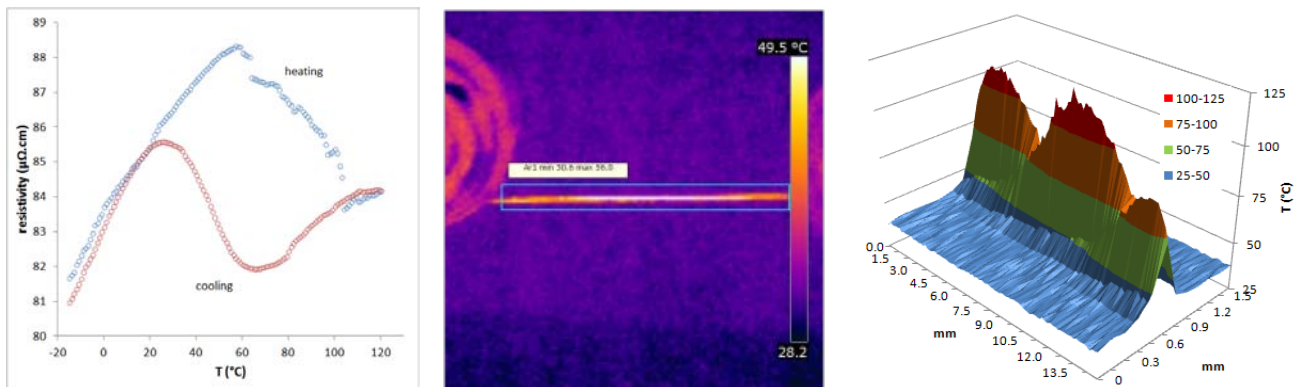
Abstract:

NiTi alloys exhibit two closely related and unique properties: shape memory effect and superelasticity. Shape memory is the ability of NiTi wires to undergo deformation at one temperature, and then recover its original, un-deformed shape upon heating above its transformation temperature. NiTi-based materials are widely accepted as one of the best families of shape memory alloys (SMA). SMA materials are sensitive to temperature and/or stress, producing a large macroscopic strain, through the so-called martensitic transformation.

Martensitic transformation is a thermoelastic reversible crystallographic phase transition from high-temperature phase (Austenite), to a low temperature phase (Martensite). In some cases (depending on alloy's composition, thermal history and manufacturing) an intermediate phase known as R-phase, appears during cooling; resulting in a two-stage process: the high-temperature Austenite phase first transforms into the intermediate R-phase and then to Martensite, at low-temperature.

The transformation behaviour has been studied by different methods, namely, electrical resistivity, differential scanning calorimetry (DSC), magnetic susceptibility, and thermoelectric power. Several studies have shown that electrical resistivity measurements can be a useful and reliable probe for the identification of both temperature and stress induced transformations. Their electrical properties reveal a potential to be used as memristive devices, thus, the exact assessment of the alloy's temperature-profile is critical.

In this work we report the resistivity measurements as well as the thermal imaging of four commercial $\text{Ni}_{1+x}\text{Ti}_{1-x}$ wires, with different composition and hence different transformation temperatures. Two of the wires were un-annealed and two annealed. Resistivity measurements were performed under constant current in a custom-made thermal bath, capable of varying the temperature in the range of -50°C to 200°C . Thermal Imaging was performed while heating the samples with constant current (up to 2A), using an i-7 FLIR thermal camera equipped with Ge close-up lenses and the whole results are presented.



(a) Typical resistivity curve (b) thermal imaging and (c) temperature profile of a NiTi wire

Surface degradation of aluminium matrix composites reinforced by WC nanoparticles and aluminide particles

A. Lekatou¹, N. Gkikas¹, A.E. Karantzalis¹, G. Kaptay², Z. Gacsi³, P. Baumli², A. Simon³

¹ Department of Materials Science & Engineering, University of Ioannina, Ioannina 45110, Greece

² Department of Nanotechnology, University of Miskolc, 3515 Miskolc-Egyetemváros, Hungary

³ Institute of Physical Metallurgy, Metalforming and Nanotechnology, The University of Miskolc, 3515

Abstract:

The present work is part of a greater effort to fabricate particulate reinforced AMCs with the following objectives: (i) low cost conventional casting assisted by stirring and salt fluxing for improved particle wetting and distribution; (ii) addition of submicron carbide particles aiming at combining the advantages of ultra-fine dimensions with the excellent intrinsic properties of carbides and the good particle-liquid metal wetting compatibility of carbides with a strong metallic character; (iii) employment of ex-situ reinforcement volume fractions sufficiently low to limit segregation; (iv) optimization of surface property performance by attaining extra in-situ reinforcement. Within the above framework, aluminum matrix composites were prepared by adding submicron sized WC particles into a melt of Al 1050 under mechanical stirring, with the scope to determine: (a) the most appropriate salt flux amongst KBF_4 , K_2TiF_6 , K_3AlF_6 and Na_3AlF_6 for optimum particle wetting and distribution and (b) the maximum carbide volume fraction (CVF) for optimum responses to surface properties. The nature of the wetting agent notably affected particle incorporation, with K_2TiF_6 providing greater particle insertion. A uniform aluminide and WC particle distribution was attained. Sliding wear testing showed that at low CVFs ($\leq 1.5\%$), crack propagation was delayed by the dispersion; at high CVFs (2.0%), crack propagation was obstructed by a tribolayer. Reverse polarization in 3.5 wt.% NaCl revealed impurity-induced intergranular corrosion. The reinforcement/matrix interphase remained corrosion-free.

Corrosion and wear behaviour of HVOF WC-Co-Cr nanostructured and conventional coatings

A. Lekatou¹, D. Sioulas¹, D. Manitsas¹, A.E. Karantzalis¹, D. Grimanelis²

¹ *Department of Materials Science & Engineering, University of Ioannina, Ioannina 45110, Greece*

² *Dept. of Special Processes, Hellenic Aerospace Industry, S.A., 32009 Schimatari, Greece*

Abstract:

Thermal sprayed WC-Co based coatings are widely used for wear and corrosion resistance applications such as aerospace, automotive, biomedical, chemical, power plants etc. applications. Recently, nanostructured cermet thermal spray coatings have attracted great research interest owing to superior hardness and improved wear resistance compared to the conventional coatings, as a result of high grain boundary density. In this work, conventional and nanostructured WC-10%wt Co-4%wt Cr powders were deposited by HVOF (High Velocity Oxygen Fuel) on Al 7075 T6. The nanocoating presented higher porosity (nevertheless, still less than 1%), less decarburization and less oxidation due to the compact grain morphology of the nanopowder feedstock. Its hardness was higher than that of the conventional coating due to the greater specific surface of the carbide phase. Both coatings exhibited high sliding wear resistances. The nanocoating, however, presented even higher wear resistance than the conventional one. Electrochemical tests (cyclic polarization and chronoamperometry) in 3.5% NaCl revealed similar corrosion mechanisms for the nano- and conventional coatings. Both coatings were found susceptible to localized forms of corrosion. The nanocoating showed better performance to salt spray test without any apparent corrosion signs after 45 days of exposure to the salt chamber.

XAFS study of hydroxyapatite and fossil bone apatiteI. M. Zougrou¹, M. Katsikini¹, M. Brzhezinskaya², F. Pinakidou¹,
L. Papadopoulou³, E. Tsoukala³, E. C. Paloura¹¹School of Physics, Aristotle University of Thessaloniki, 54124 Thessaloniki, Greece²Main Department Scientific-Technical Infrastructure II, Helmholtz Zentrum Berlin,
12489, Berlin, Germany³School of Geology, Aristotle University of Thessaloniki, 54124 Thessaloniki, Greece

Abstract: Ca L_{2,3}-edge XANES spectroscopy is applied for the study of variations in fossil bone apatite crystallinity due to heavy bacterial alteration and catastrophic mineral dissolution. The results are referred to those from well-preserved fossil apatite, fresh bone, and geologic apatite. In order to identify the origin of the peaks in the Ca L_{2,3}-edge XANES spectrum of hydroxyapatite, Ca^[1]₄Ca^[2]₆(PO₄)₃(OH)₂, the spectrum was simulated using the CTM4XAS code. The atomic multiplet spectrum arising from the distorted octahedral bonding geometry of the Ca^[2] site was simulated using octahedral (O_h) crystal field symmetry (10Dq=0.76 eV). The simulation gives rise to the 1, 2, a₁, a₂, b₁ and b₂ peaks (Fig. 1). The Ca^[1] nine-fold coordinated site, that was simulated using D_{4h} symmetry (10Dq=-0.6 eV, Dt=0.06 eV, Ds=0 eV), gives rise to the a₁₀, 3 and b₁₀ peaks and also contributes to the intensity of the 2, a₂ and b₂ peaks. As shown in Fig. 1, the simulated spectrum, that results after summing up the contribution of the Ca^[2] and Ca^[1] sites and taking into account the site occupancy, reproduces very well the experimental spectrum. In fossil bone samples the apatite crystallinity was determined from the energy difference between the a₂ and the average position of the a₁ and a₁₀ peaks in the Ca L_{2,3}-edge XANES spectra. The highest and lowest crystallinity values were observed for the bone with increased microbial porosity and the well preserved fossil bone respectively, indicating that bioerosion influences the crystallization process presumably *via* its by-products. The local bonding environment of Sr and the Ca site-preference with varying Sr/Ca content in fossil bone apatite was studied by Sr K-edge EXAFS spectroscopy. The analysis reveals a mixed Ca^[1] and Ca^[2] occupancy for Sr with a small preference for the Ca^[2] site for Sr/Ca = 0.017–0.024 gr/gr and a definite preference for the Ca^[2] site for Sr/Ca = 0.040 gr/gr.

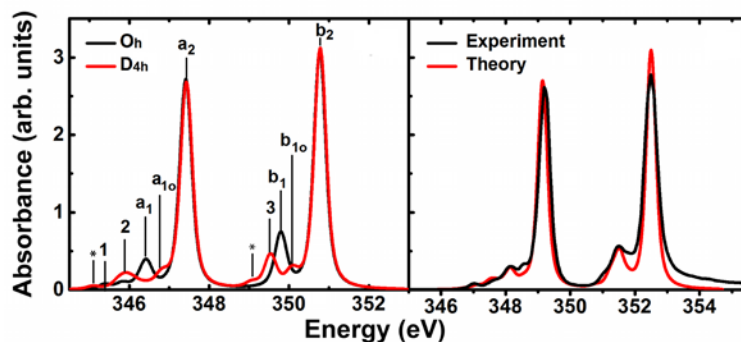


Fig. 1: CTM4XAS simulation of the Ca L_{2,3}-edge XANES spectra of hydroxylapatite: (Left) Simulated contribution of the Ca^[1] and Ca^[2] sites with point symmetry D_{4h} and O_h, respectively; (Right) Comparison of the simulated and experimental spectra.

Acknowledgments: Financial support from the European Community's 7th Framework Programme (FP7/2007-2013-grant agreement Nr. 312284) is greatly acknowledged.

Vitrification and devitrification treatment for the stabilization of chromium containing tannery ash

S. Varitis¹, P. Kavouras¹, G. Kaimakamis¹, G. Vourlias¹, E. Pavlidou¹, K. Chrissafis¹,
 E. Pantazopoulou², A.I. Zouboulis², M. Mitrakas³, Th.Karakostas¹, A.Xenidis⁴, Ph. Komninou¹

¹Physics Department, Aristotle University of Thessaloniki, Thessaloniki 541 24, Greece

²Chemistry Department, Aristotle University of Thessaloniki, Thessaloniki 541 24, Greece

³School of Chemical Engineering University of Thessaloniki, Thessaloniki 541 24, Greece

⁴School of Mining and Metallurgical Engineering, National Technical University of Athens, Greece

Abstract: We report on the vitrification and devitrification of chromium containing ashes originated from the incineration of tannery sludge. The waste was retrieved from the tannery effluent treatment facilities in the industrial area of Thessaloniki in the form of a dried sludge. The sludge was homogenized and characterized structural, morphological and chemical. Due to the high quantities of the contained organic species and Cr the waste could not be safely disposed. Two different incineration conditions were applied in order to remove the organic content while the speciation of Cr in the resulting ash was monitored. The first included incineration in oxygen abundance (oxic) conditions and resulted to complete removal of the organic content and oxidation of Cr to the hexavalent state. On the other hand, incineration under oxygen absence (anoxic) conditions removed part of the organic content and Cr was maintained in the trivalent form [1].

Vitrification was conducted utilizing the Cr-ash from the anoxic conditions which was mixed either with glass forming (SiO_2) and network modifying (Na_2O and CaO) oxides in different proportions [2] or combined with Red Mud and Fly ash, exploiting that they contain high quantities of glass forming and network modifying species. The batch mixtures were melt in a Pt crucible at 1400°C . Subsequently devitrification was conducted in temperatures determined by DTA and resulted to separation of different crystalline phases. Characterization included XRD, SEM-EDS and DTA analysis while TEM observations were conducted to study the local structure in the nanoscale. Leaching tests revealed that most of the products were chemically inert.

Finally, stabilization/solidification was conducted through mixing of Cr-ash with scrap soda lime glass in different proportions and sintering in different temperatures. The resulting products were either opaque ceramics or resembled the as-vitrified ones [3].

Acknowledgement

This research has been co-financed by the European Union (European Social Fund - ESF) and Greek national funds through the Operational Program "Education and Lifelong Learning" of the National Strategic Reference Framework (NSRF) - Research Funding Program: THALES: Reinforcement of the interdisciplinary and/or inter-institutional research and innovation.

Reference

- [1] P. Kavouras, E. Pantazopoulou, S. Varitis, G. Vourlias, K. Chrissafis, G.P. Dimitrakopoulos, M. Mitrakas, A.I. Zouboulis, Th. Karakostas, A. Xenidis. Incineration of tannery sludge under oxic and anoxic conditions: Study of chromium speciation. *J. Haz. Mat.* 283 (2015) 672-679
- [2] S. Varitis, E. Pavlidou, P. Kavouras, G. Vourlias, K. Chrissafis, A. Xenidis, Th. Karakostas Devitrification routes of a vitrified chromium-loaded ash *Journal of Thermal Analysis and Calorimetry* Vol 121, 1, pp 203–208
- [3] S. Varitis, P. Kavouras, G. Vourlias, E. Pavlidou, Th. Karakostas, Ph. Komninou "Production of Composite Materials by Mixing Chromium-Rich Ash and Soda-Lime Glass Powder: Mechanical Properties and Microstructure" *Int J. Chem, Nucl, Mat Met. Eng* Vol:9, No:6, 2015

Ionic Conductivity comparative study of LiZnVO_4 and LiMgVO_4

A. Kazakopoulos¹, C. Sarafidis², O. Kalogirou²

¹*Department of Electronics, T.E.I. of Thessaloniki 57 400 Thessaloniki Greece*

²*Dept. of Physics, Aristotle University of Thessaloniki, 54124 Thessaloniki, Greece*

Abstract:

LiMgVO_4 and LiZnVO_4 are materials used in electrochemical devices and in humidity sensors. In particular LiMgVO_4 has interesting properties related to luminescence due to the tetrahedrally coordinated V^{5+} atoms. The information related to the cation distribution in the LiMgVO_4 structure is still under debate. The LiMgVO_4 has been assigned to the olivine Pnma space group. The purpose of this work is to study and compare the conduction mechanisms of LiMgVO_4 and LiZnVO_4 at temperatures from 25 to 500 °C, using impedance spectroscopy measurements at frequencies from 42 Hz to 1 MHz, in order to deduct useful information about the Li ion diffusion and mobility in its structure. The bulk activation energy values were calculated to be around 1.20 eV, while two grain boundary conductivity processes were detected with activation energies almost half of the bulk (at near room temperature area) and 1.4 eV at higher temperatures. In both stoichiometries the loss factor ($\tan\delta$) versus frequency presents one peak in the temperature range from 400 – 500 °C which suggests the presence of relaxation procedures. The modulus master curves present a scaling behavior that suggests non Debye type conductivity relaxation and ion migration via hopping.

Structural Analysis of Waste Material from Mafic Rock Quarries Used for CO₂ Sequestration

A. Delimitis¹, I. Rigopoulos², Th. Kyratsi²

¹Chemical Process & Energy Resources Institute (CPERI), Centre for Research & Technology Hellas (CERTH), 6th km. Charilaou - Thermis road, 57001 Themi, Thessaloniki, Greece

²Department of Mechanical and Manufacturing Engineering, University of Cyprus, 1678 Nicosia, Cyprus

Sequestration of carbon dioxide by *ex situ* mineral carbonation has the potential to safely store CO₂ as carbonate minerals, which are stable over geological time scales. This method could become more economically viable by using solid wastes rich in Ca²⁺, Mg²⁺ and Fe²⁺, generated from quarrying processes. In the present study, the structural characteristics of a representative sample of waste material, obtained from a mafic rock quarry is investigated using Transmission Electron Microscopy (TEM) methods. The waste material was subjected to the ball milling process, in order to produce a nanostructured material with enhanced CO₂ adsorption capacity.

TEM experiments were carried out in both the unmilled and the ball-milled sample with the highest CO₂ uptake. A comparison of TEM images from the quarry waste before and after the ball milling process, shown in Fig. 1(a) and (b), confirms the significant reduction of particle size due to mechanical activation: the unmilled sample is predominantly composed of particles with sizes larger than 600 nm, whereas the majority of the particle sizes after ball milling is in the 30-50 nm range. Furthermore, TEM revealed that in the ball-milled sample a great percentage of particles are highly disordered or even, amorphous, implying that ball milling not only leads to nanoscale particle size reduction, but also to crystal structure amorphization of the constituent minerals. Energy dispersive X-ray spectroscopy (EDS) confirmed that the dominant mineral phases are chlorite (clinochlore, cc), actinolite (ac), albite, augite, anorthite, quartz (q) and magnetite. Such structural modifications in the crystal structure of the constituent silicate minerals are considered to be the most significant factor towards the enhancement of the CO₂ uptake of the quarry waste under study.

Although the sizes of the primary augite crystals are quite small, ranging between 8 and 40 nm, they are still highly crystalline as proved by selected area diffraction (SAD) and HRTEM experiments. The fact that these particles retain their crystallinity even after extensive ball milling, demonstrates their high resistance to mechanical activation. Having in mind that augite is an anhydrous Ca-, Mg-, Fe-bearing silicate mineral, it is suggested that the presence of augite nanocrystals in the milled quarry waste is closely linked to the high CO₂ adsorption capacity of this material. Specifically, it is considered that augite nanocrystals comprise a significant number of surface sites that promote the carbonation process.

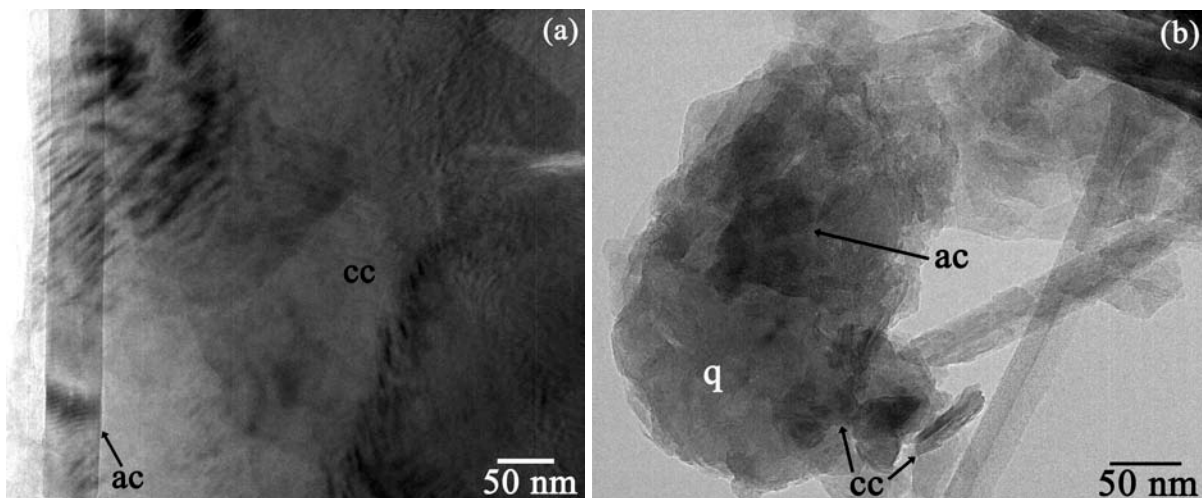


Fig. 1: TEM images of quarry waste material (a) before and (b) after ball milling.

POSTER SESSION II

Tuesday 20 September 2016, 19:00-20:30

*Electronics, photonics and
optoelectronics*

*Strongly correlated systems,
magnetism & superconductivity*

*Polymers, organic materials and
biomaterials*

**Ab-initio structure prediction
and electronic properties of $[\text{Si}_x\text{Sn}_{1-x}]_3\text{N}_4$ ternary nitrides**Th. Pavloudis¹, M. Zervos², Ph. Komninou¹, J. Kioseoglou¹¹*Department of Physics, Aristotle University of Thessaloniki, GR-54124 Thessaloniki, Greece*²*Nanostructured Materials and Devices Laboratory, Department of Mechanical and Manufacturing Engineering, PO Box 20537, Nicosia 1678, Cyprus*

Abstract: Group IV-Nitrides with spinel structures i.e. $\gamma\text{-M}_3\text{N}_4$ (M= Si,Ge,Sn) exhibit electronic bandgaps which span the visible spectrum making them suitable for optoelectronic devices. $[\text{Si}_x\text{Sn}_{1-x}]_3\text{N}_4$ is the most challenging ternary compound, with a bandgap tunable over a broad area. The USPEX evolutionary structure prediction code interfaced with the VASP code is used in order to predict the structure of Sn_3N_4 . The energetically preferable is found to be the spinel structure, while the second best is the hexagonal $\beta\text{-Si}_3\text{N}_4$ -like structure. Following these results, an in depth analysis of the $[\text{Si}_x\text{Sn}_{1-x}]_3\text{N}_4$ ternary alloy is performed, resulting in the preferable atom configurations for both cubic and hexagonal $[\text{Si}_x\text{Sn}_{1-x}]_3\text{N}_4$ for the full range of x. The cubic structure is found to be preferable for small Si content, but before $x=0.33$ a switch to the hexagonal structure occurs. Finally, hybrid functional calculations are employed to accurately construct the bandstructures of all the examined configurations and the corresponding bandgaps are calculated. A quadratic fit is applied and the bowing parameters of the bandgaps for both structures are extracted.

Comparison between beta and ultraviolet (UV) induced Thermoluminescence in Lithium Fluoride (LiF)

L. Dodoleri¹, P. Kesidou¹, I.K. Sfampa¹, G. Kitis¹

¹Nuclear Physics Laboratory, Aristotle University of Thessaloniki, 54124, Thessaloniki, Greece.

Introduction: Crystals of Lithium Fluoride (LiF) have been studied widely for several years as is one of the most commonly used Thermoluminescence dosimetric material (TLD). It is well known that LiF has several individual glow peaks observed in both low Temperatures and high Temperatures. The aim of the present study is to photo transfer (study photo transferred TL, PTTL) the electrons from deep traps (high Temperature, T) to shallow traps ($T < 400\text{ }^{\circ}\text{C}$) using UV light. It was also examined the possibility of having UV induced TL instead of PTTL.

Experimental Procedure: The sample used in this experiment is LiF TLD-100 crystals. TL measurements were carried out using Harshaw-3500 TLD-Reader. The irradiations were applied through a $^{90}\text{Sr}/^{90}\text{Y}$ beta particle source, delivering a beta dose of 0,028 Gy/s. All measurements were performed in a nitrogen atmosphere with a low constant heating rate of $2\text{ }^{\circ}\text{C/s}$ in order to avoid significant temperature lag.

Table I: Two experimental procedures were applied in two LiF crystals:

Steps	Procedure A	Procedure B
1	Test Dose: 1,72 Gy	-
2	TL up to $T_{\max}=350\text{ }^{\circ}\text{C}$	-
3	TD 1,72 Gy	-
4	TL up to $T=250^{\circ}\text{C}$	-
5	Exposure to UV for t_i	Exposure to UV for t_i
6	Repeat steps 3, 4 and 5	Repeat Step 5

Where $t_i = 1\text{min}, 2\text{min}, 4\text{min}, 8\text{min}, 16\text{min}, 32\text{min}, 1\text{hr}$ and 2hr .

Results and Discussion: Following are presented the results of the experimental procedure. In figure 1, on the left is the comparison between the two crystals for 32min UV with beta dose added and without. On the right is the comparison of normalized TL intensity for various times. The two figures show that beta induced TL is higher than the UV induced TL.

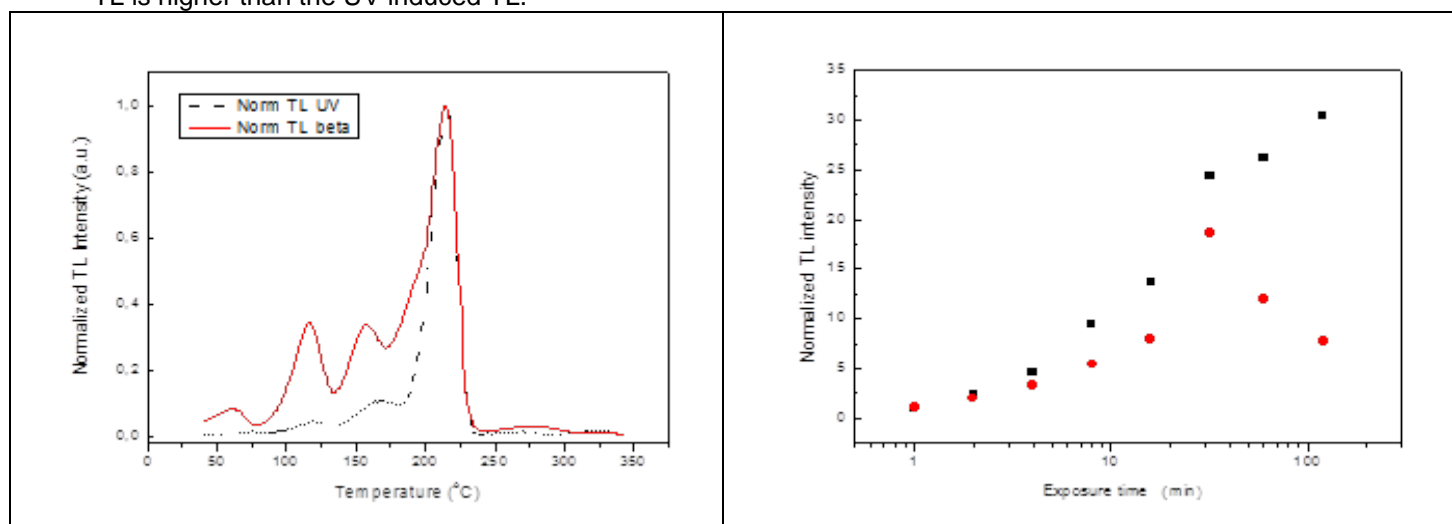


Figure 1: (left) Comparison of TL in two crystals, for $t=32\text{min}$ UV exposure, (right) Comparison of Normalized TL for various times. Red circles are for the UV exposed crystal and black squares for the Irradiated crystal.

References:

- [1] Budzanowski, M., Sas-Bieniarz, A., Bilski, P., Bubak, A., Kopeć, R., Rad. Meas, 56 (2013), 389-392
 [2] Benevides, L., Voss S., Nita. I, Rotunda J, Velbeck. K, Luo L.Z., Moscovitch M., Rad. Prot. D., 144 (2011) 199-201

Photoconductive properties of nanocrystalline TiO₂ powders prepared in acidic environment

T. Georgakopoulos^{1*}, N. Todorova², C. Trapalis² and K. Pomoni¹

¹Department of Physics University of Patras, 26500 Patras Greece

²Institute of Nanoscience and Nanotechnology, National Centre for Scientific Research "Demokritos" 15343, Ag. Paraskevi Attikis, Greece

For the preparation of the samples in acidic environment, 3.32 mL TBO were digested in 100 mL of 0.5 M aqueous solution of sulphuric acid (SA) for 30 min under vigorous stirring at room temperature. Then, the solution was poured into a 100 mL Teflon-lined autoclave occupied 80% of its volume. Two different solution heat treatments were used, the first at 180 °C for 10h and the second at 180 °C for 24h. Moreover, TiO₂ nanocrystalline powder, TiO₂-W, was prepared in neutral environment. After natural cooling to room temperature, the powder products were washed with distilled water to neutral conditions, and then dried at 70 °C for 24 h. The powders obtained were abbreviated as sample TiO₂-SA 10h and TiO₂-SA 24h, respectively. By means of XRD measurements the phase of the TiO₂-SA samples was found only anatase, in agreement with Z. Zhao et al., while for TiO₂-W a mixture of anatase and brookite phase was identified.

Fig.1 shows the diffuse reflectance spectra. The effective band gap of these samples was estimated from the absorption function $[f(R) \times E]^{1/2}$ was plotted against E (eV), where $F(R) = (1 - R)^2/2R$ is the Kubelka-Munk function expressed through the measured diffuse reflectance R (fig.2).

The transient photoconductivity (σ_p) of the samples TiO₂-SA 10h, TiO₂-SA 24h and TiO₂-W, in vacuum at 300K, is illustrated in Fig.3. The σ_p of all samples after a quick rise show the usual sublinear behavior indicating the competition between photogeneration, recombination and thermal release rates [2]. The TiO₂-SA samples present higher σ_p values when compared to TiO₂-W sample attributed to their anatase phase [3]. The TiO₂-SA 24h sample reaches larger σ_p values (fig. 4) due to the better nucleation and growth because of the prolonged reaction time [1].

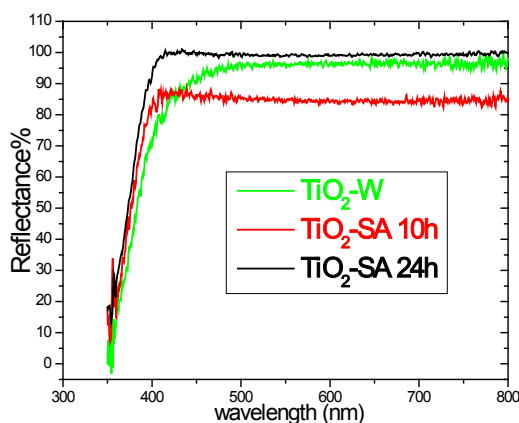


Fig.1. Measured diffuse reflectance spectra of the samples TiO₂-W, TiO₂-SA 10h and TiO₂-SA 24h

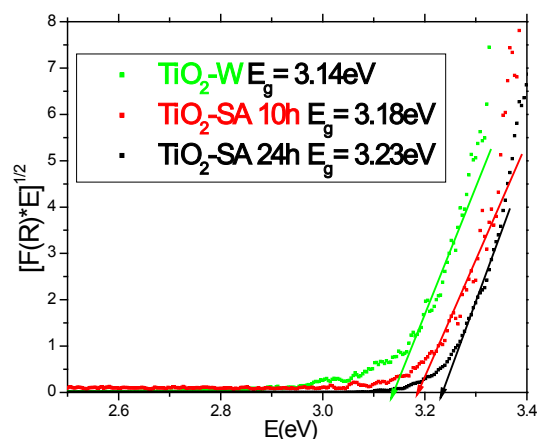


Fig. 2. Absorption function $[f(R) \times E]^{1/2}$ vs energy E for the samples TiO₂-W, TiO₂-SA 10h and TiO₂-SA 24h

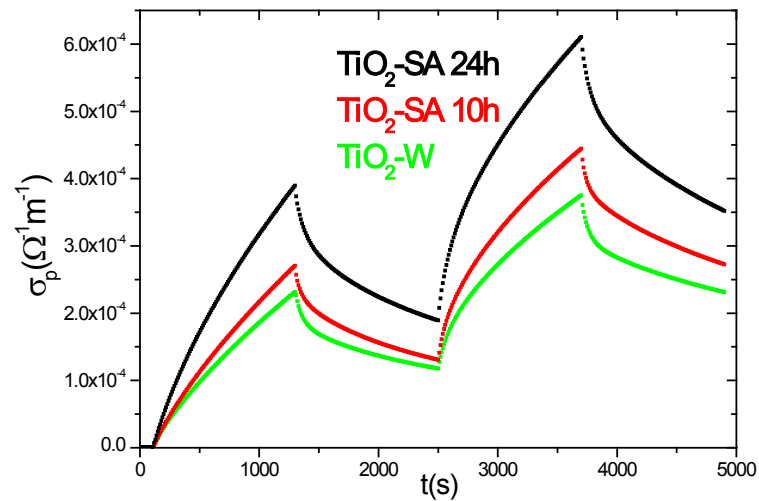


Fig.3. The photoconductivity response at 300K, in vacuum, of the samples $\text{TiO}_2\text{-SA 24h}$, $\text{TiO}_2\text{-SA 10h}$ and $\text{TiO}_2\text{-W}$

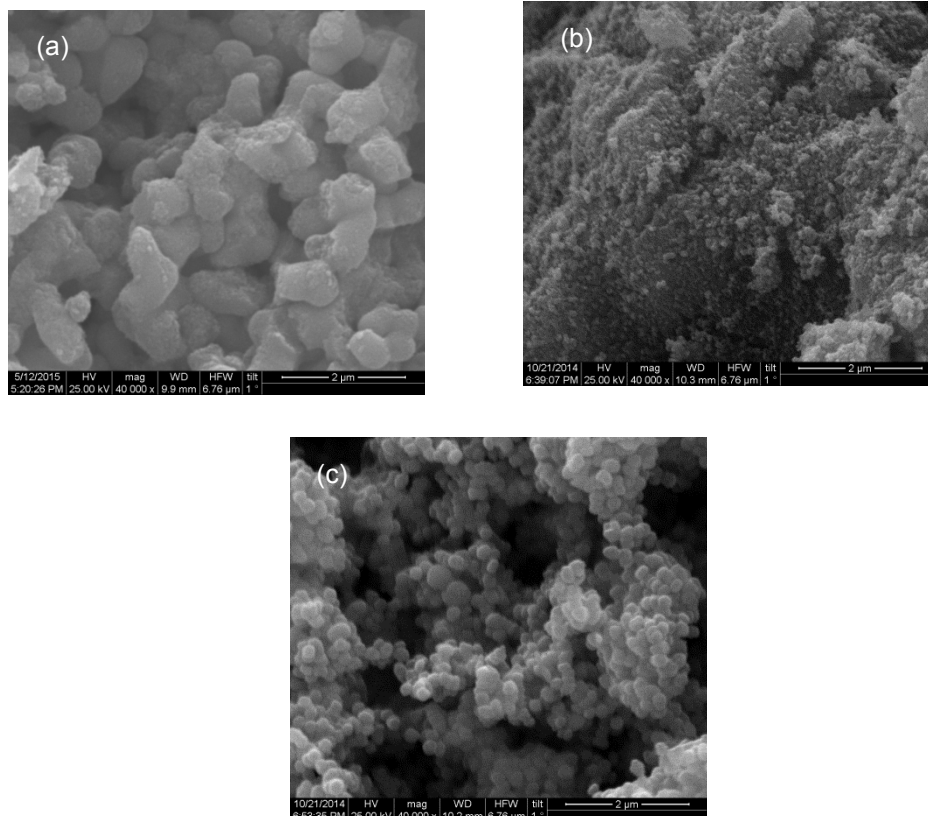


Fig.4 SEM images of samples a) $\text{TiO}_2\text{-W}$, b) $\text{TiO}_2\text{-SA 10h}$ and c) $\text{TiO}_2\text{-SA 24h}$

References

- [1] Z. Zhao, Z. Sun, H. Zhao, M. Zheng, P. Du, J. Zhao and H. Fan, J. Mater. Chem. 22 (2012) 21965-21971
- [2] K. Pomoni, T. Georgakopoulos, M.V. Sofianou, C. Trapalis, J. Alloys Compd. 558 (2013) 1-5
- [3] C. Colbeau-Justin, M. Kunst, D. Huguenin, J. Mater. Sci. 38 (2003) 2429-2437

Deconvolution on CaF:N glowcurves induced by ultraviolet (UV)

P. Kesidou¹, L. Dodoleri¹, I.K. Sfampa¹, G. Kitis¹

¹Nuclear Physics Laboratory, Aristotle University of Thessaloniki, 54124, Thessaloniki, Greece.

Introduction: Calcium fluoride, CaF:N, is one of the earliest known thermoluminescence (TL) materials and was among the first used for TL dosimetry due to their high sensitivity. In this study we deal with the computerized glow curve deconvolution analysis of thermoluminescence glow curves. The information by the CGCD is very useful in order to understand the thermoluminescence mechanism of materials.

Experimental Procedure: The sample used in this experiment was natural (fluorite) in the form of powdered crystals in two colours green and violet. All samples were first annealed up to 500°C for 1 hour. TL measurements were carried out using a Harshaw 3500 TLD-Reader. The irradiations were applied through a ⁹⁰Sr/⁹⁰Y beta particle source. All measurements were performed in a nitrogen atmosphere with a low constant heating rate of 2°C/s, in order to avoid significant temperature lag, and the samples were heated up to the maximum temperature of 400°C. The following experimental procedure was applied:

S1: Test Dose (TD) 1,72Gy and TL up to T_{max}: 400 °C.

S2: Exposure in UV light for t_i and TL up to T_{max}: 400 °C.

S3: Repeat S2 for various times. Where t_i= 10sec, 20sec, 40sec, 80sec, 160sec, 320sec, 640sec, 1280sec, 2560sec, and 5120sec.

Results: All glow-curves were analysed using a (CGCD). The analytical expression used was that of general order kinetic (GOK)[3], examples of CGCD are shown in fig1:

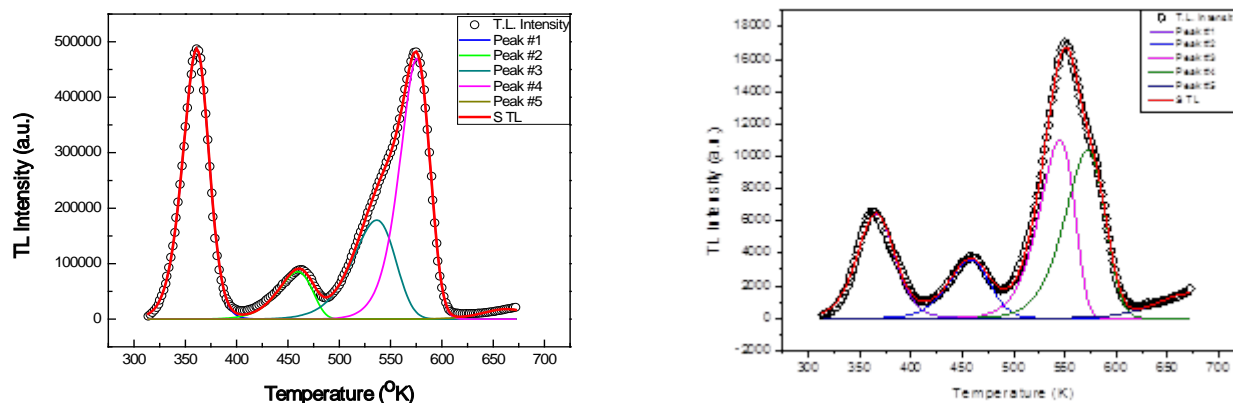


Fig. 1: Deconvolution on CaF:N exposed in UV light for t_i=640sec (left: green sample) (right: violet sample)

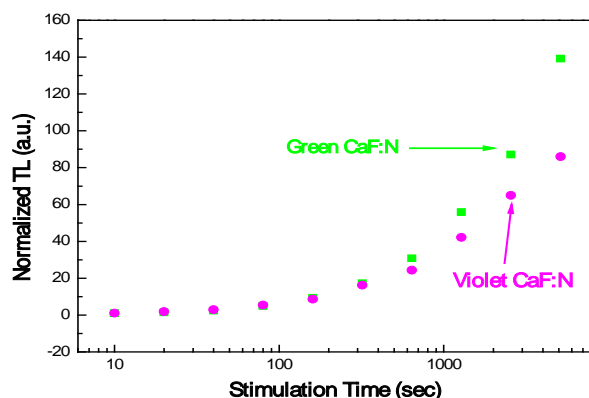


Fig.2: normalized TL vs stimulation time on UV irradiation

References:

1. H. Tugay, Z. Yegingil, T. Dogan, N. Nur, N. Yazici, NIM B 267 (2009) 3640–3651.
2. F.O. Ogundarea, F.A. Balogun, L.A. Hussaina, Radiation Measurements 38 (2004) 281 – 286
3. G Kitis, J M Gomez-Ros and J W N Tuyn, J. Phys. D: Appl. Phys. 31(1998)2636-2641

Dose rate dependence of Anomalous Fading (AF) in natural apatites.

P. Konstantinidis¹, F. Okkarides¹, I.K. Sfampa¹, G. Kitis¹

¹Nuclear Physics Laboratory, Aristotle University of Thessaloniki, 54124, Thessaloniki, Greece.

Introduction: Apatite crystals are well known for their use as thermoluminescence (TL) dosimetric material. Several studies about their luminescence properties have taken place. Present work has the aim to study the Dose Rate effect as well as the initial rise of natural apatites which exhibit the AF effect, with the laboratory names Durango and Mexico A1.

Experimental Procedure: The samples used in this experiment were crashed gently in an agate mortar and grains 30-80 μ m were selected. TL measurements were carried out using Harshaw-3500 TLD-Reader. The irradiations were applied through a ⁹⁰Sr/⁹⁰Y beta source, delivering a dose rate of 0,02 Gy/sec. All measurements were performed in a nitrogen atmosphere with a low constant heating rate of 2 °C/s.

The first protocol applied was (Initial Rise):

Step 1: Dose of 35Gy.

Step 2: Record TL glowcurve up to $T_{max}= 50^{\circ}C$

Step 3: Repeat Step 2 for a new T_{max} , where the measurement step is 5 $^{\circ}C$ and the final TL is up to 400 $^{\circ}C$.

Step 4: Dose of 52Gy on a fresh aliquot.

Step 5: Repeat Step 2-Step 3 after storage of 22hours in dark room.

The protocol applied for the second experiment is:

Step 1: Record of S_0 up to $T_{max}:400^{\circ}C$ for each sample (10 samples) after TD: 61.6Gy.

Step 2: TD on each sample

Step 3: Different storage time (t_i) for each one.

Step 4: Record of S_f for each sample after TD.

t_i : 0, 20min, 1hour, 1.6h, 3.2h, 6.9h, 11.5h, 17h, 24.5h.

Results: Following are presented in figure 1 the results of the first experimental protocol. On the right of the figures is the activation energy as a function of temperature. It is obvious that the AF affects especially the traps of lower energy. The plateau corresponds to the 300 $^{\circ}C$ peak, since a shift towards lower temperatures is observed after the Initial Rise method.

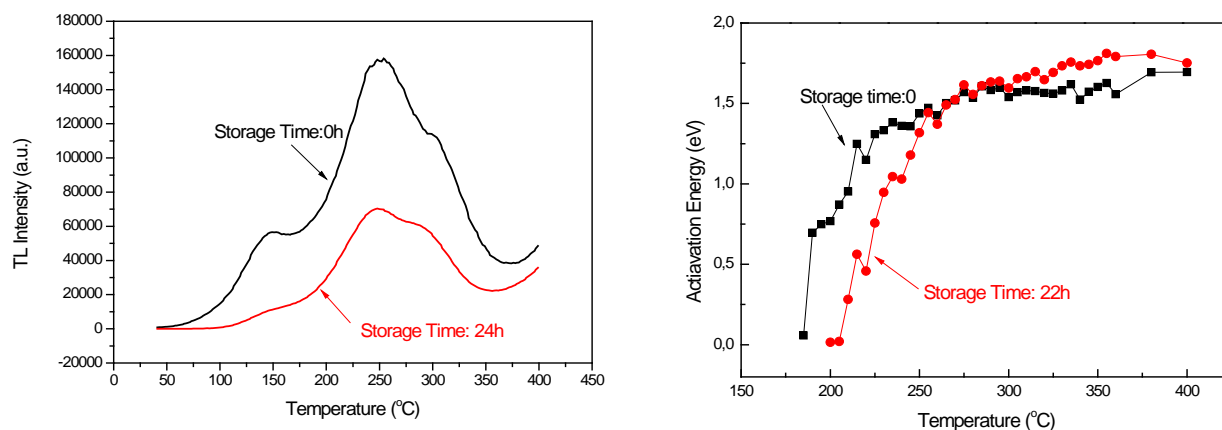


Figure 1: (left): Glowcurves recorded right after irradiation (black) and after 24hours (red). (right):Initial rise for Durango apatite crystal after irradiation (black) and after 24hours (red).

References:

1. G. S. Polymeris, V. Giannoulatou, I. K. Sfampa, G. Kitis. J. of Lum.153 (2014) 245-251
2. Sfampa, I.K., Polymeris, G.S., Tsirliganis, N.C., Pagonis, V. Kitis, G. NIMB, PRVol. 320, (2014), Pages 57-63
3. Kitis, G., Polymeris, G.S., Pagonis, V., Tsirliganis, N.C. Phys.Stat.Solid.Appl.Mat.Science, Vol. 203, Issue 15, (2006), 3816-3823

Electrical conductivity mechanisms of nanocrystalline TiO₂ powders prepared in acidic environment

V. Lionas^{1*}, T. Georgakopoulos¹, N. Todorova², K. Pomoni¹ and C. Trapalis²

¹Department of Physics University of Patras, 26500 Patras Greece

²Institute of Nanoscience and Nanotechnology, National Centre for Scientific Research "Demokritos" 15343, Ag. Paraskevi Attikis, Greece

For the preparation of the samples in acidic environment, 3.32 mL TBO were digested in 100 mL of 0.5 M aqueous solution of sulphuric acid (SA) for 30 min under vigorous stirring at room temperature. Then, the solution was poured into a 100 mL Teflon-lined autoclave occupied 80% of its volume. Two different solution heat treatments were used, the first at 180 °C for 10h and the second at 180 °C for 24h. Moreover, TiO₂ nanocrystalline powder, TiO₂-W, was prepared in neutral environment. After natural cooling to room temperature, the powder products were washed with distilled water to neutral conditions, and then dried at 70 °C for 24 h. The powders obtained were abbreviated as sample TiO₂-SA 10h and TiO₂-SA 24h, respectively. From XRD spectra (Fig.1), the phase of the TiO₂-SA samples was found only anatase while for TiO₂-W a mixture of anatase and brookite phase was identified.

The temperature dependence of the conductivity for all samples, plotted as $\ln(\sigma)$ versus $10^3/T$, in vacuum, is given in Fig.2. Several conductivity mechanisms are shown, acting at different temperature regions for each sample. Looking for the suitable conduction mechanism, in the temperature range 199-130K for TiO₂ -SA 24h, 277-187K for TiO₂ -SA 10h and 247-193K for the TiO₂ -W samples, the best fit of electrical conductivity data was attained for the $\ln(\sigma T^{1/2})$ versus $T^{-1/4}$ plot, indicating that it obeys to the Mott's variable range hopping (VRH). In Fig.4, the temperature dependence of $\ln(\sigma T^{3/2})$ versus $10^3/T$ suggests the SPH non-adiabatic conduction mechanism in the temperature regime 292-214K for TiO₂ -SA 24h, 343-277K for TiO₂ -SA 10h and 322-247K for the TiO₂-W, respectively. At high temperatures, the best fit was achieved for the $\ln(\sigma T^{1/2})$ versus $10^3/T$ plot related to grain boundary model (GB) for polycrystalline semiconductors (Fig.5), indicating that grains are partially depleted of charge carriers.

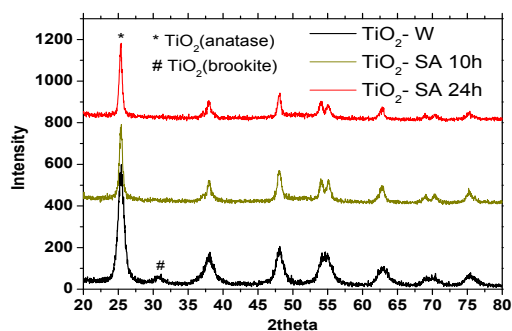


Fig. 1. XRD pattern

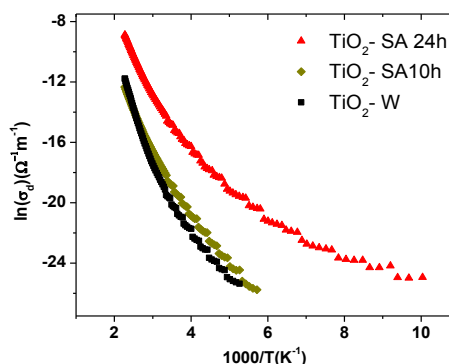


Fig. 2. Temperature dependence of the electrical conductivity plotted as $\ln(\sigma)$ versus $10^3/T$ in vacuum

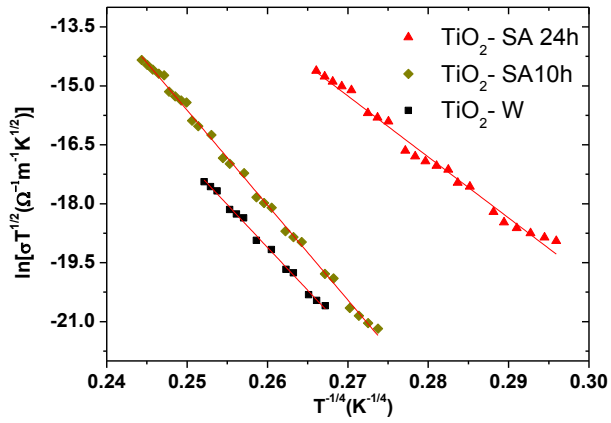


Fig. 3. Temperature dependence of $\ln(\sigma T^{1/2})$ versus $T^{-1/4}$, in vacuum

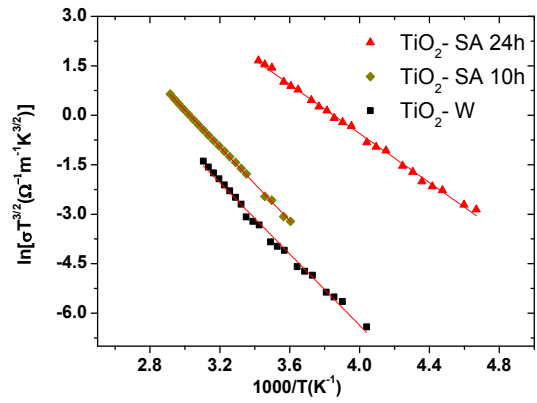


Fig. 4. Temperature dependence of $\ln(\sigma T^{3/2})$ versus $10^3/T$, in vacuum

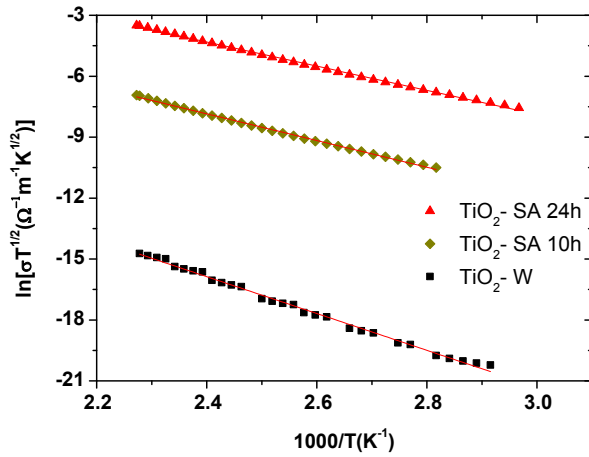


Fig.5. Temperature dependence of the electrical conductivity plotted as $\ln(\sigma T^{1/2})$ versus $10^3/T$ in vacuum

References

- [1] K. Ponomi, T. Georgakopoulos, M.V. Sofianou, C. Trapalis, J. Alloys Comp. 586 (2014) 52-58

XXXII Panhellenic Conference on Solid State Physics and Materials Science
Conference Center "Carolos Papoulias", 18-21 September 2016, Ioannina, Greece

EIS studies in incandescent lamps' tungsten wires

I. Karagiannis, I. Samaras,

Physics Department of Aristotle Univ. of Thessaloniki, Greece

Incandescent light bulbs, in addition to providing illumination, are useful from the context of basic and teaching basic physics to engineering, multi-physics and chemistry, as many other application driven applications. The electrical properties of incandescent lamps' W-wires are revised. It is based on two new experimental observations. One is the valuable information retrieved from the measured non-zero phase φ between voltage V and current i that registers in complex impedance $Z (=V/i)$. The other is the DC voltage V_{DC} background polarization used for DC power supply ensuring a constant temperature profile conditions in W-wires during the measurement of $Z(f)$ spectra. The frequency f of importance is in the wide range of 10^{-3} to 100 Hz and the phase (Z_φ) is in the "capacitive" range from near zero values to -90° . The maximum dynamic capacitive charge behavior, before lighting, was applied from HP in an innovative commercial (1955) AC function generator model HP200A helping HP to grow from a spin off (1954) to a big company we know today. This job will provide us the experimental tools to understand the electrical behavior of incandescent lamps' W-wires upon lighting, before lighting and the critical conditions just before lighting.

Solution-processed reduced graphene-based electrodes for organic photovoltaicsC. Petridis,^{1,2} D. Konios,¹ M. M. Stylianakis,¹ E. Stratakis,³ E. Kymakis¹¹*Center of Materials Technology and Photonics & Electrical Engineering Department, School of Applied Technology, Technological Educational Institute (TEI) of Crete, Heraklion 71004, Crete, Greece.*²*Department of Electronic Engineering Technological Educational Institute (TEI) of Crete, Chania 73132, Crete, Greece.*³*Institute of Electronic Structure and Laser Foundation for Research and Technology-Hellas, Heraklion 71110, Crete, Greece.*

Abstract: Since the isolation of free standing graphene in 2004, graphene research has experienced a phenomenal growth.^[1,2,3] Due to its exceptional electronic, optical and mechanical properties, it is believed to be the next wonder material for optoelectronics. The enhanced electrical conductivity, combined with its high transparency in visible and near-infrared spectra, enabled graphene to be an ideal low cost indium-tin oxide (ITO) substitute. Solution-processed graphene combines the unique optoelectrical properties of graphene with large area deposition and flexible substrates rendering it compatible with roll-to-roll manufacturing methods. This work provides an overview of recent research progress in the application and consequent physical-chemical properties of solution-processed graphene-based films as transparent conductive electrodes (TCEs) in organic photovoltaic (OPV) cells.^[4] Reduced graphene oxide (rGO) can be effectively utilized as the TCE in flexible OPVs, where the brittle and expensive ITO is incompatible.

Special attention is paid to the preparation of solution processable reduced graphene oxide micromesh (rGOMM) electrodes, using a laser-based patterning technique.^[5] This compatible with flexible, temperature sensitive substrates method allows to accurately control and enhance the electrode transparency, with a subsequent slight increase in the sheet resistance, and therefore improve the tradeoff between transparency and conductivity of reduced graphene oxide (rGO) layers. In addition, the effect of rGO flakes decoration with metal NPs (Au, Ag) on the sheet resistance and the transparency of rGO and rGOMM electrodes is also investigated. It is likely that the fabrication of mesh will increase the TCE transparency and at the same time the incorporation of metal NPs will boost its conductivity compared to pure rGO micromesh.

References

- [1] E. Stratakis, K. Savva, D. Konios, C. Petridis, E. Kymakis, *Nanoscale*, 6, 6925, (2014).
- [2] G. Kakavelakis, D. Konios, E. Stratakis, E. Kymakis, *Chemistry of Materials*, 26, 5988, (2014).
- [3] D. Konios, G. Kakavelakis, C. Petridis, E. Stratakis, E. Kymakis, *Journal of Materials Chemistry A*, 4, 1612-1623 (2016)
- [4] C. Petridis, D. Konios, M. M. Stylianakis, G. Kakavelakis, M. Sygletou, K. Savva, P. Tzourbakis, M. Krassas, N. Vaenas, E. Stratakis, E. Kymakis, *Nanoscale Horizons*, DOI: 10.1039/C5NH00089K (2016)
- [5] D. Konios, C. Petridis, G. Kakavelakis, M. Sygletou, K. Savva, E. Stratakis, E. Kymakis *Advanced Functional Materials*, (2015), 25, 2213-2221

Spectrometer free molecular sensing with graphene plasmons

S. Doukas, E. Lidorikis¹

¹*Department of Materials Science and Engineering, Univ. of Ioannina, GR 45110 Ioannina, Greece*

Abstract: Graphene plasmons have emerged as an attractive alternative to noble metal plasmonics for applications regarding infrared sensing. Both the tunability and the higher quality of graphene plasmons make them ideal for surface-enhanced infrared absorption experiments. With this technique molecular resonances, which are unique for each molecule, can be recorded for a wide range of wavelengths. In this work we study a recently proposed apparatus [1-3] where absorption is integrated over photon energy as a function of graphene doping level. Doing so, one can utilize this method without the use of spectrometers and laser sources in order to resolve the light wavelength. Instead, a molecular resonance corresponds to a certain doping level which in turn can be corresponded to specific photon energy. We investigate, via FDTD simulations, all these factors that can influence the device's spectral resolution, including graphene's short relaxation time in the spectral vicinity of graphene's phonons. By using the plasmon quality factor, which is critical for the method's efficiency, as a figure of merit we conclude that the simple addition of an Au mirror at a certain distance can dramatically enhance the resolution of the device. We also explore the possibility of using graphene's much sharper quadrupolar term, instead of the broader dipolar term which is commonly used, in order to be able to identify molecular resonances that are indistinguishable when a broad plasmon resonance is used.

[1] Marini et al, ACS Photonics 2015

[2] Rodrigo et al, Science 2015

[3] Farmer et al, ACS Photonics 2016

Optimal designs of plasmonic organic photovoltaics

I. Vangelidis, E. Lidorikis

Department of Materials Science and Engineering, Univ. of Ioannina, GR 45110 Ioannina, Greece

Incorporation of plasmonic nanoparticles inside optimized organic solar cells is a promising technique for increasing the optical thickness of the photovoltaic absorber layer while keeping the physical thickness fixed. This can be achieved with either, or both, the effects of near-field focusing and far-field scattering of the plasmonic resonances of noble metal nanoparticles. Despite several efforts in literature to incorporate plasmonic enhancers in OPVs, the overall benefits in performance enhancement remain limited and contradicted. This occurs due to the trade-offs between the various parameters that affect the utility of metallic nanoparticles, such as nanoparticle dispersion and device geometry. In this work a full evaluation and optimization of all parameters in MNPs implementation (metal, size, position and periodicity of NPs, as well as device layer thicknesses) is conducted. The different phase spaces of plasmonic enhancement mechanisms are found (i.e. of near-field focusing and far-field scattering), and interesting interplays with the device layer architecture are revealed. These interplays are the main reason for contradictory results and predictions found in the literature. Being now able to simultaneously optimize device architecture and plasmonic nanoparticle dispersion, more than 20% photocurrent enhancement can be achieved for the highly efficient low band-gap polymer blend PCDTBT:PCBM.

Critical temperature investigation in high temperature superconductors by means of magnetic susceptibility measurements

I. Hanis, E.Halevas and G.Litsardakis,
*Laboratory of Materials for Electrotechnics,
Department of Electrical & Computer Engineering,
Aristotle University of Thessaloniki, Greece*

The Laboratory of Materials for Electrotechnics operates a QD Versalab system, capable of measurements up to 3 T at temperatures 50-400K, as well as a QD PPMS (Physical Properties Measurement System), with a 9 T magnet operating at 4-400 K. The Versalab is equipped with a VSM head and the PPMS with AC susceptibility, DC magnetization extraction and electric transport probes. Cooling of the superconducting magnets is achieved by closed cycle Gifford-McMahon cryopumps that do not require the prohibitively expensive liquid helium, but a moderate supply of affordable helium gas.

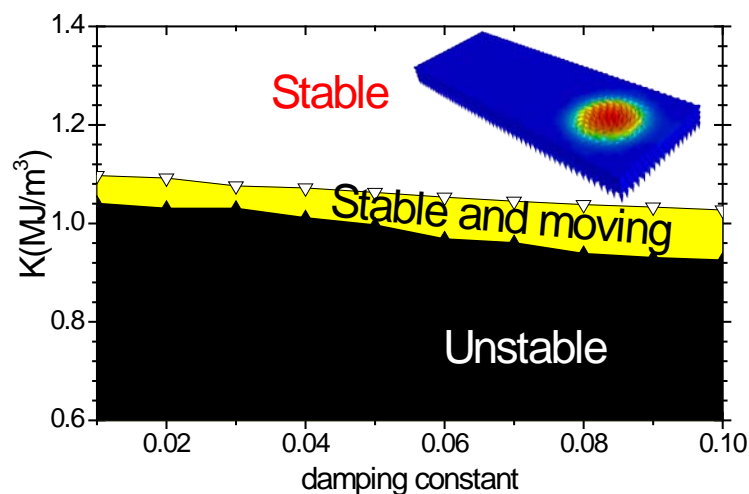
Thanks to the open architecture of the instruments and to in-house modifications, these measurement probes can now be interchangeably used in both systems, allowing for greater versatility and cost efficiency in their use.

In order to demonstrate the capabilities of the instruments, which are open to access by the scientific community, either as a service or in cooperation projects, in this poster we present magnetic properties investigations of high temperature superconductors and vanadium complexes.

Motion of Magnetic Bubbles by Electric Currents in Perpendicular Anisotropy Films

Th. Tzartzas¹, L.N. Gergidis¹, I.Panagiotopoulos¹
¹*Department of Materials Science and Engineering,
 University of Ioannina, Ioannina 45110, Greece*

Recently "topologically protected" spin textures as Skyrmions have attracted a lot of interest for future spintronic devices [i] due to their unique properties as stability, rapid and defect-insensitive current-driven motion [ii]. Here we present a micromagnetic study of the stability and current-driven motion of Skyrmions in elongated thin film structures (180nm x 60nm x10nm) which technically simulate magnetic wires as the demagnetization factors along the three directions do not differ substantially from the \square x 60nm x10nm case. The stabilization is done solely by perpendicular anisotropy i.e. without any Dzyaloshinskii–Moriya underlayers. The initial Skyrmion configuration rapidly relaxes to a bubble formation which under the presence of a current of 10^8 A/cm² can move with velocities from 32 m/s for damping constant $\alpha=0.01$, to 62 m/s for $\alpha=0.09$. It is found that there is only a narrow range of magnetocrystalline anisotropy values (which depend weakly on the α) that permit the stabilization and current driven motion of Skyrmion-like structures along the wire.



ⁱ Xichao Zhang, Motohiko Ezawa and Yan Zhou, Nature Scientific Reports 5 (2015) 9400

ⁱⁱ J. Sampaio, V. Cros, S. Rohart, A. Thiaville And A. Fert Nature Nanotechnology 8 (2013) 839

A novel approach for Plastic Bonded Magnets of the type MQU-F melt spun NdFeGaB –type alloys

S. Karamanou¹, M. Gjokas¹, E. Devlin¹, V. Psycharis¹, A. Ioannidou¹, G. Vekinis¹ and D. Niarchos¹

¹INN, NCSR Demokritos, Athens, Greece

Abstract:

Two routes are used to make bonded magnets: [injection molded magnets](#) can be formed into complex shapes and be insert molded directly onto other components to produce assembly parts, and [Compression bonded magnets](#) offer higher magnetic output than injection-molded magnets, but are limited to more simple geometries. The densities obtained with the former technique are in the range of 55-65 % of the theoretical magnetic density and for the second technique can reach up to 75 % and in special cases 78 %. These densities are much less of the one's achieved for sintered magnets, which approach 99 %, resulting to energy products $(BH)_{\max}$ of the 50-60 % of the theoretical density of the used powder.

In order to increase the energy density in bonded magnets we introduce a novel technique we termed "plastic sintering", an approach that simulates the classical sintering of magnetic powders of NdFeB.

We have employed a magnetic powder provided by Molycorp of the type MQU-F and as plastic binder MMA. We have coated a distribution of micron sized particles with a very thin < 1 micrometer with MMA, dried and then subjected to compression up to 1.5 GPa. To polymerize the compressed powders we used a conventional furnace and a microwave furnace at around the polymerization temperature of 85 °C, for the conventional furnace for a period of 3 hours and for the microwave furnace for 10-15 minutes.

We observed that:

- It is possible to plastic sinter MQU-F powders with a density in excess of 80 %
- Sintering time is at least ten times faster with microwaves compared to the conventional way. Care must be taken not to overheat the alloy, because it decomposes
- This approach is very promising for the formation of strong plastic bonded magnets with an energy product higher than the commercial ones

Work supported by the H2020-INAPEM project.

**Numerical Study of the Exchange Bias properties of
MnFe₂O₄/γ-Fe₂O₃ core/disordered shell nanoparticles**M. Vasilakaki¹, K. N. Trohidou¹, F.G.Silva^{2,3,4}, R.Aquino^{2,5}, R. Perzynski^{3,4}, J.Depeyrot²¹ *Institute of Nanoscience and Nanotechnology, NCSR Demokritos, Aghia Paraskevi, Greece*² *Complex Fluids Group, Instituto de Física, UnB70919-970, Brasília (DF), Brazil*³ *Sorbonne Universités, UPMC Univ Paris 06, UMR8234, PHENIX, F-75005 Paris, France*⁴ *CNRS, UMR8234, PHENIX, F-75005 Paris, France*⁵ *Laboratório de Nanociência Ambiental Aplicada - NAA, Faculdade UnB Planaltina, UnB73300-000, Brasília (DF), Brazil*

Abstract: The structure and the low-temperature magnetic properties of non-textured diluted frozen dispersions of single 3.3 nm sized nanoparticles (NPs) consisted of a soft MnFe₂O₄ core protected by a disordered maghemite shell have been experimentally investigated [1,2]. We use Monte Carlo simulations technique to study the exchange bias behaviour of these systems [3,4] in an atomic scale.

The model assumes spherical ferrimagnetic soft core/hard disordered shell nanoparticles with Heisenberg exchange interaction between the spins. We consider uniaxial anisotropy along the z-axis in the core and at the interface and random anisotropy in the shell and at the surface. To take into account the random distribution of the NPs in the ferrofluid, the cooling field has been applied in different directions and the hysteresis loop is calculated by averaging on the hysteresis loops along each magnetic field direction. Our simulations have been performed for several cooling field sizes and they show that the optimum exchange bias field is achieved for a cooling field of the order of the anisotropy field. Higher cooling fields lead to the decrease of the exchange bias value. Our numerical results reproduce well the experimental findings confirming that the NPs consist of a well-ordered ferrimagnetic core surrounded by a disordered spin glass-like surface layer [1,2].

[1] F. G. Silva, R. Aquino, F. A. Tourinho, V. I. Stepanov, Yu. L. Raikher, R. Perzynski and J. Depeyrot, *J. Phys. D: Appl. Phys.* 46 (2013) 285003 (9pp)

[2] R. Cabreira-Gomes, F.G.Silva, R.Aquino, P.Bonville, F.A.Tourinho, R. Perzynski, J.Depeyrot, *J. M. M.* 368 (2014) 409–414

[3] M. Vasilakaki and K. N. Trohidou, *Phys. Rev. B.* 79 (2009) 144402

[4] Marianna Vasilakaki, Kalliopi Trohidou, Josep Nogués, *Scientific Reports*, 5 (2015) 9609

Electrical properties of VO₂ layers on Y-ZrO₂ substrates

A. Theodorou¹, E. Syskakis²

¹*Section of Solid State Physics, Department of Physics, National and Kapodistrian University of Athens, Panepistimiopolis, GR-15784, Zografos*

The VO₂ metal insulator transition (MIT) at about 340 K is a topic of long standing research. Apart from the elucidation of the transition mechanism, it has attracted intensive application-oriented research interest originating by the dramatic change of electrical resistivity accompanying this ultrafast structural transition. Emphasis is given to emerging devices operable by triggering the MIT transition by small thermal, electrical or optical perturbation at around RT.

In the present work, VO₂ layers with typical thickness of 10 μm were investigated by electrical resistivity, I-V measurements, XPRD and SEM. Using Y-ZrO₂ substrates, sintered as well as dense VO₂ layers were obtained by annealing V₂O₅ layers in the range 450-600 °C under vacuum (10⁻²mbar).

Specimen show semiconducting behaviour at 80 K < T < T_{MIT} with an activation energy E_a ≈ 0.1 eV. The observed MIT at T_{MIT} = 327.1 K results in an up to 3 orders of magnitude drop of the electrical resistivity, taking place within a ~4 K temperature interval. According to the I-V measurements the MIT can be triggered by a dc applied electric field as well as by joule heating.

Magnetic ordering and low field CMR in $\text{La}(\text{Mn}, \text{Cr})\text{O}_{3+\delta}$ ($\delta \approx 0.09, 0.12$) compounds

K. Georgalas¹, E. Syskakis², A. Samartzis³

¹Section of Solid State Physics, Department of Physics, National and Kapodistrian University of Athens, Panepistimiopolis Gr-15784 Zografos, Athens, GREECE

Cr^{3+} substituting Mn^{3+} in LaMnO_3 -based compounds can be viewed as a "big" immobile hole, since it has the same electronic configuration ($t_{2g}^3 e_g^0$), as Mn^{4+} and an ionic radius $r_{\text{Cr}^{3+}} = 0.615 \text{ \AA}$ almost equal to that of Mn^{3+} . It has been claimed that Cr^{3+} participates to the DE mechanism, while it is known to aid the long range ferromagnetic (FM) ordering in the low doping regime.

In the present work, electrical resistivity, $\rho(T)$ ($80 < T < 1100\text{K}$), $\chi_{\text{ac}}(T)$ and LFMR(T) ($H=2\text{kG}$) ($80 < T < 300\text{K}$) measurements were carried out on O_2 -enriched $\text{LaMn}_{1-x}\text{Cr}_x\text{O}_{3+\delta}$ specimen. The powders were prepared by solid state reaction from high purity La_2O_3 , $\text{Cr}(\text{NO}_3)_3 \cdot 9\text{H}_2\text{O}$ and MnO_2 and the specimen were sintered at $T=1300^\circ\text{C}$ in air. In order to obtain high O_2 excess they were heated in O_2 and in air ($T=900^\circ\text{C}/t=100\text{h}$). XRPD patterns confirmed that the specimen were single phased with the O_2 treated specimen having $R\bar{3}c$ symmetry.

Specimen show small polaron semiconducting behavior at $80 < T < 1100\text{K}$. The Cr^{3+} substitution for Mn^{3+} increases the $\rho(T)$ and the activation energy, E_a , due to the gradual decrease of the delocalized electrons concentration and increase of (Mn, Cr)-O bond distance. According to the $\chi_{\text{ac}}(T)$ measurements, long range FM order is established in all samples at $T < 170\text{K}$. The Curie temperatures, T_C , vary non-monotonously with x , displaying a maximum value close to $x=0.12$, caused by the competition of the DE FM Mn^{3+} - Mn^{4+} with SE AFM Mn^{3+} - Cr^{3+} interactions. LFMR(T) show low negative magnetoresistance approximately of the order of 2-3%. The broad peaks of $-\text{MR}$ observed close to the corresponding T_C 's, are attributed to intrinsic DE CMR. The progressive decrease of $-\text{MR}$ versus x , implies that Cr^{3+} does not participate in the DE mechanism.

Processing of MnBi particles by high energy surfactant assisted ball milling

K. Kanari¹, C. Sarafidis¹, M. Gjoka², D. Niarchos² and O. Kalogirou¹

¹Dept. of Physics, Aristotle University of Thessaloniki, 54124 Thessaloniki, Greece

²INN, NCSR Demokritos, Athens 15310, Greece

Nowadays, the field of magnetic applications is dominated by high performance permanent magnets containing rare-earth metals. However, the high cost along with limited supply of rare-earth elements resulted in search of potential substitutions. The intermetallic compound MnBi is a rare-earth-free permanent magnetic material and its low temperature phase (LTP) has large magnetocrystalline anisotropy ($K \approx 10^7 \text{ erg cm}^{-3}$) [1] due to its hexagonal NiAs crystal structure and a positive temperature coefficient of coercivity [2], which makes it an excellent candidate for high temperature applications [3].

Due to the peritectic reaction of Mn with Bi it is rather challenging to prepare single-phase MnBi particles. We followed a mechanochemical approach, with surfactant assisted high energy ball milling. MnBi ingots were arc-melted and subsequently annealed, then grinded and mechanically milled along with oleic acid and oleylamine as surfactants. Crystal structure of the samples were examined by X-ray powder diffraction (XRD) and chemical composition was measured with EDS. Scanning electron microscopy (SEM) and magnetic hysteresis loops by using a vibrating sample magnetometer (VSM) were also performed.

We began with MnBi particles (Fig. 1) smaller than 50 μm . Samples were extracted from the mill in $t = 1, 2, 3, 5, 10, 20, 40, 80 \text{ h}$. From the first hour of milling the coercivity plummeted and did not increase with further processing. In a similar tone, MnBi has magnetic remanence (M_r) of $18.05 \text{ Am}^2/\text{kg}$ at the beginning; however it drops to almost $0.1 \text{ Am}^2/\text{kg}$ in all the samples. A new non-magnetic phase $\text{Bi}(\text{Mn})_2\text{O}_3$ was detected. It seems that the surfactant is not adequate protection for the brittle MnBi LTP phase at least when high energy ball milling is used.

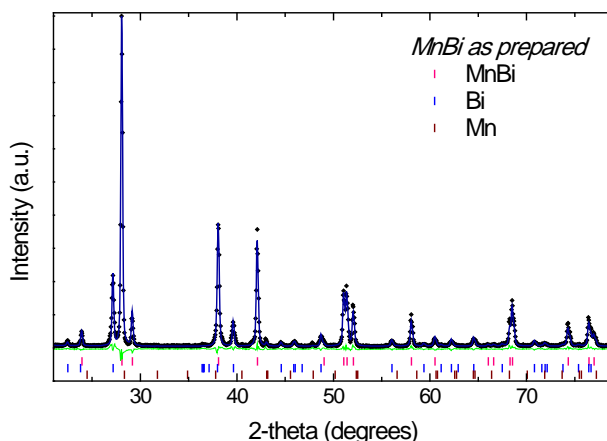


Fig. 1 – XRD analysis of initial MnBi powder.

Acknowledgement: This work is partially supported by AUTH Research Committee (Project No 93282 - Support of new researchers: Advanced Magnetic Materials).

References

- [1] N.V. Rama Rao, A.M. Gabay, X. Hu, G.C. Hadjipanayis, J. Alloys Compds. **586** (2014) 349-352.
- [2] Y. B. Yang et al., J. Appl. Phys. **111** (2012) 07E312.
- [3] Jian Shen, Huizhong Cui et al, RCS Adv. **5** (2015) 5567-5570.

Synthesis, processing and characterization of FeMnGa nanoparticles for permanent magnet applications

G. Sempros¹, K. Kanari¹, C. Sarafidis¹, M. Gjoka², C. Chrissafis¹, N. Lupu³, G. Ababei³, D. Niarchos², O. Kalogirou¹

¹*Dept. of Physics, Aristotle University of Thessaloniki, 54124 Thessaloniki, Greece*

²*Institute of Nanoscience and Nanotechnology, NCSR "Demokritos", Athens, Greece*

³*National Institute of R&D for Technical Physics, 47 Mangeron Blvd., 700050 Iasi, Romania*

Abstract:

In recent years, there is a great demand in materials suitable for permanent magnets which led to shortages in the supply of rare earth elements, a basic ingredient of high performance magnets. Research for rare earth free magnetic materials is considered as a viable alternative. Various Heusler alloys are investigated as possible candidates. Among them, the binary compound Mn_xGa has gained interest. A method of improving the magnetic properties of intermetallic compounds is the introduction of a magnetic atom like Fe in replacement of a 3d metal, in our case, by replacing a quantity of Mn with Fe. In this study $Mn_{0.4}Fe_{0.3}Ga_{0.3}$ alloys were prepared in a high purity Ar atmosphere with the arc-melting technique followed by melt-spinning in order to get nanostructured ribbons. The samples were further treated (annealing, mechanical processing) in order to tune the microstructure, mostly to reduce the grain size and obtain single phase particles with optimum magnetic properties. Magnetization measurements were performed by using a Vibrating Sample Magnetometer (VSM), versus temperature and field. The structure of the samples was observed with the X-Ray Diffraction Patterns (XRD). The $L1_2$ structure was observed for the first time, among the other ones $D0_{19}$ and $L2_1$ which are already observed in Mn_3Ga studies. A deeper observation was performed with Scanning Electron Microscopy (SEM) and Thermogravimetric Analysis (TG), in which the stoichiometry and the homogeneity were confirmed. Saturation magnetization of the basic material was measured at $81.4 \text{ Am}^2/\text{kg}$ while remanence and coercive field were low. The effect of the grain size on the magnetic properties, due to mechanical processing, is presented.

Acknowledgement: This work is partially supported by AUTH Research Committee (Project No 93282 - Support of new researchers: Advanced Magnetic Materials).

Study of Magnetization Reversal in Layered Heterostructures by Vector-Magnetometry

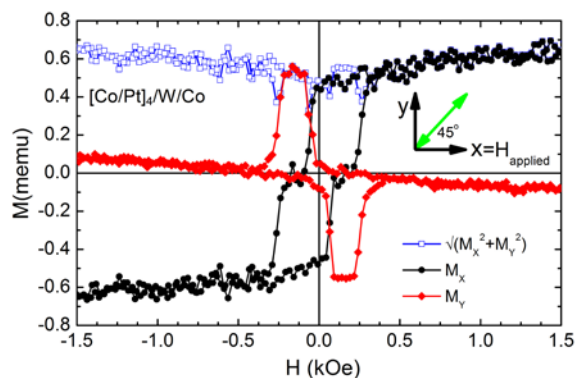
A. Markou^{1,2}, A. Mourkas¹, A. Koume¹, D. Vartzioti¹, I. Panagiotopoulos¹

¹Department of Materials Science and Engineering,
 University of Ioannina, Ioannina 45110, Greece

²Current Address: Max Planck Institute for Chemical Physics of Solids,
 Nöthnitzer Straße 40, 01187 Dresden, Germany

Vector magnetometry refers to simultaneous measurement of two magnetization components (along the applied field M_x and perpendicular to it M_y) during the hysteresis measurement. This offers the possibility to distinguish between different mechanisms of reversal as for a domain wall dominated reversal the perpendicular component remains negligible while in contrast for a homogeneous rotation a strong contribution is expected. Thus $\sqrt{M_x^2 + M_y^2}$ can be used as measure of the homogeneity of the reversal as it remains constant for a purely homogeneous rotation while it dips to zero (at coercivity) for a purely domain wall based one. Here the reversal mechanisms are studied by Vector magnetometry at different angles ($\theta=0^\circ, 15^\circ, 30^\circ, 45^\circ, 60^\circ, 75^\circ, 90^\circ$) to the film plane in different multilayered heterostructures with mixed anisotropies: For the $[\text{Co}(6\text{\AA})/\text{Pt}(15\text{\AA})]_4/(\text{Pt}(t))/[\text{Co}(10\text{\AA})/\text{Pt}(15\text{\AA})]_4$ with $t=0-45\text{\AA}$ series consisting of a perpendicular anisotropy bottom four-bilayer-stack coupled to a vanishing anisotropy top four-bilayer-stack through a variable thickness Pt interlayer, evidence of decoupling and homogeneous rotation of the top stack is clearly observed at for $\theta=30-75^\circ$. Similar behavior is observed for a $[\text{Co}(6\text{\AA})/\text{Pt}(15\text{\AA})]_4/\text{W}(15\text{\AA})/\text{Co}(24\text{\AA})$ sample consisting of a perpendicular anisotropy bottom four-bilayer-stack coupled to a vanishing anisotropy top Co layer through a non-magnetic W layer (permitting only dipolar coupling) in the plateau between the reversal of the two components. In contrast for the $\text{Co}(6\text{\AA})/\text{Pt}(15\text{\AA})]_4/\text{W}(15\text{\AA})/[\text{Co}(6\text{\AA})/\text{Pt}(15\text{\AA})]_4$ sample where two identical perpendicular anisotropy stacks are separated by a decoupling W layer the reversal follows the typical domain-wall propagation reversal. The same holds for $[\text{Co}(5\text{\AA})/\text{Pt}(10\text{\AA})]_6/\text{Pt}(x)/[\text{Ni}(15\text{\AA})/\text{Pt}(5\text{\AA})]_6$ series consisting of two six-bilayer-stacks having both perpendicular anisotropy but different coercivities.

Fig.1 Typical Vector Magnetometry measurement for a $[\text{Co}/\text{Pt}]_4/\text{W}/\text{Co}$ multilayer sample.



Magnetic nanoparticle heating in an AC magnetic field; an *ex vivo* approach

Z. Kalpaxidou¹, K. Kazeli^{1,2}, A. Makridis¹, E. Myrovali¹, N. Maniotis¹, D. Sakellari¹,
 T. Samaras¹ and M. Angelakeris¹

¹Physics Department, Aristotle University of Thessaloniki, Thessaloniki, 54124, Greece

²Physics Department, Aristotle University of Ioannina, Ioannina, 45110, Greece

Abstract:

Magnetic fluid hyperthermia (MFH) is the ever-promising "fourth leg" of cancer treatment. This thermotherapy is based on the fact that magnetic nanoparticles can transform electromagnetic energy from an external high-frequency field to heat, thus affecting the viability of malignant cells. In this work, in order to address the current challenges in clinical magnetic hyperthermia and due to the lack of tissue heat dissipation in *in vitro* studies, hyperthermia experiments were performed in phantom systems and eventually in *ex vivo* environment. For this purpose, iron oxide nanoparticles were chosen as hyperthermia magnetic carriers, and injected in tissue mimicking phantom models (by using appropriate dispersion medium such as agarose), while various substances (e.g. albumin) were utilized as a tool for visualisation of the heating area. For *ex vivo* systems magnetic carriers injected in bovine liver and sausage pork. All prepared samples were subjected in hyperthermia experiment, with magnetic field amplitude of 30 mT and frequency of 760 kHz (Fig.a). Heat diffusion of our studies was illustrated using an infrared digital camera while optical images revealed the final heating effect in each case. More specifically, our results revealed thermal denaturation of albumin protein as well as color changes in irradiated liver (Fig.b-e) at highest recorded temperatures of 70°C and 100°C respectively. Moreover, heat dissipation results of the computational analysis developed using COMSOL Multiphysics®, showing good agreement with available experimental findings, are also discussed.

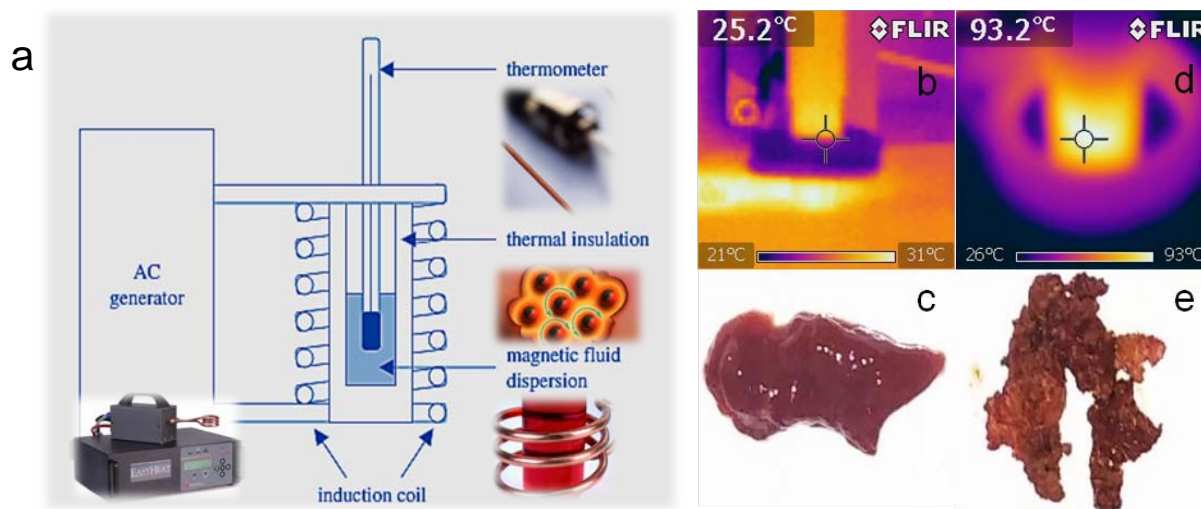


Figure: Scheme of magnetic hyperthermia setup (a). Heat map and bovine liver image without (b,c) and with (d,e) magnetic nanoparticles after the application of AC magnetic field. It is obvious that the sample with injected magnetic nanoparticles was successfully submitted to heating treatment.

Numerical simulations of interactions between magnetic nanoparticles and living matter through magnetothermal and magnetomechanical experimental setups

N. Maniotis, A. Makridis, E. Myrovali, T. Samaras and M. Angelakeris

Department of Physics, Aristotle University of Thessaloniki, 54124 Thessaloniki, Greece

In this work we quantify numerically the interactions between magnetic nanoparticles (MNPs) and the living matter which take place under varying external magnetic fields and frequencies through two different procedures: The MNPs magnetic energy density transformation (i) into mechanical forces and (ii) into heat. For the first case magnetic field gradients are induced by permanent magnets which are placed on a 3D polymer disk and in close proximity to seeded cells (above the magnets in Fig1a). With COMSOL 3.5a Multiphysics we estimate the mechanical forces exerted on different lines of cancer cells by cell-internalized MNPs. Those forces are generated by high-gradient magnetic fields (Fig.1d) and dictate MNPs movements within the cellular environment. Mechanical stress mediated by localized nanoparticles in HT.29 (human colorectal adenocarcinoma) and CT 26 cells leads to a significant decrease of cells viability. On the other hand in magnetic hyperthermia (Figs 1b, 1c) the combination of alternating magnetic fields and magnetic nanoparticles allows one to cause apoptosis via heat induction. We simulate the heating process of a single MNP inserted in a biological tissue under an external applied magnetic field. The thermal response of MNPs with different morphological features is analysed. The results demonstrate the impact of nanoparticle shape and surface coating in temperature dissipation in and around the nanoparticle. Finally we model the experimental setup of magnetic hyperthermia for in – vitro experiments. The simulations are repeated for both experimental setups of the laboratory, one consisting of two circular coils and one of eight squared coils surrounding the solution (Figs 1e, 1f). COMSOL can easily extend convectional models for one type of physics into multiphysics models that solve coupled physics phenomena simultaneously and so the electrical and the thermal problem were solved, calculating the magnetic field and the temperature of the coil and the solution respectively.

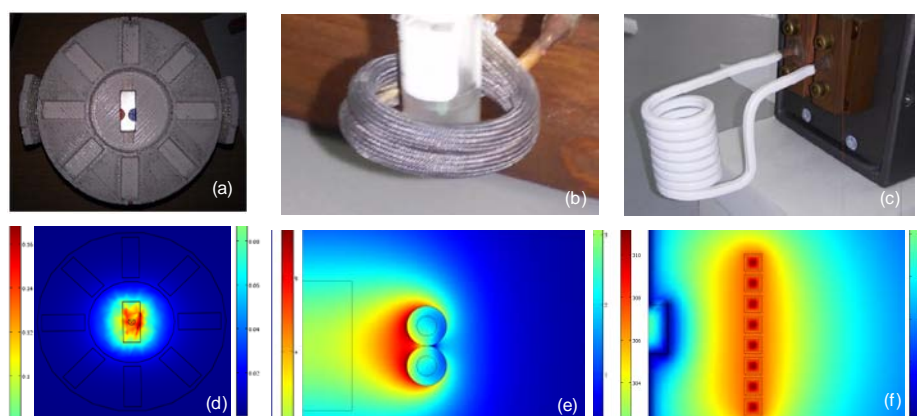


Figure 1: From theory to experiment and vice versa: Magnetic flux density mapping of a permanent NdFeB magnet placed in the centre of the 3D polymer magnetomechanical disk (1a, 1d), Magnetic field distribution generated by two circular coils (1b, 1e) and temperature distribution in the eight squared coils (1c, 1f).

Finite Elements Micromagnetic Simulation of the domain wall resonance

N. Ntallis, K.G. Efthimiadis,

Department of Physics, Aristotle University, 54124 Thessaloniki, Greece

In this work simulations of the domain wall oscillations under the influence of alternating external magnetic fields were performed.

The simulation method is based theoretically on Brown's classical micromagnetic approach and computationally on the finite element method. The magnetization dynamics is not simply described by the classical Landau – Lifshitz – Gilbert equation, but it is generalized in order to include, besides the precession, the nutation of the magnetization vector as well. In a compact vector form with respect to the magnetization vector, \vec{M} , the used partial differential equation is

$$\frac{\partial \vec{M}}{\partial t} = \gamma \vec{M} \times \left(\mu_0 \vec{H} - \eta \frac{\partial \vec{M}}{\partial t} - \frac{J}{M_s^2} \frac{\partial^2 \vec{M}}{\partial t^2} \right),$$

where γ is the gyromagnetic ratio, η is the Gilbert damping parameter, J is the moment of inertia regarding the magnetization nutation and \vec{H} is a local effective field acting on the magnetization. The last one was defined by the variational derivative of the free micromagnetic energy, in which the main contributions arise from exchange, magnetocrystalline, magnetostatic and Zeeman energies. In this context, assuming a uniaxial anisotropy

$$\vec{H} = \ell^2 \nabla^2 \vec{M} + \kappa^2 (\hat{k} \cdot \vec{M}) \hat{k} + \vec{H}_d + \vec{H},$$

where $\ell = \sqrt{2A/\mu_0 M_s^2}$ is the exchange length with A the exchange stiffness constant and $\kappa = \sqrt{2K/\mu_0 M_s^2}$ is the hardness parameter with K the first order anisotropy constant and \hat{k} the direction of the anisotropy axis, i.e. the easy magnetization axis. In the absence of conducting media, the demagnetizing field, \vec{H}_d , was calculated from the gradient of a magnetic scalar potential φ , which obeys the Poisson equation $\nabla^2 \varphi = -\nabla \cdot \vec{M}$. The last term, \vec{H} , is the external field, which is parallel to the easy axis. The governing equations were supplemented with the boundary condition $\partial \vec{M} / \partial \hat{n} = 0$, where \hat{n} represents the unit vector normal to the surface of the particle.

The simulations were performed for soft ferromagnetic spherical particles of uniaxial magnetocrystalline anisotropy, in which the magnetic domains were created during the demagnetization from saturation (figure 1).

The simulation results indicate multiple resonances in different points of the susceptibility spectrum, due to different oscillation modes of the domain wall (figure 2).

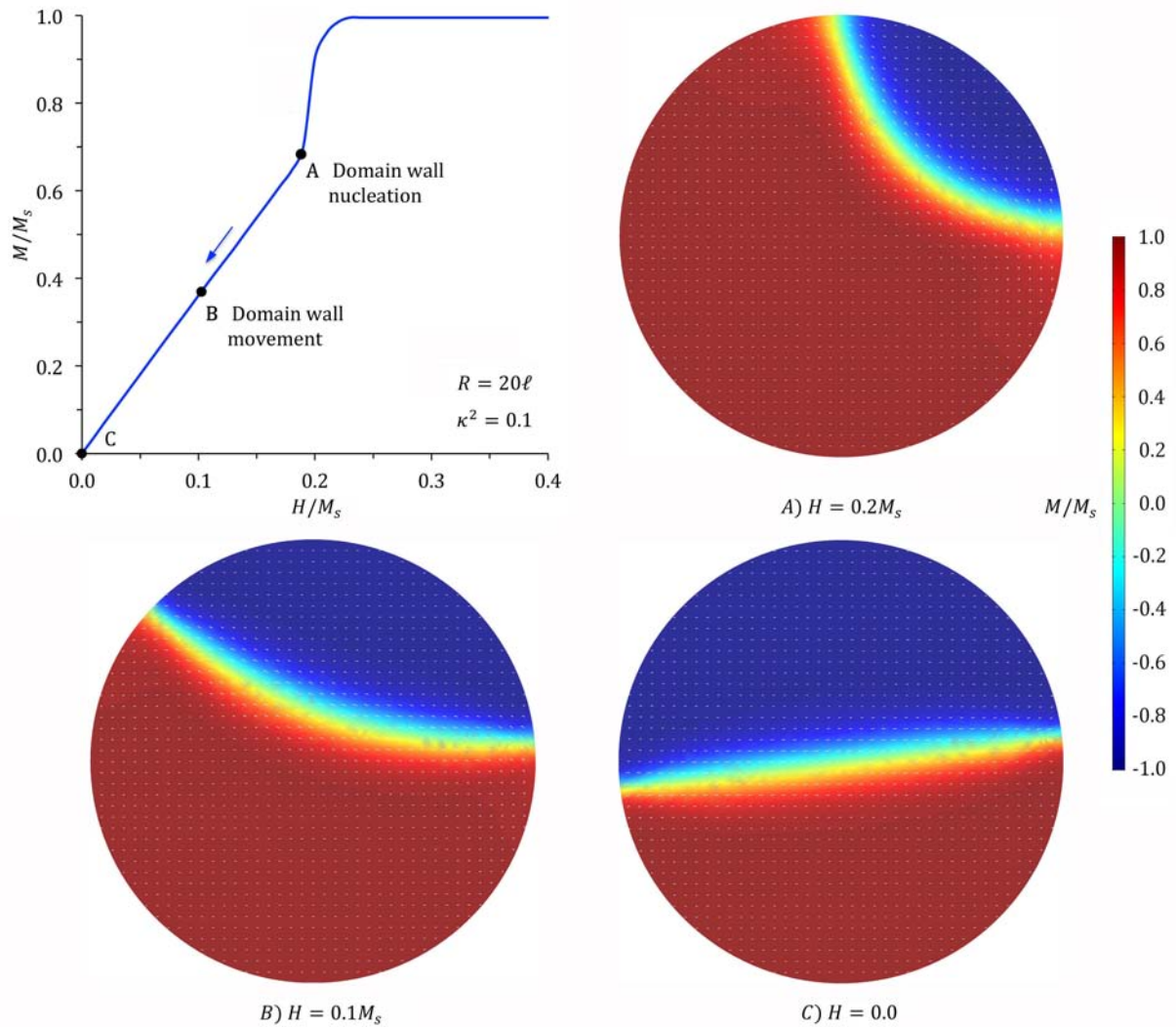


Fig. 1 Nucleation and expansion of a magnetic domain wall during the demagnetization.

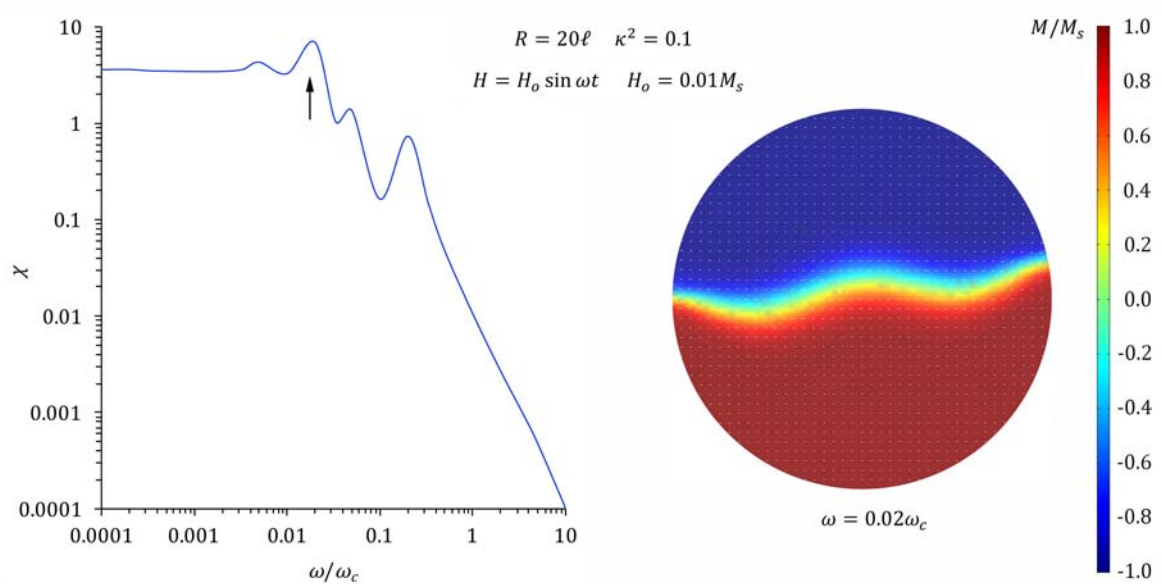


Fig.2 Susceptibility spectrum and a snapshot of domain wall oscillation in one of the resonance frequencies.

Conductivity Degradation Study of Polypyrrole and Polypyrrole/5% w/w TiO₂ nanocomposite under Heat Treatment in He and Atmospheric Air

E. Vitoratos¹, K. Emmanouil, E. Dalas² and S. Sakkopoulos¹

¹Department of Physics, University of Patras, 265 00 Patras, Greece

²Department of Chemistry, University of Patras, 265 00 Patras, Greece

The thermal aging of the d.c. electrical conductivity σ in pure polypyrrole (PPy) and in the nanocomposite PPy/5%w/w TiO₂ was investigated for thermal treatment times from 0 to 50 hours at different temperatures $T = 100, 300$ and 380 K under atmospheric air and inert He gas. In both materials the fluctuation induced tunneling (FIT) of charge carriers was followed revealing a granular metal structure.

The isothermal variation of σ with time under atmospheric air and inert He indicates the coexistence of two antagonistic mechanisms, the one increasing and the other decreasing σ , as it is shown in Fig.1.

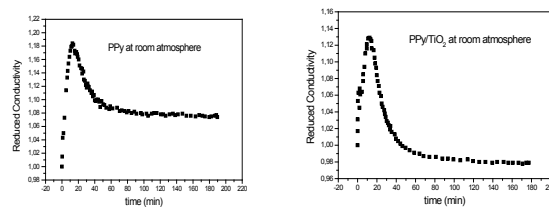


Fig.1. The reduced conductivity of pure PPy and PPy/TiO₂ at 300 K under room atmosphere for times from 0 to 200 min.

In XRD patterns from PPy and PPy/5%w/w TiO₂ (Fig.2), the sharp peaks of TiO₂ coexist with the broad peak of amorphous PPy, which shifts to smaller angles with the addition of TiO₂ revealing a greater departure between pyrrole rings, which turns up to be about equal to the diameter of O²⁻ indicating the diffuse of oxygen from TiO₂ into PPy.

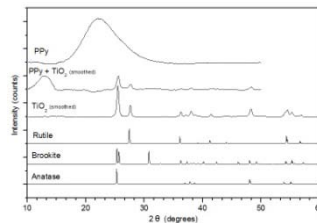
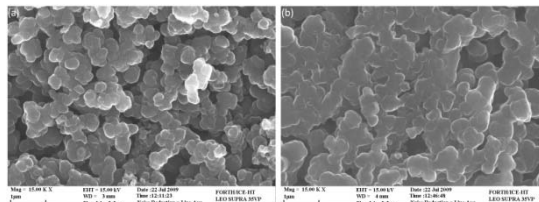


Fig.2 XRD spectrograms from pure PPy, PPy+5%w/wTiO₂ and TiO₂.

In the SEM pictures, shown in Fig.3., the decrease of the more light regions and the smoothing of the surface with aging confirm the removal of Cl⁻ and the rearrangement of the



SEM pictures from pristine PPy on the left and thermally aged polymer at 380 K for 36 h on the right.

polymer chains, two antagonistic mechanisms the first decreasing, the second increasing conductivity.

Laser Induced Forward Transfer technique for the immobilization of biomaterialsM. Chatzipetrou¹, M. Massaouti¹, S. Papazoglou¹, I. Zergioti¹*1. National Technical University of Athens, Physics Department, Heroon Polytehneiou 9, 15780, Zografou, Greece***Abstract:**

Laser Induced Forward Transfer (LIFT) is a direct write technique, able to create micropatterns of biomaterials on sensing devices. In this conference we will present a new approach of using LIFT technique for the printing and direct immobilization of biomaterials on a great variety of surfaces, for bio-sensor applications. In our approach, we use LIFT technique for the direct immobilization of biomaterials, either by physical adsorption or by covalent bonding. The physical adsorption of the biomaterials, occurs on hydrophobic or super-hydrophobic surfaces, due to the transition of the wetting properties of the surfaces upon the impact of the biomaterials solution with high velocity. The unique characteristic of LIFT technique to create high speed liquid jets, leads to the penetration of the biomaterial in the micro/nano roughness of the surface, resulting in their direct immobilization and avoiding any chemical functionalization layer. In this conference we will present the direct immobilization of enzymes and proteins on Screen Printed Electrodes (SPEs), for the fabrication of electrochemical biosensors able to detect phenolic compounds and herbicides. For the enzymatic biosensor, used for the detection of phenolic compounds, the observed LOD for catechol was 150 nM, while for the protein biosensor, used for the detection of herbicides, the observed LOD was 8-10 nM. Moreover, regarding the covalent immobilization of biomaterials, we will present the direct immobilization of thiol modified aptamers, on alkene and alkyne modified Si₃N₄ surfaces, by laser-mediated "click chemistry" reactions, where a laser pulse is used both for the printing and the photo-activation of the aptamers that react with the alkene/yne surfaces by thiol-ene/yne reactions. This approach effectively combines the classical benefits of click reactions with the advantages of a photoinitiated process, which can be activated at specific times and locations, resulting in a powerful method for chemical immobilization of biomaterials.

Ionic Conductivity in Discotic Liquid Crystals of hexa-*peri*-benzocoronenes (HBC) doped with lithium triflate (LiTf)

A. Pipertzis¹, K. Wunderlich², K. Müllen², G. Floudas¹

¹Department of Physics, University of Ioannina, P.O. Box 1186, 451 10 Ioannina, Greece

²Max-Planck Institute for Polymer Research, D -55128 Mainz, Germany

Abstract:

Discotic liquid crystals (DLCs) have attracted considerable interest because of their unique self-organization behavior into columnar superstructures¹. Their self-assembly is driven by noncovalent intermolecular interactions favoring the π -stacking of aromatic cores.²⁻⁴ Herein we explore the possibility of electronic and ionic conduction in model DLCs, in possible applications as Solid Polymer Electrolytes⁵ in lithium ion batteries⁶. For this purpose we design a DLC of hexa-*peri*-benzocoronenes (HBC) with six chains of triethylene glycol dimethyl ether (TEG) doped with lithium triflate (LiTf) in three salt concentrations [EO]:[Li⁺]=12:1, 8:1 and 3:1. The columnar organization ("hard nanophase") supports the electronic conductivity (i.e. molecular wires⁷⁻⁸) whereas TEG functionalization ("soft nanophase") and addition of lithium triflate (LiTf) results in ionic conductivity. We have employed (a) differential scanning calorimetry (DSC) to investigate the thermal properties of DLCs, (b) X-ray scattering to determine the unit cell and the nanodomain structure, (c) dielectric spectroscopy (DS) to determine the ionic conductivity and the molecular dynamics and (d) rheology to determine the viscoelastic properties. The bulk HBC-TEG6 undergoes a low temperature phase transition from crystalline (Cr) phase to liquid-crystalline (LC) phase and a transition at higher temperatures due to the change of unit cell. The addition of lithium triflate (LiTf) stabilizes the high temperature unit cell and in addition organized into a superstructure that is detected in DSC, X-rays, DS and in rheology. The ionic conductivity is $\approx 3.6 \times 10^{-6}$ S/cm at T= 363 K of the HBC-TEG6/LiTf with salt concentration [EO]:[Li⁺]=3:1. Ionic conductivity of these composite systems is reduced by 2 decades in comparison to the respective TEG6/LiTf with the same salt concentration. Furthermore DS revealed that ion transport is coupled to the segmental dynamics.

References

- [1] Handbook of Liquid Crystals; Demus, D., Goodby, J., Gray, G. W., Spiess, H.-W., Vill, V., Eds.; Wiley-VCH: Weinheim, **1998**.
- [2] Boden, N.; Bushby, R J.; Clements, J.; Movaghar, B.; Donovan, K J.; and Kreouzis, T.; **1995 Phys. Rev. B** 52 13274
- [3] Haase, N.; Grigoriadis, C.; Butt, H. J.; Müllen, K.; Floudas, G., *J Phys Chem B* 115, 5807 (**2011**)
- [4] Wunderlich, K.; Grigoriadis, C.; Zardalidis, G.; Klapper, M.; Graf, R.; Butt, H.-J.; Müllen, K.; Floudas, G., *Macromolecules*, **2014**, 47, pp 5691.
- [5] Agrawal, R.C.; Pandey, G.P. *J. Phys. D: Appl. Phys.* **2008**, 41, 223001.
- [6] Osaka, T.; Ogumi, Z. Eds, *Springer* **2014**.
- [7] Feng, X.; Marcon, V.; Pisula, W.; Hansen, M. R.; Kirkpatrick, J.; Grozema, F.; Andrienko, D.; Kremer, K.; Müllen, K. *Nat. Mater.* **2009**, 8, 421–426.
- [8] Van de Craats, A. M.; Warman, J. M.; Fechtenkotter, A.; Brand, J. D.; Harbison, M. A.; Müllen, K. *Adv. Mater.* **1999**, 11, 1469.

Synthesis of a glass-ceramic nano-material in the ternary system SiO-CaO-MgO-CuO: effect of ball milling on the particle size, morphology and bioactive behavior

G. K. Pouroutzidou¹, G. S. Theodorou¹, L. Papadopoulou², N. Kantiranis², E. Kontonasaki³, C. B. Lioutas¹, K. M. Paraskevopoulos¹

¹Department of Physics, ²School of Geology, ³School of Dentistry, Aristotle University of Thessaloniki, 54124 Thessaloniki, Greece

Various studies have reported that, Si-, Ca-, Mg- and Cu containing glasses, are highly bioactive and could be used in biomedical applications such as bone tissue regeneration [1]. Moreover, Cu is a trace element in the human body, known to play a significant role in angiogenesis [1]. Nanotechnology has a great potential to improve biomaterials used in tissue engineering [2]. Nano-bioceramics are preferable compared to their micro-scale counterparts, because of their increased surface area which can improve both mechanical properties and apatite formation ability due to the increased nucleation sites provided [3]. The aim of this study was to produce nano-sized glass-ceramics of the ternary system SiO-CaO-MgO-CuO.

Sol-gel derived bioactive glasses with composition in wt%: 60 SiO₂, 30 CaO, 7.5 MgO, 2.5 CuO were produced by the hydrolysis of TEOS in a mixture of d.d. H₂O, ethanol and HNO₃. Afterwards Ca, Mg, Cu were added as nitrate salts while ammonia solution was inserted dropwise under stirring in an ultrasonic bath [4]. The synthesized glass-ceramics were inserted in a planetary system (Retsch S100) for 6h with different rpm (300, 400 and 500). Bioactivity evaluation was conducted in SBF, with a ratio of 1.5 mg/mL for 1, 3, 5, 15 and 20 days under renewal conditions [5]. FTIR, TEM, XRD and SEM/EDS were used for the characterization of the samples.

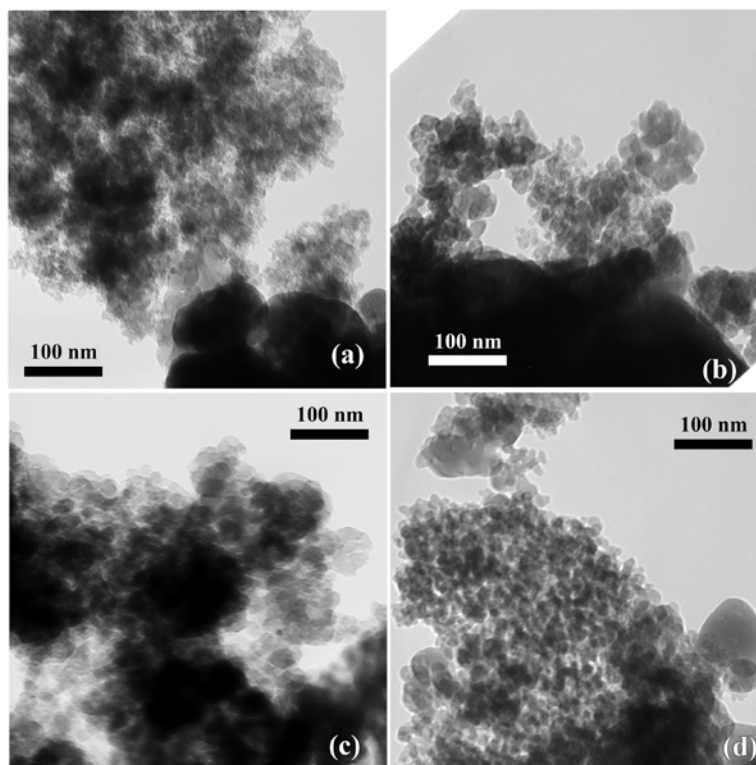


Fig. 1: TEM microphotographs of glass ceramic material before (a) and after ball milling treatment with different rpm: (b) 300 rpm, (c) 400 rpm and (d) 500 rpm. (The bar of 100nm stands for all images)

TEM microphotographs of pristine and milled materials show the coexistence of both nano-crystalline and amorphous phases (Fig.1).

The size of the nano-agglomerates decreases as the rpm are increased. Simultaneously, the amorphous proportion of the glass-ceramic material is increased. Finally, the bioactivity test revealed the formation of apatite after 5 days of immersion. Thus, a bioactive glass-ceramic nano-material was successfully synthesized and the milling process had no significant effect on the agglomerate size although a slight increase in the amorphous phase was observed.

References

- [1] A. Hoppe, N.S. Gldal and A.R. Boccaccini, *Biomaterials* 32 (2011) 2757-2774.
- [2] G. M. Luz and J. F. Mano, *Nanotechnology* 22 (2011) 494014 (11pp).
- [3] B. Kankilic, S. Kose, P. Korkusuz, M. Timucin and F. Korkusuz, *Curr. Stem Cell Res. Ther.* (Feb. 2015)
- [4] A. M. El-Kady, M.M. Farag, *Journal of Nanomaterials* (2015), Article ID 839207.
- [5] C. Wu and G. Chang, *J Biomed Mater Res* 83B (2006) 153-160

Effect of Confinement on the Structure and Dynamics of two Rod-like Liquid Crystals

A. Selevou^{1*}, M. Steinhart², G. Floudas¹

¹*Department of Physics, University of Ioannina, P.O. Box 1186, 45110, Ioannina, Greece*

²*Institut für Chemie neuer Materialien, Universität Osnabrück, Germany*

8CB (n-octylcyanobiphenyl) and 8OCB (n-octyloxycyanobiphenyl) are two rod-like mesogens belonging to the cyanobiphenyl liquid crystal group, structurally different in the addition of an oxygen atom in the latter. We investigate 8CB and 8OCB, firstly, in the bulk by means of X-ray diffraction and Polarizing Optical Microscopy to determine the unit cell structure and liquid crystalline textures respectively. Self-ordered nanoporous AAO templates with pore diameters ranging from 25 nm to 400 nm are used as a confining medium. Differential Scanning Calorimetry (DSC) and Dielectric Spectroscopy (DS) are employed in identifying phase transitions from the heat of fusion and temperature dependence of the dielectric permittivity, respectively, both in the bulk and in confinement. Comparison of the bulk transition temperatures and the dynamic order parameter, S , obtained from DS implies greater order in 8OCB than 8CB. The effect of confinement is investigated with respect to changes of the phase transition temperatures and molecular dynamics and is further discussed in view of previous experimental [1], [2] and computational results [3], [4].

[1] Suppression of Phase Transitions in a Confined Rodlike Liquid Crystal, C. Grigoriadis, H. Duran, M. Steinhart, M. Kappl, H. Butt, G. Floudas, ACS Nano 5, 9208-15 (2011)

[2] Dielectric Spectroscopy of Liquid Crystals in Smectic, Nematic and Isotropic Phases Confined in Random Porous Media, G. Sinha, F. Aliev, Phys. Rev. E 58, 2001-2010 (1998)

[3] Rounding of Phase Transitions in Cylindrical Pores, D. Wilms, A. Winkler, P. Virnau, K. Binder, Phys. Rev. Lett. 105, 045701 (2010)

[4] Computer Simulation Study of a Liquid Crystal Confined to a Spherical Cavity, Y. Trukhina, T. Schilling, Phys. Rev. E, 77, 011701 (2008)

Glass Transitions of Amorphous Polymers Confined in Nanopores: Dependence on Interfacial Energy and Thickness

S. Alexandris¹, P. Papadopoulos¹, M. Steinhart², G. Floudas¹

¹*Department of Physics, University of Ioannina, Greece*

²*Institut für Chemie neuer Materialien, Universität Osnabrück, Germany*

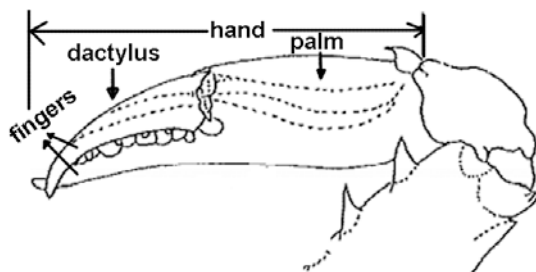
We report on the influence of confinement on the segmental dynamics of a series of amorphous polymers (PVA_c, PB, PS, PDMS, PMPS, Glycerol, PMMA and PI) and of two semicrystalline polymers (PEO and PCL). The confining medium is always the same, namely, self-ordered anodic aluminum oxide, abbreviated as AAO. AAO templates contain arrays of discrete-isolated, parallel, cylindrical pores that are uniform in length and diameter that have been employed as model confining systems. Dielectric spectroscopy reveals that dynamics become faster in confinement and thus a large depression in glass temperature is generally observed with decreasing pore diameter. In a second step we are exploring a possible connection of the glass temperature in the pores with the interfacial energy. To this end, the interfacial energy between the different polymers and AAO surface is calculated by means of the Fowkes-Oss-Chaudhury model. We find a general relation of the depression in glass temperature with increasing interfacial energy. Additional effects could relate to the density near the pore walls and surface roughness.

Spectroscopic study of the role of Br and Sr in colored parts of the *Callinectes sapidus* crab claw

M. Katsikini

School of Physics, Aristotle University of Thessaloniki, 54124 Thessaloniki, Greece.

Abstract: The exoskeleton of crustaceans comprises of a composite material consisting of chitin biopolymers and inorganic biominerals, mainly calcium carbonate, that determine their mechanical properties. Crabs accumulate Sr with the Sr/Ca ratio being directly related to the concentration of Sr in the water. Br is another element that is accumulated by crustaceans though feeding with algae. The claw of the *Callinectes sapidus* crab exhibits vivid coloration (white and blue in the palm and orange in the fingers), caused by the presence of chromo-proteins that trap the astaxanthin (AXT) carotenoid chromophore. X-ray Fluorescence (XRF), Raman, visible light Reflectance, and Br- and Sr-K-edge X-ray Absorption Fine Structure (XAFS) spectroscopies were applied for the study of the color variations along the claw. The macroscopic color at different regions is consistent with the reflectance spectra that exhibit variations related to the selective absorption caused by the electronic transitions of the conjugated polyene chain of AXT. The interaction of the protein with the chromophore molecule modifies its light absorption properties giving rise to different colors. Combination of the XRF and Raman spectra indicate that Br is present only in the stained parts of the claw (orange and blue) where the chromo-protein is also detected. Analysis of the Br-K-edge EXAFS spectra recorded from the stained parts reveals that Br is bonded to benzene rings most probably of the chromo-protein amino acid residues. Combined Sr-K-edge XAFS and Raman analysis discloses that Sr substitutes for Ca in the calcium carbonate. Nano-crystalline calcite and aragonite phases prevail in the finger and the palm of the claw, respectively. In the latter case, an amorphous phase was found to coexist with the nano-crystalline one. The variations in the biomineralization in the fingers of the claw are attributed to the necessity for improved mechanical properties at its end.



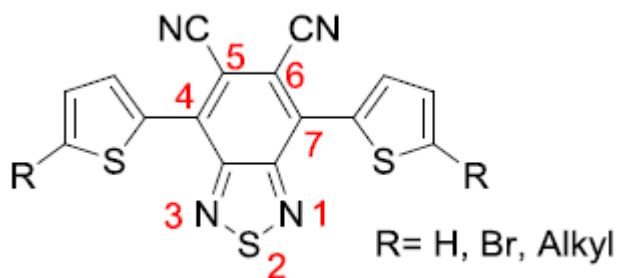
Liquid Crystals of Hexasubstituted Benzenes bearing ultra strong dipole moments

T. Nevolianis^{1*}, J. Wudarczyk², K. Müllen², G. Papamokos¹, G. Floudas¹

¹Department of Physics, University of Ioannina, P.O. Box 1186, 45110, Ioannina, Greece

²Max Planck Institute for Polymer Research, 55128 Mainz, Germany

Hexasubstituted benzenes bearing dipole moments exceeding 10 debye have been recently reported in the literature via functionalization of diaminophthalonitrile to its brominated and tetracyanated derivatives.[1] By their transformation into dithienyl derivatives (4,7-di(thiophen-2-yl)benzo[c]-[1,2,5]thiadiazole-5,6-dicarbonitrile – Figure 1) the cyano groups further increase the electron-withdrawing ability of the acceptor. In this work we study three rod-like liquid crystals (Fig. 1, R=C₆H₁₃, C₁₆H₃₃ and R=C₆H₁₃ with hydrogens at positions 5 and 6 instead of the CN) bearing strong dipole moments perpendicularly to the molecular axes. We investigated them by means of X-ray diffraction (XRD) and Polarizing Optical Microscopy (POM) to determine the unit cell structure and liquid crystalline textures respectively. Differential Scanning Calorimetry (DSC) and Dielectric Spectroscopy (DS) were employed to identify phase transitions from the heat of fusion and temperature dependence of the dielectric permittivity, respectively. For the monomers carrying either CN groups or hydrogens at positions 5 and 6 and for R=H, C₆H₁₃, C₁₆H₃₃, the energetics and their dipole moments, total molecular polarizabilities (α), and first order hyperpolarizabilities (β) are reported via state of the art DFT calculations. Such molecules may lead to enhanced charge separation efficiency by decreasing the exciton binding energy and thus become potentially applicable to organic photovoltaics. [2]



[1] J. Wudarczyk, G. Papamokos, V. Margaritis, D. Schollmeyer, F. Hinkel, M. Baumgarten, G. Floudas and K. Müllen *Ang. Chem. Int. Ed.* **2016**, 55, 3220-3223.

[2] N. Camaioni, R. Po, *J. Phys. Chem. Lett.* **2013**, 11, 1821-1828.

MODELING AND QUANTIFYING DRUG RELEASE KINETICS

G. Kalosakas^{1,2}, A. Hadjithodorou³, D. Martini⁴

¹ University of Patras, Materials Science Department, GR-26504, Rio, Greece

² Crete Center for Quantum Complexity and Nanotechnology (CCQCN), GR-71003, Heraklion, Greece

³ Stanford University, Bioengineering Department, CA-94305, Stanford, California, USA

⁴ University of Patras, Medicinal Chemistry, GR-26504 Rio & CBL Patras S.A., GR-26000 Patras, Greece

Drug release profiles from various formulations (spheres, composite spheres, and slabs) are calculated: *i*) numerically, using Monte Carlo simulations and *ii*) analytically, through the solution of diffusion equation. Diffusion-controlled release is considered. The obtained release profiles are described and quantified through the stretched exponential function (known also as Weibull function), Eq. (1) [1,2].

$$\frac{M_t}{M_\infty} = 1 - \exp[-(t/\tau)^b] \quad (1)$$

In Eq. (1), M_t is the amount of drug released at time t , M_∞ is the total amount of drug released at infinite time, and b, τ are the two stretched exponential parameters. We investigate the dependence of these parameters on the device characteristics [3,4,5].

Equation (1) has the advantage over other popular descriptions, like the Higuchi [6] or Peppas [7,8] models, that it exhibits the proper asymptotic behavior of the release at relatively long times. Such a qualitatively appropriate description of the whole release profile is achieved without introducing more parameters than for example the well known and extensively used power-law model.

Acknowledgement: This work has been supported by the Thales project MACOMSYS, co-financed by the European Union (ESF) and Greek national funds (ΕΣΠΑ) and by European Union's Seventh Framework Programme (FP7-REGPOT-2012-2013-1) under grant agreement n° 316165.

References:

- [1] K. Kosmidis, P. Argyrakis and P. Macheras, *Pharm. Res.* **20** (2003) 988.
- [2] V. Papadopoulou, K. Kosmidis, M. Vlachou and P. Macheras, *Int. J. Pharm.* **309** (2006) 44.
- [3] A. Hadjithodorou and G. Kalosakas, *Mater. Sci. Eng. C* **33** (2013) 763.
- [4] A. Hadjithodorou and G. Kalosakas, *Mater. Sci. Eng. C* **42** (2014) 681.
- [5] G. Kalosakas and D. Martini, *Int. J. Pharm.* **496** (2015) 291.
- [6] T. Higuchi, *J. Pharm. Sci.* **50** (1961) 874.
- [7] N.A. Peppas, *Pharm. Acta Helv.* **60** (1985) 110.
- [8] P.L. Ritger and N.A. Peppas, *J. Control. Release* **5** (1987) 23; *ibid* **5** (1987) 37.

Electronic structure of purines, pyrimidines and similar molecules with LCAO

Ch. Zacharaki, M. Mantela, A. Morphis, M. Tassi, and C. Simserides

National and Kapodistrian University of Athens, Faculty of Physics, Department of Solid State Physics, Panepistimiopolis, Zografos, GR-15784, Athens, Greece

Abstract: We study the electronic structure, including the lowest ionisation and excitation energies, and the transition dipole moments of biologically important heterocyclic planar molecules like purines, pyrimidines and similar molecules e.g. carbazole, luminol, acetophenone, phenanthroline etc. We use the linear combination of atomic orbitals (LCAO) method, taking only p_z atomic orbitals into account. In other words, we use a type of Hückel model but with the parametrizations proposed either by Hawke *et al.* [1] or by Mantela *et al.* [2]. These parametrizations can be employed to molecules containing carbon, nitrogen, or oxygen atoms with sp^2 hybridization. For the diagonal matrix elements, four empirical parameters are used, corresponding to carbon, nitrogen with one or two p_z electrons and oxygen atoms. For the non-diagonal matrix elements between neighbouring atoms, bond-length dependent formulae like the one of Harrison [3] are used. The methods have already been successfully applied among other molecules to adenine, guanine, cytosine, thymine, and uracil [1,2] and used to obtain the tight binding parameters pertinent to charge transfer along DNA [4]. We compare our results to experimental ionization energies, HOMO-LUMO gaps and transition dipole moments.

[1] L.G.D. Hawke, G. Kalosakas, C. Simserides, *Molecular Physics* 107 (2009) 1755

[2] M. Mantela, A. Morphis, M. Tassi and C. Simserides, *Molecular Physics* 114 (2016) 709

[3] W.A. Harrison, *Electronic Structure and the Properties of Solids*, 2nd ed. (Dover, New York, 1989); *Elementary Electronic Structure* (World Scientific, River Edge, NJ, 1999)

[4] L.G.D. Hawke, G. Kalosakas, C. Simserides, *Eur. Phys. J. E* 32 (2010) 291; *ibid.* 34 (2011) 118

Mesomorphic Behaviour and dielectric response of symmetric difluoroterphenyl methylene-linked dimers

E.E. Zavvou¹, E. Ramou^{1,2}, Z. Ahmed², C. Welch², P.K. Karahaliou¹, G.H. Mehl²

¹*Department of Physics, University of Patras, 26504 Patras, Greece*

²*Department of Chemistry, University of Hull, HU6 7RX, UK*

The recent discovery of a new unusual liquid crystal phase, formed by symmetric odd-membered dimers, has attracted considerable interest towards these liquid crystal systems [1-3]. The new mesophase, termed originally Nx to indicate an unknown nematic-like mesophase and also found in the literature as twist-bend nematic (Ntb), is characterized, in common with the conventional nematic, by the absence of long range positional order and by a spontaneous spatial modulation of a phase axis [1]. Moreover the fact that Nx/tb phase is chiral in nature even though comprised by achiral molecules, poses new challenges in the research field of liquid crystals. Several complementary characterization techniques have been implemented to probe this mesophase, but its structural features and physical properties are still under debate.

In this work we investigate the mesophase behaviour and dielectric response of new symmetric difluoroterphenyl methylene-linked dimers. The phase characterization and thermal behaviour are investigated by means of Polarizing Optical Microscopy (POM) and Differential Scanning Calorimetry (DSC), while dielectric anisotropy and relaxations are investigated by means of Broadband Dielectric Spectroscopy. The results are to be discussed in connection to the molecular shape and molecular conformations, the molecular order within both nematic phases and contribute to better understanding the nematic-nematic transition in liquid crystalline dimers.

References

- [1] V. Borshch, et al., Nat. Commun., 4, 2635, (2013)
- [2] V. Panov, et al., Phys. Rev. Lett., 105, 167801, (2010)
- [3] M.G. Tamba, et al., RSC Adv., 5, 11207, (2015)
- [4] S.M. Salili, et al., Phys. Rev. Lett., 116, 217801, (2016)

Modelling of drug particles behavior near the release boundary: a classical and fractional dynamics approach

E. V. Christidi¹, G. Kalosakas^{1,2}

¹*Materials Science Dept., University of Patras, Rio GR_26504, Greece*

^{1,2}*Crete Center for Quantum Complexity and Nanotechnology (CCQCN), Physics Dept., University of Crete, 71003 Heraklion, Greece*

Abstract: In first place, investigation of the evolution of the fraction of drug molecules that are sufficiently close to the release boundary, in order to check the validity of the assumption underlying the theoretical derivation of a stretched exponential (Weibull) release kinetics [1]. Secondly, exploration of the use of fractional order differential equations for the analysis of datasets of various drug processes that present anomalous kinetics, i.e. kinetics that are non-exponential and are typically described by power-laws [2]. This approach takes place also for the drug release behavior near the release boundary. A fractional differential equation corresponds to a differential equation with a derivative of fractional order. The main mechanism that describes the drug release is diffusion. For the aforementioned cases, the Diffusion-controlled drug release from slabs and spheres is considered. Both analytical results and Monte Carlo simulations are used to calculate the evolution of diffusive drug particles.

Both analytical and Monte Carlo simulations data show an inverse power-law time dependence of the fraction of diffusive drug particles near the boundary, after an initial short time, followed by saturation. The power-law dependence starts early during the process, at around 1% of the release and lasts up to at least 80% of the release. The obtained results indicate an agreement between the values of the power-law exponent, m , and the Weibull exponent, b , as predicted from the relation $b=1-m$ [1]. The fraction of drug molecules near to an exit, as a function of time, follows an inverse power-law in a substantial part of the release problem, justifying an approximate description of the release kinetics through a stretched exponential function. Fractional kinetics though, can describe all the cases of drug release systems, including the Weibull classical kinetics and offers an elegant description of anomalous kinetics, i.e. nonexponential terminal phases, the presence of which has been acknowledged in pharmaceutical literature extensively.

[1] K. Kosmidis, P. Argyrakis, P. Macheras, *Pharm. Res.*, 988 (2003) 988-995

[2] A. Dokoumetzidis, P. Macheras, *J. Pharmakokinet. Pharmakodyn.* 36, (2009) 165-178

CoFe₂O₄ Nanoassemblies as Dual agents: Carriers of Anti-inflammatory Drug and Imaging Probes

V. Georgiadou¹, D. Papagiannopoulou², I. Tsoukos³, C. Dendrinou-Samara¹

¹Department of Chemistry, Aristotle University of Thessaloniki, GR-54124 Thessaloniki, Greece

²Department of Pharmaceutical Chemistry, School of Pharmacy, Aristotle University of Thessaloniki, 54124 Thessaloniki, Greece

³Department of Medical Physics, University Hospital of Larissa, University of Thessaly, Biopolis, GR-41110 Larisa, Greece

Abstract:

The emerging need for multimodal clinical nanoagents for theranostics points out the demand for magnetic nanoparticles (MNPs) with optimum size, shape, magnetization, surface chemistry and stability. The targeted synthesis of MNPs permits new inventive surface modification ways with a view to ensure their *in vivo* fate and clinical performance. In addition, these drug carriers undergo certain limitations concerning the drug release mechanism and kinetics, while easy post-release removal is a prerequisite for the avoidance of *in vivo* side effects (1). Herein, we present the development of a stable dual system: anti-inflammatory **drug delivery** and **T2 imaging system** (DD/T2S) for the first time (Fig. 1). CoFe₂O₄ magnetic nanoparticles <10 nm, with moderate magnetic properties (~60 emu g⁻¹), coated with octadecylamine, were synthesized solvothermally. The DD/T2S was formed by an inverse micelles method with sodium dodecyl sulfate (SDS) chains that also allowed the introduction of the anti-inflammatory drug Naproxen. The resulted DD/T2S is stable and has a small hydrodynamic size ($d_H = 320$ nm), which is also confirmed by Transmission Electron Microscopy (TEM) imaging. The enhancement of proton transverse relaxivity was evaluated by MRI ($r_2 = 24$ mM⁻¹ s⁻¹, $r_1 = 2.8$ mM⁻¹ s⁻¹, measured at 3 T) and by NMR measurements ($r_2 = 50$ mM⁻¹ s⁻¹, 11.7 T). The relaxivity values of DD/T2S are compared with their non Naproxen carrying analogue system ($r_2 = 30$ mM⁻¹ s⁻¹, $r_1 = 1.1$ mM⁻¹ s⁻¹, measured at 3 T). The Naproxen release by the DD/T2S was also studied and compared with other functionalization routes presented before by us (1).

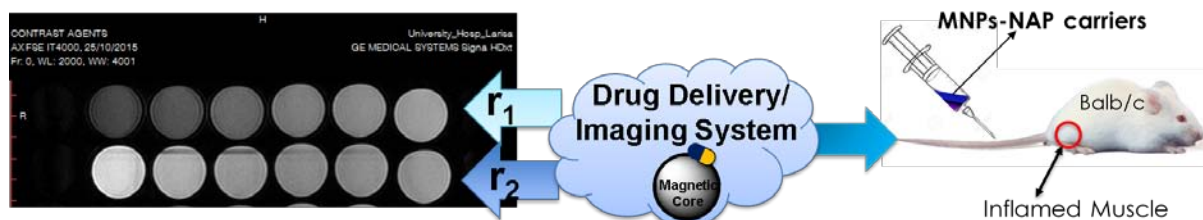


Figure 1. CoFe₂O₄ Nanoassemblies as Dual agents (DD/T2S).

(1) *ACS Appl. Mater. Interfaces*, 2016, 8, 9345-9360